USING THE “KITE” FRAMEWORK FOR UNDERSTANDING LANDSCAPE CHANGE AND IMPROVING EAST AFRICAN AGRICULTURAL SYSTEMS UNDER CLIMATE CHANGE

By

Dan Wanyama

A DISSERTATION

Submitted to
Michigan State University
in partial fulfillment of the requirements
for the degree of

Geography – Doctor of Philosophy

2021

ABSTRACT

USING THE “KITE” FRAMEWORK FOR UNDERSTANDING LANDSCAPE CHANGE AND IMPROVING EAST AFRICAN AGRICULTURAL SYSTEMS UNDER CLIMATE CHANGE

By

Dan Wanyama

The Mount Elgon Ecosystem (MEE), an important hydrological and socio-economic area in East Africa, has exhibited significant landscape changes, driven by both natural factors and human activities, therefore leading to more frequent natural disasters (frequent and extended droughts, floods, and landslides). Yet, few studies have focused on the MEE socio-ecological system; no comprehensive knowledge exists of how humans and nature interact, at multiple scales, to drive ecosystem-wide landscape changes.

This dissertation focuses on three interrelated questions: (1.) What is the nature and magnitude of change in MEE greenness for the period 2001-2018, and how is this change related to long-term trends and variability in MEE precipitation? (2.) How is ecological and environmental (eco-environmental) vulnerability distributed across the MEE, and what are the major factors driving these patterns? and (3.) How will the MEE landscape change in the future, and what opportunities exist for streamlining livelihood improvement and environmental conservation efforts?

Study 1 characterized comprehensively, over multiple time scales, recent patterns and trends in MEE vegetation greening and browning. The MEE was found to exhibit significant variability in vegetation dynamics and precipitation regimes. There was persistent greening and browning at different time scales and this change was attributed to both natural factors (including changing precipitation) and anthropogenic factors (especially the vegetation-to-cropland conversion). The study also concluded that MEE precipitation had increased substantially in the post-2000 era, which influenced greening and browning patterns observed in the 2006-2010 period. The integration of Mann–Kendall, Sen’s slope and bfast (breaks for additive season and

trend) proved useful in comprehensively characterizing recent changes in vegetation greenness within the MEE.

Study 2 examined eco-environmental vulnerability for the MEE using freely available remote sensing (RS), topographic, and socio-economic data. The study found that the majority of the MEE (comprising savannas, grasslands, and most of the agricultural land in Ugandan MEE) was moderately vulnerable based on the analysis methods and variables used. The eco-environmental vulnerability index (EEVI) showed a marked increase in vulnerability with decrease in elevation. Eco-environmental vulnerability was strongly associated with multi-year variables based on precipitation, temperature, and population density. Moreover, precipitation distribution was changing especially in the wet season, thus adding another layer of risk for agriculture and ultimately for local community livelihoods.

Study 3 simulated possible future land use changes in the MEE based on existing RS LULC products and a well-known land use change model. The study projected that agriculture will possibly expand from approximately 58% in 2001 to more than 64% in 2033 if current and future LULC transformation follows rates in 2001-2017. These new croplands will occur mostly around edges of the protected forest and zones of transition between mixed vegetation and existing croplands. Due to the unpredictable LULC transitions in the MEE, simulating forest-to-cropland conversion was less accurate compared to mixed-to-cropland conversion.

This research provides a more complete explanation of the underlying complex human-environment interactions shaping the MEE landscape. This is the first study to comprehensively assess landscape dynamics at multiple scales (10-day, 16-day, monthly, seasonal, and household). It is also the first to define and assess at the annual scale, eco-environmental vulnerability as influenced by climate, topographic and socio-economic variables. In addition, by simulating future LULC change, this research provides the opportunity to quantify and anticipate possible LULC changes in the MEE. This research relies on publicly available RS and geospatial datasets and therefore analyses conducted here can easily be translated to other similar regions.

I dedicate this work to the two women who have inspired a big part of my life. To Salome, my mum, thank you! And to Susan, my loving wife, I love you too!

ACKNOWLEDGEMENTS

My academic journey has been successful due to the many awesome people I have met. First, I am very grateful to Dr. Nathan Moore, my advisor, mentor, and friend. I appreciate that you believed in me, listened to me, challenged me, and nurtured me into an all-rounded scholar and person. I always loved our weekly chats about life and research. Thank you! I am very grateful to Dr. Kyla Dahlin for introducing me to analysis of remotely sensed time series data in R, and for being there to 'troubleshoot' my codes whenever I needed. Thank you for working with me on my dissertation, and the great feedback you have given me. To Dr. Bandana Kar, thank you for agreeing to work with me on my dissertation and always being available to guide me and answer my questions. I am also thankful to Dr. Erin Bunting for welcoming me to RS&GIS and giving me the opportunity to work on the diverse range of funded projects. I enjoyed working with you, and I am always grateful. And thank you for working with me on my dissertation.

I would also like to thank faculty, staff and leadership in the Department of Geography, Environment, and Spatial Sciences at Michigan State University. To Dr. Ashton Shortridge, thank you for taking the chance with me and the great advice you offered me during GeoCamp and many other times we met. Thank you Dr. Lifeng Luo for introducing me to Python programming, and always having students' interests at heart. To Dr. Raechel Portelli, thank you for always sharing advice with me about life and graduate school. I am also grateful to Sharon Ruggles for having answers to my many questions about the graduate program and MSU. To Claudia Brown, thank you for 'having a second' to chat with me every time I stopped by. Thank you to Wilson Ndovie for introducing me to Magellan and other IT services, and to Ana O'Donnell for handling our AAG and AGU conference registrations.

I am grateful too to my master's program professors at University of North Alabama. Thank you, Dr. Francis Koti and Dr. David Brommer, for the assistantship in the Department of Geography – an assistantship that started it all. My sincere gratitude to Dr. Mario Mighty for his guidance in my

master's thesis and Dr. Sunhui (Sunny) Sim for teaching me about GIS, remote sensing, and spatial statistics every semester of my program!

I am thankful to the great colleagues and friends. Many thanks to Robert Goodwin, Nicholas Weil, and Joseph Welsh at RS&GIS for the great working relationship we had. I am also grateful that I got to know and share an office with Thomas Bilintoh. Thank you for the great friendship, buddy! To my friends Dr. Ida Djenontin, Gabriela Shirkey, Dr. Rajiv Paudel, Piero Sciusco, Dr. Leah Mungai, Dr. Judith Namanya, and Jonnell Sanciangco: thank you for making my graduate school experience great! Thank you to my long-time friend and brother, Donald Akanga, for always caring, checking in and sometimes saving me from myself. To my friends Dr. Pauline Wambua and Titus Omanga, I am grateful for hosting and feeding me all those times I came to East Lansing – thanks for the friendship! And finally, I thank Dr. George Lohay and Grace Malley, the great friends we have here in State College, PA! Special thanks to my friend Eliud Akanga for the valuable support in the fieldwork portion of this research.

I also want to express my gratitude to my family for providing the support I needed to succeed in graduate school. I am thankful to Susan, my dear wife, partner, friend, and the love of my life - for her sacrifices and patience throughout my time in graduate school. Thank you to my son who has been very cooperative during these past 4 years (especially the last 1 ½ during the lockdown and working from home!). I also recognize the many sacrifices made by Salome, my mum. Thank you for the love, unending support, great advice, and always wanting me to succeed. Much appreciation to my dad (Sammy) for believing in the power of education. To my sisters (Rose and Phoebe) and brothers (Sospeter and Jeremiah), thank you for cheering me on till the end. To my uncle, Jerry Waswa, I thank you for always having good intentions and for always being in my corner.

Special thanks to the scientific community on Stack Overflow who have, over the years, provided solutions to most of the issues that people like me have encountered while coding in R, Python, and Google Earth Engine. Thank you!

Finally, I would like to express my gratitude to the College of Social Science, Department of Geography, Environment, and Spatial Sciences, and Graduate School for supporting this research financially through the 2019 and 2020 Graduate Office Fellowship (GOF) and the 2020 Research Enhancement Award. I am also grateful to RS&GIS for funding the PhD studies within which this dissertation research was conducted.

TABLE OF CONTENTS

LIST OF TABLES

LIST OF FIGURES

LIST OF ABBREVIATIONS

CSOs	Civil society organizations
EEVI	Eco-environmental Vulnerability Index
EVI	Enhanced Vegetation Index
GEE	Google Earth Engine
GIS	Geographic Information Systems
LCM	Land Change Modeler
LCS	Land Change Science
LUC	Land Use Change
LULC	Land Use and Land Cover
MEE	Mount Elgon Ecosystem
MODIS	Moderate Resolution Imaging Spectroradiometer
NDVI	Normalized Difference Vegetation Index
PAs	Protected areas
PE	Political Ecology
RS	Remote Sensing
SI	Sustainable Intensification

CHAPTER 1. INTRODUCTION

1.1 Research Context

The synergistic effects of rapid population increase, climate change and variability, economic development, and human activities have resulted in undesirable effects on the environment. Global environmental temperatures have increased, since the 20th century, causing significant changes in the global climate (Guo et al. 2019). As a result, precipitation has become more variable (Nguyen et al. 2018), animal and plant species loss has intensified, and frequencies and magnitudes of environmental hazards have increased (Guo et al. 2019). Further, in many parts of the world, populations and natural resource extraction have increased substantially, and the self-purification and restorative ability of ecosystems have declined, thus rendering both human and natural systems more fragile (Zhong-Wu et al. 2006; Nandy et al. 2015; Guo et al. 2019). As such, during these climate change times, the world faces an unprecedented double challenge: "to eradicate hunger and poverty and to stabilize the global climate before it is too late" (FAO 2016). The big task, therefore, is to increase food production while fostering sustainability of Earth's environmental systems (Atzberger 2013).

Climate change and variability threatens food security globally (Nelson et al. 2009; FAO 2016), but developing nations are more at risk due to poverty, their overdependence on local natural resources, inadequate capacity to adapt to change (Bryan et al. 2013; Kabubo-Mariara & Kabara 2015), low technological advancement (Mwendwa & Giliba 2012), and environmental stress (Norrington-Davies & Thornton 2011). These nations have large rural populations dependent on rainfed agriculture, extensive areas of low agricultural productivity, widespread poverty and high climatic risks (Vermeulen et al. 2012). These underlying characteristics are significant drivers of food insecurity in these nations. As populations increase, the need for more food also increases and this leads to the increased conversion of forests and natural vegetation to agriculture, pasture, and settlement (Government of Kenya 2009; Maitima et al. 2009). As a result, the proportion of agricultural land continues to increase while forests and other natural

vegetation shrink (Figure 1.1) – thus threatening important environmental processes. Besides, fluctuations in seasonal rainfall patterns and varying temperatures influence and sometimes diminish the suitability of land to produce certain crops – thus negatively influencing agricultural sustainability. For developing nations heavily reliant on rainfed agriculture, therefore, seeking to conserve natural resources while utilizing the resources to improve local livelihoods is a necessary but difficult undertaking.

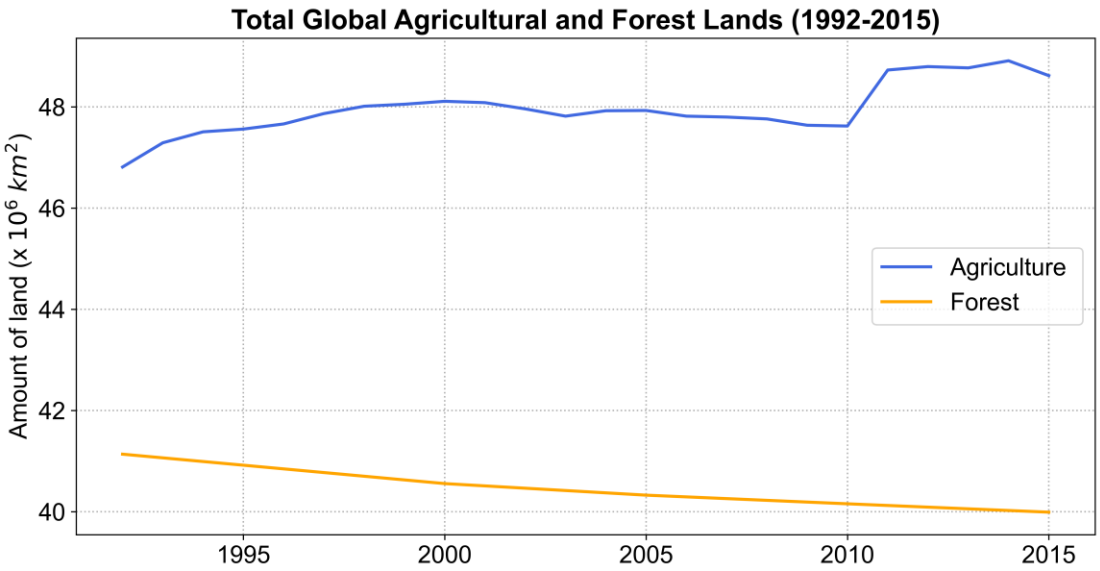

Figure 1.1. *Total global agricultural and forest land between 1992 and 2015.* The data used here was obtained from World Bank (accessed on April 17, 2019).

East Africa depends heavily on rainfed agriculture which puts food security and rural livelihoods at risk (Guzha et al. 2018). Land holdings in this region are small and steadily declining over time (Maitima et al. 2009; Guzha et al. 2018). At the same time, populations have been fast increasing thus necessitating more food production while also navigating the effects of climate change in the area. Over recent decades, therefore, East Africa has witnessed significant landscape transformation due to both human and natural drivers (Vrieling et al. 2013; Landmann & Dubovyk 2014). Generally, natural vegetation has been converted to farmlands, grazing lands and human settlements (Maitima et al. 2009). This land use and land cover (LULC) transformation has, in part, fueled climate change and variability (e.g., warming temperatures and increasingly

variable precipitation (Ongoma & Chen 2017)) which have in turn diminished nature's ability to support climate-dependent livelihoods (e.g., rainfed agriculture). Finding a common ground in which we can simultaneously conserve the natural environment and improve nature-dependent livelihoods is a matter of serious urgency in this region.

The Mount Elgon Ecosystem (MEE) is a major water catchment tower supplying water to three major lakes in East Africa (Lake Turkana [Kenya], Lake Kyoga [Uganda] and Lake Victoria [Kenya, Uganda and Tanzania] (Petursson et al. 2013)). The MEE is dominated by croplands in most locations, mixed vegetation (primarily savanna, grasslands, and shrubs) in the northern portion, and the Afromontane forest. The high population growth and densities in the area have translated into need for more land for agriculture (Mugagga et al. 2012). Coupled with political interference and corruption among park and reserve staff, this need for more land has resulted in forest encroachment and deforestation especially on fertile areas found at high elevations (Muhweezi et al. 2007; Bamutaze et al. 2010; Mugagga et al. 2012; Nakakaawa et al. 2015; EAC et al. 2016). The changes in LULC have, in part, altered the functioning of the ecosystem (Muhweezi et al. 2007) and as a result, the mountain area has experienced more frequent landslides, prolonged droughts, flooding, and diminishing soil productivity (Nakakaawa et al. 2015; EAC et al. 2016). Evidence of a changing climate has been reported (Myhren 2007) and this may be associated with the increased frequency of these events. As such, the livelihoods of at least 2 million people (Petursson et al. 2013; Nakakaawa et al. 2015) are threatened. Yet, few studies have focused on the MEE socio-ecological system and therefore little is known about processes and human-environment interactions that shape the landscape.

1.2 The Kite Framework

Environmental benefits and impacts traverse scales – goods and services are provided at the local (e.g. food and water), regional (e.g. water catchment enhancement and natural hazard mitigation) and global (e.g. climate change mitigation and global biodiversity conservation) (Vedeld et al. 2016). Due to the multiscalar nature of conservation and livelihood improvement

efforts and the complex interactions within socio-ecosystems, insights from political ecology (PE) are invaluable in unearthing any hidden dynamics and finding ways for effective intervention. This dissertation is set within the 'Kite' framework (Campbell & Olson 1991), a PE framework that emphasizes the interactions between social processes and the physical environment across space and time. The framework is built on "perspectives that view society as an intervening variable between nature and resources" (p.13).

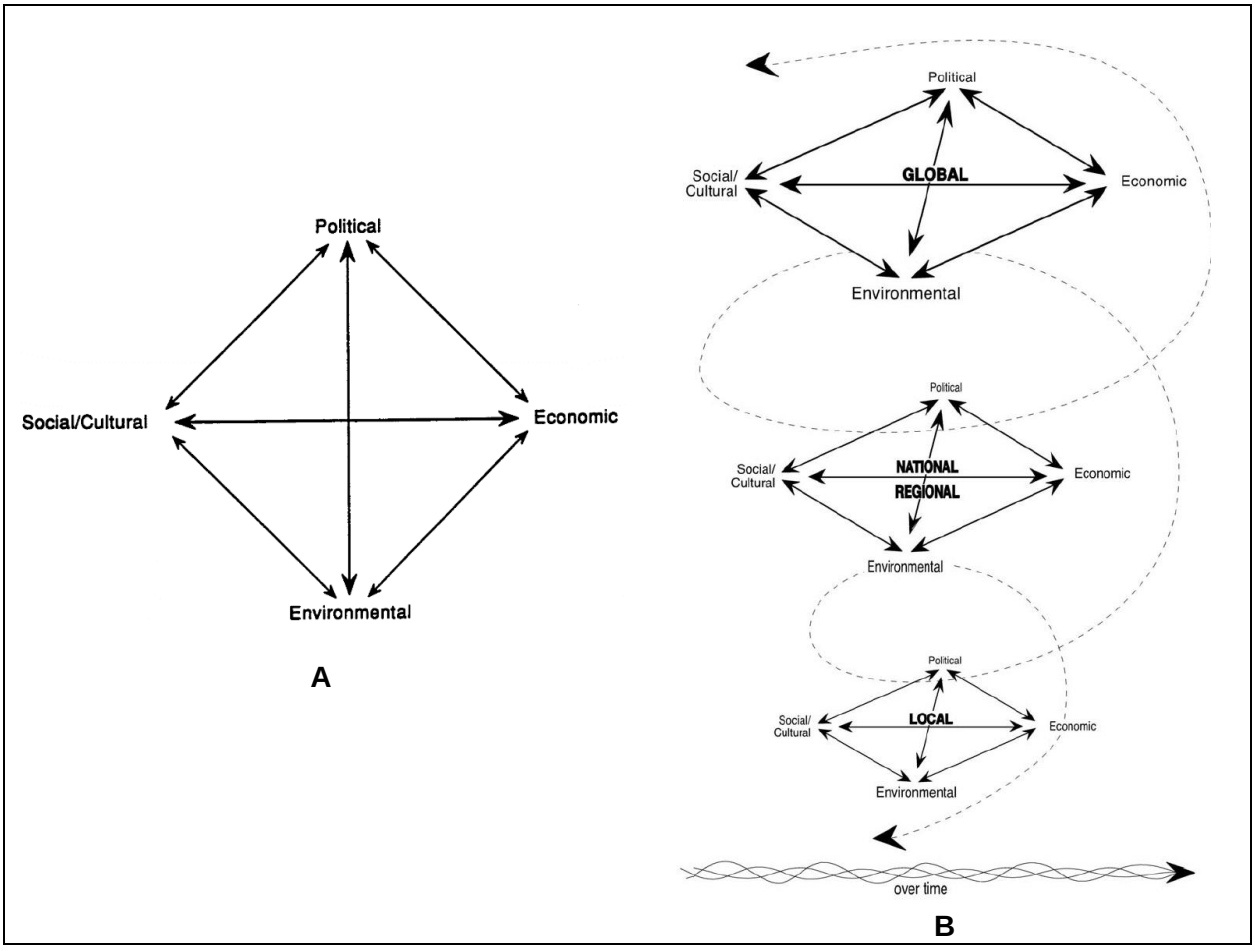

Figure 1.2. *The Kite framework showing (A) the four points (categorical variables) and (B) the various scales of interaction across time and space.* Note that time becomes complicated and thus several time scales are considered and woven together to form a 'braid of time' (Campbell & Olson 1991).

The framework has four categorical variables (political, economic, environmental, and social/cultural) of the human-environment interactions (Figure 1.3). To understand the coupled nature of human-environment systems, (Campbell & Olson 1991) propose that the above

conceptualization should be complemented by a structure that stresses the interactions among the categorical variables. These interactions have four characteristics: (i.) they occur at different scales; (ii.) they are shaped by time; (iii.) they are also shaped by space; and (iv.) their outcome is determined through the existing power structures.

1.3 Existing Challenges

1.3.1 Landscape Change Related to Human Activities and Natural Processes

A few studies about landscape change have been conducted in the MEE, most of which relied on supervised classification and change detection techniques. In their study, Petursson et al. (2013) analyzed processes that led to deforestation within protected areas (PAs) in the transboundary MEE. This study found that it was challenging to correctly quantify LULC change, especially on the Kenyan side, due to the overlap between bamboo, plantation and Shamba system farms. Shamba system refers to a Kenyan government effort meant to convert native to plantation forests (originally) and to replant trees on harvested forest land (later) by allowing local communities to farm in protected areas while tending to the growing trees in their early stages of growth (Petursson et al. 2013). Other studies were conducted on relatively smaller spatial scales, mostly on the Ugandan side. Such studies have focused on the effect of LULC change on landslide occurrence (Mugagga et al. 2012), soil organic carbon, food security and climate change vulnerability (Barasa & Kakembo 2013), carbon stocks and climate variability (Mugagga et al. 2015), among others. However, some of the studies have reported contradictory results especially about the nature and magnitude of LULC change within the agricultural land-use class. This may be due to the complex LULC orientation which causes the MEE to exhibit persistent and sometimes sudden landscape changes, thus complicating efforts to correctly characterize vegetation dynamics especially using traditional classification and change detection methods. More robust methods are therefore needed to comprehensively examine spatio-temporal landscape changes particularly for this constantly variable landscape.

Due to recent developments in Earth observation (EO) technologies, spatio-temporally contiguous remote sensing (RS) data have been collected and preprocessed. The increasing availability of ready-to-use data has made it possible to investigate landscape change more accurately and comprehensively in terms of other environmental processes, at multiple scales. For instance, there has been an uptick in the number of studies using vegetation indices (e.g., normalized difference vegetation index [NDVI], and enhanced vegetation index [EVI]) and modeled precipitation time series data (e.g., Climate Hazards group Infrared Precipitation with Stations [CHIRPS]) to characterize landscape change at finer scales. Analyses like these can circumvent issues reported in bitemporal image classification and change detection studies and have made it possible to disentangle nature- vs human-driven LULC change. Such analyses are lacking in the MEE, yet the complex human-environment interactions in the area are threatening major ecosystem processes and therefore rendering the MEE more vulnerable to the effects of climate change and further environmental change.

1.3.2 Environmental Vulnerability Related to Social and Natural Factors

The concept of vulnerability cross-cuts multiple disciplines (O'Brien et al. 2004) and is therefore viewed differently depending on context (Rama Rao et al. 2016) – making it challenging to measure. Vulnerability assessment is routine to many fields, which include livelihood vulnerability to hazards (Huong et al. (2019); Simane et al. (2016)), vulnerability to natural hazards (Han et al. (2019); Xiong et al. (2019)), vulnerability to climate change (Rama Rao et al. (2016); Torresan et al. (2012)), agricultural vulnerability (e.g. Aleksandrova et al. (2016); Baca et al. (2014); Parker et al. (2019)), groundwater (Duarte et al. 2015; Aydi 2018), and ecological and environmental (eco-environmental) vulnerability (Sahoo et al. 2016; He et al. 2018; Zhao et al. 2018; Wei et al. 2020). Eco-environmental vulnerability is closely associated with risk of damage to the natural environment (Nandy et al. 2015). As such, eco-environmental vulnerability assessment (EEVA) has been conducted to comprehensively evaluate natural resource systems

that are impacted by both natural and anthropogenic activities (Fan et al. 2009). EEVA reveals pertinent information about environmental quality, thus it is a critical step towards better formulations of environmental protection frameworks (Sahoo et al. 2016). This can aid attainment of ecological sustainability and restoration and ensure better environmental and resource management (Nguyen et al. 2016).

Previous studies related to EEVA in the MEE have mostly focused on landslide vulnerability in the Ugandan MEE. The Ugandan MEE is particularly vulnerable to landslide hazards which have become more frequent over time (Mumba et al. 2016). Broeckx et al. (2019) recently assessed landslide susceptibility and mobility rates for the area using a combination of logistic regression and Monte Carlo simulations. The study concluded that topography significantly affects landslide susceptibility. They attributed the larger landslide mobilization rates correlating highly with higher landslide susceptibilities to higher landslide quantity rather than magnitude. Ratemo & Bamutaze (2017) integrated qualitative data with GIS to analyze risk elements and household vulnerability to landslides within Manafwa District in Uganda. This study found that 95% of the community was vulnerable to landslide hazards and that vulnerability was especially high in agricultural areas. In another study, landslide susceptibility was analyzed in terms of historical land use changes in eastern Uganda (Mugagga et al. 2012). The study reported that the encroachment onto critical slopes of the ecosystem resulted in a series of landslides in the area. Thus far, only one EEVA-related study has been conducted on the Kenyan side of the MEE. Mwangi & Mutua (2015) assessed climate change vulnerability for Kenya in terms of its exposure, sensitivity, and adaptive capacity characteristics. This study found that the Kenyan MEE was either moderately or highly vulnerable. The MEE landscape exhibits significant variability thus motivating a more comprehensive spatio-temporal assessment of the complex interrelationships in the area. While EEVA is not new, such a systematic study has not been conducted in the MEE and therefore little is known about the general eco-environmental vulnerability, its spatial-temporal evolution, and variables contributing to the vulnerability. In

addition, land use change (LUC) models can provide important information about possible future LULC change trajectories. Such information is essential in policy- and decision-making aimed to simultaneously conserve the environment and improve nature-dependent livelihoods, reduce eco-environmental vulnerability, and ultimately ensure sustainability of the socio-ecological system.

1.3.3 Possible Future Landscape Changes in the MEE

LUC modeling refers to the simulation of a socio-ecological system over space and time in a manner that relates to measured LULC change (Paegelow et al. 2013; Gibson et al. 2018). LUC models serve two purposes: to identify factors or proxies that explain LULC change and to predict possible future scenarios of LULC based on the factors (Overmars et al. 2003; Eastman & He 2020). Change analysis in these models is performed using historical LULC data to assess past LULC changes and transitions (Halmy et al. 2015). The transitions are then integrated with environmental variables to estimate future LULC changes (Pijanowski et al. 2002; Halmy et al. 2015). Several LUC models have been developed including Cellular Automata (CA) (Vaz et al. 2012), CA-Markov (Halmy et al. 2015; Huang et al. 2015; Lu et al. 2019; Aburas et al. 2021), logistic regression (Das et al. 2019) and model combinations (Shafizadeh-Moghadam et al. 2017; Gharaibeh et al. 2020). Example applications of LUC modeling are an assessment of the impact of future grassland cover change on catchment water and carbon fluxes in South Africa (Gibson et al. 2018), monitoring and predicting landscape dynamics within Iran's Meighan Wetland and surrounding areas (Ansari & Golabi 2019), predicting growth and changes in urban areas (Shafizadeh Moghadam & Helbich 2013; Aburas et al. 2021), and assessing deforestation in Thailand (Waiyasusri & Wetchayont 2020), among others. LUC models provide information beyond traditional LULC change analyses, and therefore allow for future landscape changes to be anticipated and quantified.

Two LUC modeling studies exist for the Ugandan MEE and none for the Kenyan side. The study by Mwanjalolo et al. (2018) found that subsistence agricultural land and protected

grasslands in Uganda experienced highest gains and that LULC patchiness was associated with the increasingly high demand for agriculture and settlement land. The expansion of agricultural land was also estimated to continue in 2040. J. Li et al. (2016) used an agent-based model (ABM) to analyze historical LULC change (1996-2013) and later simulated possible changes in agricultural land in Uganda under business-as-usual and deforestation scenarios. The study reported that agricultural land increased from 8.98 million ha in 1996 (37%) to 10.31 million ha in 2013 (43%). Agriculture was projected to increase further in 2025 to 12.10 m ha (50%) and 12.39 m ha (51%) in the business-as-usual and deforestation scenarios, respectively. The two studies were conducted at the national scale, meaning that localized environmental relationships and patterns were not emphasized. There is therefore need for an ecosystem-wide simulation of LULC change which will inform positive environmental conservation and livelihood improvement actions within the MEE.

1.4 Approaches and Solutions

This dissertation addresses the above challenges as follows.

1.4.1 Purpose and Objectives

This dissertation examines human-environment interactions and landscape change under climate change. The focus is on how nature- and human-related factors and practices interact to influence landscape dynamics, drive eco-environmental vulnerability, and eventually threaten nature-dependent livelihoods in the MEE. Chapters 2, 3 and 4 are interrelated studies addressing the following research questions:

1. What is the nature and magnitude of change in MEE greenness for the period 2001–2018 and how is this change related to long-term trends and variability in MEE precipitation? (*Chapter 2, Study 1*)
2. How is eco-environmental vulnerability distributed across the MEE, and what are the major factors driving these patterns? (*Chapter 3, Study 2)*

3. How will the MEE landscape change in the future, and what opportunities exist for streamlining livelihood improvement and environmental conservation efforts? (*Chapter 4, Study 3)*

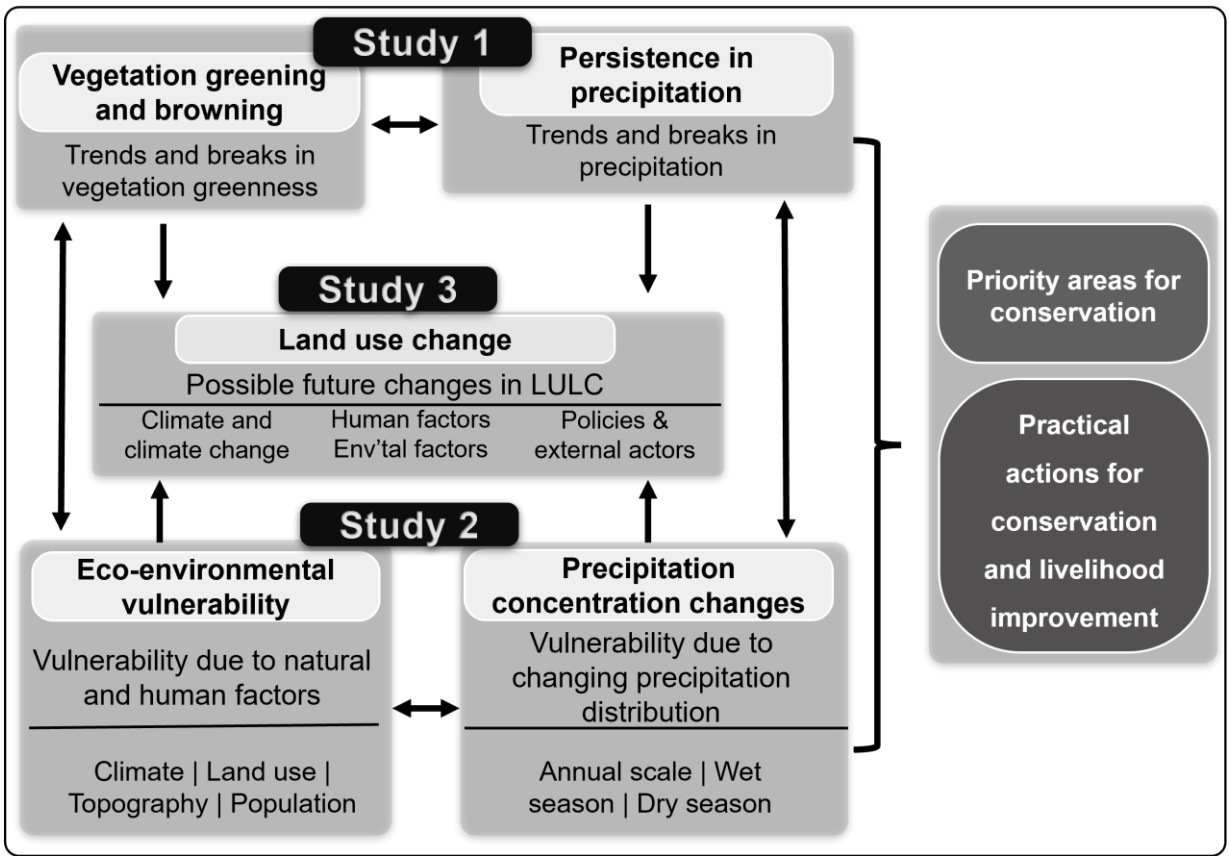

Figure 1.3. *Conceptual framework used in this study.*

In this study, the MEE was considered an integrated system, and connections between natural factors and human activities were studied to shine light on the complex human-environment dynamics and identify avenues for improving both livelihoods and nature. Analyses in this study were performed across multiple scales (10-day, 16-day, monthly, seasonal, annual, and farm-scale) – to comprehensively characterize processes in the highly variable MEE. This research is therefore a type of land change science (LCS) study embedded within a PE framework. While LCS aims to understand the changing human-environment interrelationships and the nature, magnitude and location of resultant LULC (Rindfuss et al. 2004), PE emphasizes that the interrelationships are dynamic across space and time (Campbell & Olson 1991). By using

the ‘Kite’ framework, the study reveals major factors influencing landscape change as well as their scale of influence in the highly dynamic MEE. Figure 1.2 shows the conceptual framework used in this study.

1.4.2 Study 1: Landscape Change Related to Human and Natural Processes

Study 1 characterized comprehensively, over multiple time scales, recent patterns and trends in MEE vegetation greening and browning. The study first assessed and quantified the nature and magnitude of change in greenness for the period 2001–2018. To disentangle nature- versus human-driven vegetation greening and browning, the study similarly characterized trends and variability in MEE precipitation for the period 1986-2018. It was argued here that (1) changes in climate have forced local communities in the MEE to expand croplands at the expense of the natural vegetation thus leading to deforestation and degradation; and (2) the high variability exhibited in the MEE landscape requires integration of both general and sequential time series analysis methods to be fully characterized.

This study combined trend (Mann-Kendall and Sen’s slope) and breakpoint (bfast) analysis methods to comprehensively examine recent vegetation greening and browning in Mount Elgon at multiple time scales. The study used both 16-day NDVI composites from Moderate Resolution Imaging Spectroradiometer (MODIS) and 5-day CHIRPS precipitation data and attempted to disentangle nature- versus human-driven vegetation greening and browning. Inferences from a 2019 field study were valuable in explaining some of the observed patterns. Results from this study are multi-scale maps showing areas of persistent changes in greenness (deforestation, reforestation, or vegetation degradation) associated with human activities and/or natural processes.

1.4.3 Study 2: Environmental Vulnerability Related to Social and Natural Factors

The second study examined eco-environmental vulnerability in the MEE using freely available RS, topographic and socio-economic data. This study sought to quantitatively examine spatio-temporal patterns and trends in eco-environmental vulnerability, and factors driving the high variability observed in the MEE landscape. This study hypothesized that being mountainous, environmental vulnerability in the MEE varied significantly over distances as short as 5-10 km and was influenced greatly by multiple factors.

Eco-environmental vulnerability of the MEE was assessed using a novel combination of natural, environmental, and socio-economic data. With use of spatial principal components analysis (SPCA) within GIS, this study effectively integrated variables computed from RS data (NDVI), digital elevation models (DEM), climate (precipitation and temperature), and socio-economic data (population density) to compute an eco-environmental vulnerability index (EEVI) for the MEE. The final EEVI was categorized into five qualitative classes indicative of potential, slight, light, moderate, and severe vulnerability. Temporal principal component analysis (TPCA) was also conducted to identify persistent changes in multi-year variables for the period 2001-2018. Additionally, spatio-temporal changes in precipitation concentration in the MEE were assessed using the precipitation concentration index (PCI) – to provide insights into the significant contribution of precipitation to overall vulnerability of the MEE. Outputs from this study include maps showing levels of eco-environmental vulnerability for each year in 2001-2016, and significant changes in multi-year variables (precipitation, temperature, and population density). Ultimately, this study identified areas in the MEE where urgent action and the limited resources can be targeted.

1.4.4 Study 3: Possible Future Landscape Changes in the MEE

The goal of this study was to simulate possible future land use changes in the MEE based on existing RS LULC products and TerrSet's Land Change Modeler (LCM) (Eastman 2016a;

Eastman 2016b). Here, the main objectives were (1) to forecast possible future LULC changes for the MEE using LCM; and (2) to assess the accuracy of the simulated LULC surfaces in relation to observed persistent changes in the MEE. It is argued that accelerated climate change and significant vegetation-to-cropland conversion have led to an unsystematic and rapidly changing landscape making it difficult to accurately characterize future LULC trajectories using historical change transitions.

This study first combined data from GlobeLand30 and Regional Centre for Mapping of Resources for Development (RCMRD) to generate improved LULC data for 2001, 2009, and 2017. The study then examined spatial and temporal distribution of LULC change and identified areas of major LULC changes in the periods 2001-2009 and 2001-2017. Projections to 2025 and 2033 were developed to estimate how LULC will potentially change over time. Accuracy of the simulations (for 2017) was assessed first against the 2009 and 2017 LULC maps (to generate a map of hits, false alarms and misses), and then against greening and browning surfaces over the growing season for 2001-2018. Such a comprehensive analysis of future LULC changes can support decision- and policy-making efforts towards a conserved environment and improved local livelihoods. Figure 1.2 below shows the conceptual framework used in this study.

1.4.5 Important Insights from the Field Study in the MEE

RS technologies and geospatial analyses provide important opportunities for characterizing historical, present, and predicting future landscape change. However, geospatial analyses cannot tell the whole story, especially when dealing with highly dynamic landscapes. Insights from field studies have proven important as indigenous and historical accounts of LULC change in such a constantly variable landscape can be used to fill in gaps that may not be fully explained using RS and GIS alone. In this study, human-environment interactions in the MEE were characterized based in part on insights from a field study conducted in the MEE.

CHAPTER 2. PERSISTENT VEGETATION GREENING AND BROWNING TRENDS RELATED TO NATURAL AND HUMAN ACTIVITIES IN THE MOUNT ELGON ECOSYSTEM[1]

2.1 Introduction

Vegetation plays very important roles in ecosystem processes, including the mitigation of climate change effects (Gemitzi et al. 2019) and the regulation of land surface temperatures, carbon and energy cycles (Alavipanah et al. 2015; Ballantyne et al. 2017; Forzieri et al. 2018). At the same time, significant changes in terrestrial vegetation have been reported in the recent past (Landmann & Dubovyk 2014; Pan et al. 2018). Previous studies have concluded that these changes are driven by (1) slowly-changing natural processes, such as regional climate change (e.g., changes in temperature, precipitation, etc.), nitrogen disposition and increasing atmospheric CO_2 concentrations (Zhu et al. 2016), and (2) more rapid anthropogenic activities, including land-use and land-cover (LULC) change (e.g., deforestation (Olsson et al. 2005; Le Quéré et al. 2009), overcultivation and overgrazing (Olsson et al. 2005), afforestation, expanding green areas in cities (Gemitzi et al. 2019) among others). These processes do not operate in isolation (Zhu et al. 2016) but rather interact at multiple scales, with global-scale drivers interacting with processes at the regional and local scales (Mishra & Mainali 2017), thus making vegetation change dynamics a complex phenomenon to examine. Understanding vegetation dynamics has attracted substantial attention in the past years, specifically in the wake of climate change and variability (Fensholt et al. 2012). As such, knowledge of vegetation response to climate change is critically important in the effort to maintain the supported processes as well as the human livelihoods derived from them (Murthy & Bagchi 2018). Such an analysis has been difficult in the past, due in part to limited access to consistent data both in space and time. However, with recent developments in Earth observation (EO) technologies, spatio-temporally contiguous remote sensing (RS) data have

[1] This is an accepted manuscript of an article published by MDPI in *Remote Sensing* on 1 July 2020, available online at https://doi.org/10.3390/rs12132113. Reference: Wanyama D, Moore NJ, Dahlin KM. 2020. Persistent vegetation greening and browning trends related to natural and human activities in the mount Elgon ecosystem. Remote Sens. 12(13).

been collected, making it possible to investigate vegetation dynamics accurately and comprehensively in terms of other environmental processes, at multiple scales.

The Normalized Difference Vegetation Index (NDVI), which is the normalized sum of the difference in reflectance between near infrared and red bands, has extensively been used (Chamaille-Jammes et al. 2006; Mishra & Mainali 2017; Pan et al. 2018) as an indicator of photosynthetic activity and vegetation amount (Tucker 1979). Previous studies used this vegetation index (VI) to characterize vegetation processes such as productivity decline (Landmann & Dubovyk 2014), phenology (Verbesselt, Hyndman, Zeileis, et al. 2010; Vrieling et al. 2011) and greening and browning (Mishra & Mainali 2017; Guan et al. 2018; Murthy & Bagchi 2018; Pan et al. 2018; Emmett et al. 2019; Gemitzi et al. 2019). Variability in NDVI generally follows patterns of climatic conditions, mainly precipitation (Malo & Nicholson 1990; Davenport & Nicholson 1993; Schmidt & Gitelson 2000; Fabricante et al. 2009; Fensholt et al. 2012). The NDVI–precipitation relationship is largely a strong positive one, particularly in locations where total annual precipitation is less than 1000 millimeters (Malo & Nicholson 1990; Davenport & Nicholson 1993). This relationship is further compounded in space and time by site-specific factors such as existing LULC, vegetation structure and composition (Davenport & Nicholson 1993), topography (Mishra & Mainali 2017) and soil type (Farrar et al. 1994). As a result, vegetation greenness response to climate has shown significant spatial and temporal variability. For instance, contrasting natures and strengths of the NDVI–precipitation relationship have been reported: a strong linear relationship in the Sahel (Malo & Nicholson 1990) and a log-linear one in East Africa (Davenport & Nicholson 1993). In other studies, seasonal precipitation with different lag times was found to correlate strongly with NDVI (Davenport & Nicholson 1993; Chamaille-Jammes et al. 2006). This complexity implies that (i) results from a specific regional analysis are not transferable to another region; (ii) any slight spatial and/or temporal misspecification may lead to misleading results about vegetation greenness–precipitation relationships and patterns; and (iii)

understanding vegetation change requires multiple images (time series, TS) as opposed to the extensively used traditional classification and change detection methods.

East Africa depends heavily on rainfed agriculture, which puts food security and rural livelihoods at risk (Guzha et al. 2018). The importance of land in this region cannot be overemphasized (Guzha et al. 2018), yet land holdings are small and steadily declining (Maitima et al. 2009; Guzha et al. 2018). At the same time, populations have been increasing thus necessitating expansion of food production while also navigating the effects of climate change in the area. Over recent decades, therefore, East Africa has witnessed significant landscape transformation due to both human and natural drivers (Vrieling et al. 2013; Landmann & Dubovyk 2014). Generally, natural vegetation has been converted to farmlands, grazing lands and human settlements (Maitima et al. 2009). This LULC transformation has been reported in the Mount Elgon ecosystem (MEE), a major water catchment tower supplying water to three major lakes in East Africa (Lake Turkana, Kenya, Lake Kyoga, Uganda and Lake Victoria, Kenya, Uganda and Tanzania (Petursson et al. 2013)). The MEE is dominated by croplands in most locations, mixed vegetation (primarily savanna, grasslands, and shrubs) in the northern portion and the Afromontane forest (Figure 2.1). The high population growth and densities in the area have translated into need for more land (Mugagga et al. 2012). Coupled with political interference and corruption among park and reserve staff, the need for more land has resulted in forest encroachment and deforestation as ecologically fragile land is cleared for agriculture and settlement (Muhweezi et al. 2007; Bamutaze et al. 2010; Mugagga et al. 2012; Nakakaawa et al. 2015; EAC et al. 2016). The changes in LULC have, in part, altered the functioning of the ecosystem (Muhweezi et al. 2007) and, as a result, the mountain area has experienced more frequent landslides, prolonged droughts, and flooding (Nakakaawa et al. 2015; EAC et al. 2016).

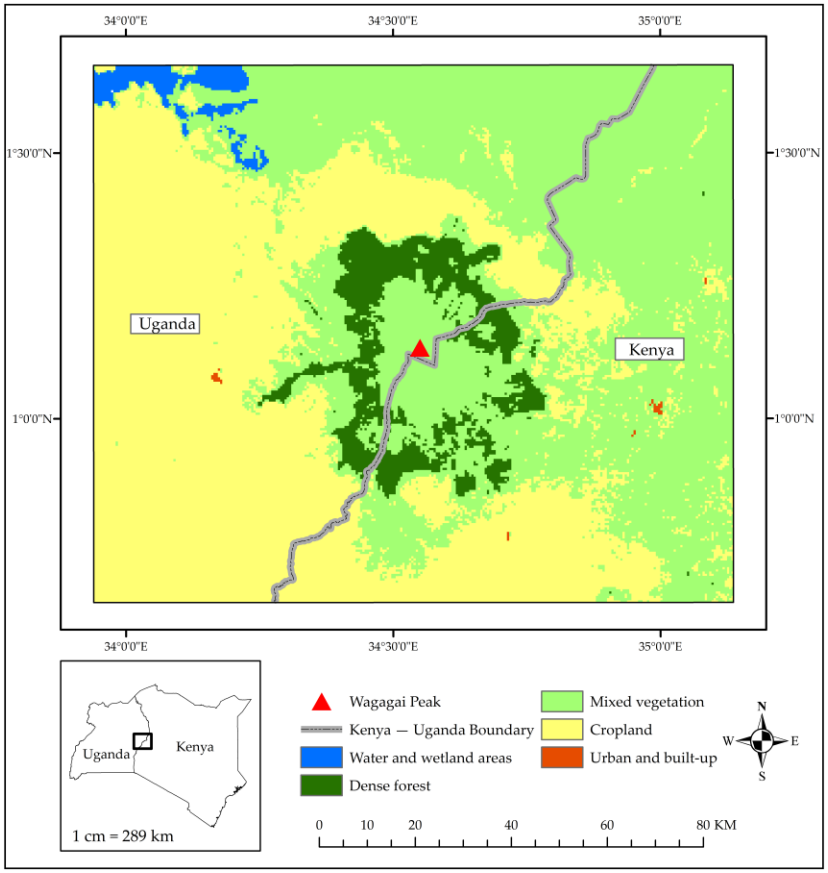

Figure 2.1. *Mount Elgon ecosystem (MEE) land-use and land-cover (LULC) in 2018.* This map was created by reclassifying Moderate Resolution Imaging Spectroradiometer (MODIS) land-cover data (MCD12Q1) created by the University of Maryland (Sulla-Menashe & Friedl 2018). Mixed vegetation includes savanna, grasslands, and shrubs. Cropland includes cropland and the cropland-vegetation mosaic classes. The black-gray line represents the boundary between Kenya and Uganda and the red triangle is Wagagai Peak, the highest point on Mount Elgon (4321 m above sea level).

Evidence of a changing climate has been reported (Myhren 2007) and this may result in increased frequency of these events. As such, the livelihoods of at least 2 million people (Petursson et al. 2013; Nakakaawa et al. 2015) are threatened. Despite this, the complex MEE landscape is currently understudied. A key study of LULC change was conducted by Petersson, Vedeld, and Sassen (Petursson et al. 2013) and employed institutional theory in analyzing processes that led to deforestation within protected areas (PAs) in the transboundary MEE. It was found that, especially on the Kenyan side, it was challenging to correctly quantify LULC change due to the overlap between bamboo, plantation and Shamba system farms. Other studies have been

conducted on relatively smaller spatial scales, mostly on the Ugandan side. Such studies have focused on the effect of LULC change on landslide occurrence (Mugagga et al. 2012), soil organic carbon, food security and climate change vulnerability (Barasa & Kakembo 2013), carbon stocks and climate variability (Mugagga et al. 2015) among others. However, some of the studies have reported contradictory results especially about the magnitude of LULC change within the agricultural land-use class. This may be due to the complex LULC orientation, which leads to persistent greening and browning in the MEE, thus making it difficult to correctly characterize vegetation dynamics especially using traditional classification and change detection methods. More robust methods are therefore needed, and TS analysis has been applied to comprehensively examine spatio-temporal landscape changes, particularly for constantly variable landscapes like the MEE.

TS analysis of RS data has been used to characterize environmental phenomena by describing both trends and discrete change events (Gómez et al. 2016). In recent years, application of TS methods has increased and this has been driven by improved access to RS imagery (for instance, due to opening up of the Landsat archive in 2008 (Woodcock et al. 2008)), improvements in the integration of RS and GIS (Geographic Information Systems) and general advancements in computing power (Badjana et al. 2015). As such, analysis of LULC change, including vegetation greening and browning, has significantly evolved from the traditional bitemporal image analysis to using multiple and continuous observations. Common methods for TS analysis include Fourier analysis (Bradley et al. 2007; Hermance et al. 2007), principal components analysis, (Crist E.P. & Cicone R.C. 1984; Anyamba & Eastman 1996) and the Mann-Kendall statistic (Mann 1945). The Mann-Kendall statistic has been used to identify the presence and nature of monotonic trends in vegetation time series (Mishra & Mainali 2017; Lamchin et al. 2018; Pan et al. 2018). It is a non-parametric statistic; thus, data does not have to conform to any specific distribution (Khambhammettu 2005). Besides, Mann-Kendall compares relative

magnitudes of sample data instead of raw data values and therefore missing values are allowed in the analysis. The Mann-Kendall analysis is often followed by the Sen's slope estimator (Sen 1968), which quantifies the strength of the monotonic trends (Lamchin et al. 2018; Murthy & Bagchi 2018). The Sen's slope estimator calculates the median of the set of slopes generated from Mann-Kendall (Sen 1968). Mann-Kendall and Sen's slope have been found to be more robust for TS with outlying values as compared to parametric statistics like ordinary least squares (Murthy & Bagchi 2018). These two statistics identify and quantify any overall trends in a time series and are therefore well suited for examining vegetation greening and browning. Previous studies have successfully used these methods in assessing the consistency of greening and browning patterns across spatio-temporal scales in northern India (Murthy & Bagchi 2018) and assessing variability in greening and browning patterns caused by use of different RS imagery in the boreal forest of central Canada (Alcaraz-Segura et al. 2010). However, the assumption that the vegetation trend preserves its change rate throughout the period of study means that some greening and browning changes are masked (Pan et al. 2018). For instance, later greening in a consistently browning vegetation may not be detected using Mann-Kendall and Sen's slope. To counter this issue, more TS decomposition methods have been proposed, including *Breaks for Additive Season and Trend*, bfast (Verbesselt, Hyndman, Zeileis, et al. 2010). Using bfast, even subtle changes in vegetation can be monitored. This algorithm has successfully been used in delineating anthropogenic, fire and elephant damage within forest ecosystems in Kenya (Morrison et al. 2018). Complementing Mann-Kendall and Sen's slope with bfast can therefore be valuable in examining vegetation greening and browning trends, especially in a dynamic environment like the MEE. In such an analysis, the latter can be used to characterize changes detected by the former. Vegetation trends can then be characterized in more detail and this can be the basis for understanding effects of climate on terrestrial ecosystems (Pan et al. 2018) and the development of ultimate strategies for the sustainable management of ecosystems (Mishra & Mainali 2017).

The goal of this study was to characterize comprehensively, over multiple time scales, recent patterns and trends in MEE vegetation greening and browning. Here, the main objectives were; (1) to assess and quantify the nature and magnitude of change in MEE greenness for the period 2001–2018; and (2) to characterize trends and variability in MEE precipitation as a way to disentangle nature- versus human-driven vegetation greening and browning. It is hypothesized that (1) changes in climate have forced local communities in the MEE to expand croplands at the expense of the natural vegetation thus leading to deforestation and degradation; and (2) the high variability exhibited in the MEE landscape requires integration of both general (such as Mann-Kendall and Sen's slope) and sequential (such as bfast) TS analysis methods to be fully characterized. To achieve these goals, the study analyzed spatio-temporal trends and patterns in Moderate Resolution Imaging Spectroradiometer (MODIS) NDVI (2001–2018) and Climate Hazards group Infrared Precipitation with Stations (CHIRPS) precipitation (1986–2018) at multiple temporal scales (dekadal (10-day), 16-day, seasonal), using an integration of Mann–Kendall, Sen's slope and bfast algorithms. The study also incorporates inferences from a field study conducted in the MEE in 2019 to explain some of the vegetation change dynamics in the area. This analysis thus produces a more comprehensive characterization of vegetation dynamics in the MEE, which would not be possible using traditional classification and change detection methods. Results would help fill in some of the existing gaps in literature about nature and magnitude of LULC change and the stability of LULC in the MEE. Such a comprehensive description of MEE vegetation dynamics is an important first step to initiate dialogue aimed to instigate policy changes for simultaneously conserving the environment and improving livelihoods dependent on it.

2.2 Study Area Description

The MEE is located in western Kenya and eastern Uganda (Figures 2.1 and 2.2). The studied area covers approximately 15,000 km^2 and extends from 1°37'42.82" N, 33°55'45.07" E and 0°42'15.76" N, 35°14'18.84" E. Mount Elgon is a solitary volcano and is among the oldest in

East Africa (Bamutaze et al. 2010; Mugagga et al. 2012). The highest point, Wagagai Peak, is 4321 meters (Hamilton & Perrott 1981; Mugagga et al. 2012) and is found on the Ugandan side. This area rises from a plateau that lies 1850–2000 meters in the east and 1050 –1350 meters to the west with a caldera that extends 8 kilometers wide (Hamilton & Perrott 1981).

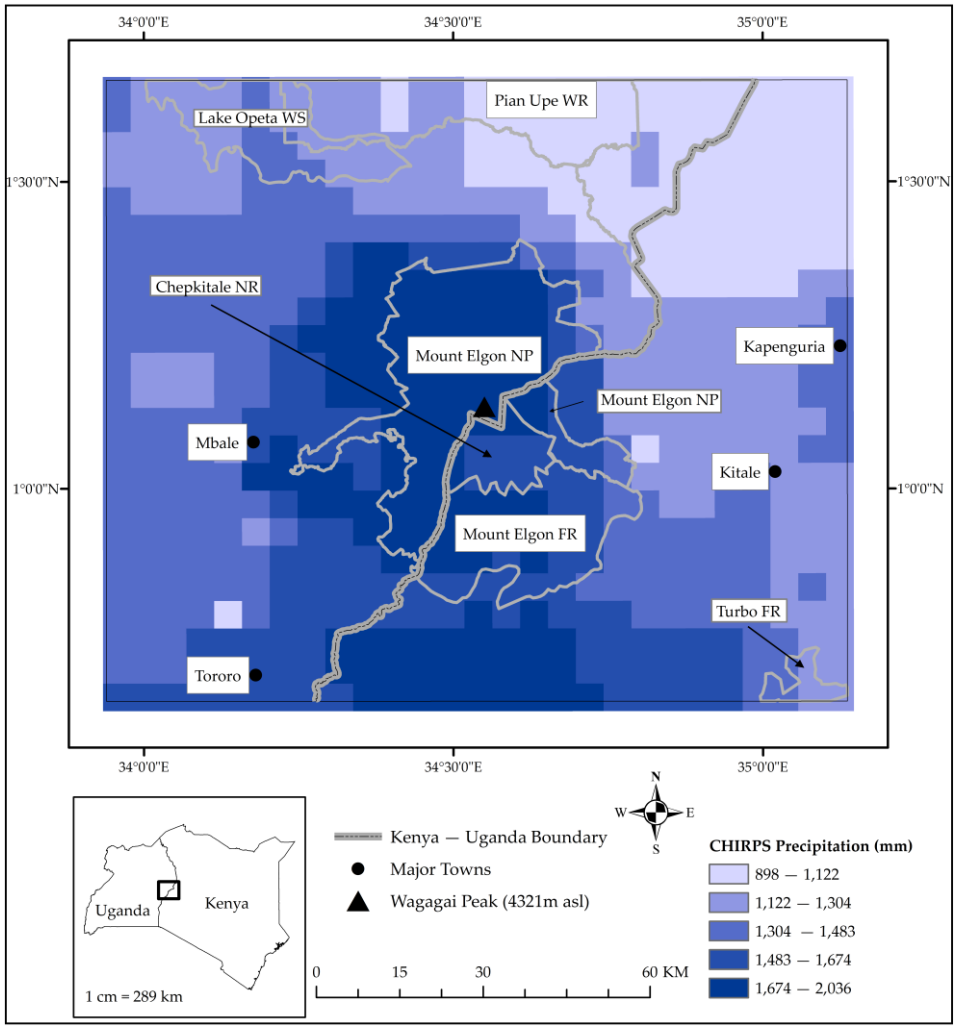

Figure 2.2. *Map of the MEE in eastern Uganda and western Kenya showing long-term (1986–2018) mean annual total precipitation (CHIRPS (Funk et al. 2015)).* Generally, the driest parts are the grasslands in northeastern MEE. The study area is wettest in the south and around the mountain region. Major protected areas and towns are shown for reference. FR is shorthand for forest reserve, NR is national reserve, NP is national park, WS is wetland system and WR is wildlife reserve.

Vegetation in this area is zoned by altitude and mountain forest, farmland and Afro-Alpine heath and moorland are the common land covers (Petursson et al. 2013). Declared a protected area in

1968 and 1992 in Kenya and Uganda, respectively (Anseeuw & Alden 2010; Nakakaawa et al. 2015), Mount Elgon Forest, a montane rainforest (Doumenge et al. 1995), is home to many important indigenous tree species (Petursson et al. 2013).

The MEE receives rainfall in a bimodal pattern (two rainy seasons) and, according to Mugagga, Kakembo and Buyinza (Mugagga et al. 2012), most of the rainfall is received between April and October on the Ugandan side (with mean annual amounts ranging from 1500 to 2000 millimeters). The Kenyan side receives long rains between March and June and short rains between September and November—average annual rainfall ranging from 1400 to 1800 millimeters (Okello et al. 2010; Musau et al. 2015). There is minimal temperature variation for the area—an average minimum of 15°C and a maximum of 23°C on the Ugandan side (Mugagga et al. 2012) and 14 and 24°C on the Kenyan side (Musau et al. 2015). However, temperatures and precipitation have a strong variation with changes in altitude (Petursson et al. 2013).

2.3 Materials and Methods

The present study integrated Mann–Kendall, Sen's slope and bfast in the analysis of NDVI and precipitation trends to characterize recent greening and browning patterns and trends within the MEE.

2.3.1 Data and Sources

This study utilized the following datasets (Table 2.1) in the analysis of greening and browning trends in the MEE.

2.3.1.1 MODIS NDVI and CHIRPS Precipitation

This study used MODIS NDVI data in the TS analysis of spatio-temporal changes in MEE vegetation greenness signal. The 16-day NDVI composite MOD13Q1.V6 (Didan 2015) with a 250-meter spatial resolution was obtained through AppEEARS (https://lpdaacsvc.cr.usgs.gov/appeears/) (AppEEARS Team 2019). Data for the period 2001–2018 were used. While Landsat data (USGS) have a better spatial resolution and historical

coverage, and are therefore better suited for this study, they were limited by the many data gaps in the TS over the MEE due to persistent cloud cover and Landsat's long (16-day) revisit time. As such, MODIS NDVI, which has previously been used successfully in similar studies in East Africa (Davenport & Nicholson 1993; Landmann & Dubovyk 2014; Hawinkel et al. 2016), was used in this study. This study also used CHIRPS precipitation data (Funk et al. 2015). These data have a spatial resolution of 5 kilometers and provide global daily and pentad records from 1981 to present. For this study, these data for the period 1986–2018 were obtained and preprocessed within Google Earth Engine (GEE) (Gorelick et al. 2017). It is worth noting here that there were no observation data to assess the accuracy of the CHIRPS dataset over the MEE. However, this dataset has been used extensively in similar studies (Georganos et al. 2017; Chen et al. 2018; Murthy & Bagchi 2018). Moreover, this dataset was recently validated (Muthoni et al. 2019) and the results showed that the CHIRPS data are reasonably accurate in estimating rainfall over east and south Africa.

NDVI preprocessing involved quality assessment using the associated VI quality files. Pixels with low quality, high aerosol content, cloud cover and possible shadows were excluded during this exercise. NDVI and precipitation composites for specific time scales were then generated. First computed were mean NDVI TS during the wet season for the period 2001–2018. Here, imagery in April, May and June was used. The TS of mean NDVI for each 16-day period during the season were also created. As a result, there were generally two TS for each month and were labeled h1 and h2 for TS created from NDVI composites recorded roughly in the first and second half of the month, respectively. For precipitation, the TS of total amount over the wet season were computed for different periods; 1986–2018 (33 years); 1986–1996 (first 11 years); 1997–2007 (median 11 years); 2008–2018 (last 11 years); 1986–2005 (first 20 years); 1999–2018 (last 20 years); and 2001–2018 (18 years, similar to the NDVI TS length). While the present study was aimed at characterizing changes in vegetation greenness from 2001 to 2018, analysis of longer precipitation TS was necessary to understand any longer-term precipitation patterns in

the MEE that may influence the vegetation patterns. TS were also generated of total precipitation amounts for each dekad over the wet season. In this analysis, these dekads for the month of April were labelled April d1 (for dates 1–10), April d2 (for dates 11–20) and April d3 (for the rest of the month). The same nomenclature was used for dekad TS in May and June. These were used to assess nature and strength of relationship between vegetation greenness and precipitation variability over a shorter time scale, in which case results from dekad precipitation TS were compared to results from 16-day NDVI. The 16-day NDVI composites were used here due to unavailability of data to compute dekad NDVI composites. Finally, monthly precipitation composites were generated for the period 1986–2018, for use in analyzing breakpoints in MEE precipitation.

2.3.1.2 Field-collected Data

Environmental data from local communities and government officers within the MEE were collected using semi-structured interviews and direct observation in July–September 2019 (IRB Number: STUDY00002404). Most of the interviewees were from significantly changing landscapes (areas showing significant changes in vegetation greenness). The participants in this study were interviewed about perceptions of climate change and land-use change, and historical patterns of agriculture and land-use change. Interviews were conducted and written responses recorded using Qualtrics software (Qualtrics 2019). The fusion of such qualitative data with quantitative RS data is important because indigenous and historical accounts of LULC change in such a constantly variable landscape can be used to fill in gaps that may not be fully explained using RS and GIS alone.

Table 2.1. *Description of original datasets used in the study.*

Dataset	Spatial Resolution	Temporal Resolution	Duration	Source
MODIS MOD13Q1.V6	250 m	16-day	2001 – 2018	https://lpdaacsvc.cr.usgs.gov/appeears/
CHIRPS	5 km	5-day	1986 – 2018	https://earthengine.google.com/

2.3.2 Methods

This section describes the methods and analyses performed on NDVI and precipitation TS to identify areas and characterize patterns of vegetation greening and browning within the MEE. These two analyses were performed in R (R Core Team 2018) and trends were assessed at the 95% significance level. After analysis of monotonic trends in greenness and precipitation, it was necessary to perform breakpoint analysis on these time series, to detect any significant breaks within the data. These two types of analyses are described in more detail below. Figure 2.3 highlights major methods used in this study.

2.3.2.1 TS Analysis: Mann-Kendall and Sen's Slope

To analyze initial spatiotemporal changes in vegetation greening and browning trends in the MEE, the current study borrowed from methodologies presented by Landmann and Dubovyk (Landmann & Dubovyk 2014). However, since NDVI TS often do not meet assumptions for parametric analysis (Alcaraz-Segura et al. 2010), the current study used the nonparametric Mann-Kendall test rather than linear regression. To calculate the Mann-Kendall test statistic, data values are evaluated as an ordered TS (Khambhammettu 2005) and each value is then compared to all subsequent values (Khambhammettu 2005; De Beurs & Henebry 2010). The Mann-Kendall S statistic is initially assumed to be 0 and a value of 1 is added to (subtracted from) the test statistic if the value of an observation is higher (lower) than that of the previous observation (Khambhammettu 2005; De Beurs & Henebry 2010). There is no change to the statistic if the values are equal. Equation 1 below shows the Mann-Kendall test equation. High positive and low negative values of S, respectively, indicate increasing and decreasing trends, but the strength of

the trend is statistically quantified by computing probability associated with S and the size of the data sample (Khambhammettu 2005).

$$S = \sum_{k=1}^{n-1} \sum_{j=k+1}^{n} sign(x_j - x_k) \quad (1)$$

where $sign(x_j - x_k)$ = 1 if $x_j - x_k > 0$

= 0 if $x_j - x_k = 0$

= -1 if $x_j - x_k < 0$ **Source:** Khambhammettu (Khambhammettu 2005)

The magnitude of the trends was quantified using Sen's slope estimator (Sen 1968). These algorithms were used in this study first to characterize and quantify any general patterns in MEE greenness during the growing season (April, May, and June). The analysis then investigated more subtle changes in vegetation greenness over shorter (16-day) periods during the growing season. From these, areas of increasing (decreasing) greenness were mapped as areas of vegetation greening (browning).

To disentangle changes due to human and natural forcings, monotonic trends were assessed in the precipitation TS and magnitude of the trends quantified. The analysis was performed on precipitation series at different temporal scales—based on the length of the time series (including 33-, 20-, 18- and 11-year periods) and TS resolution (including dekad totals, and general growing season totals). From these analyses, areas with significant positive (negative) precipitation trends were mapped as areas experiencing significant and consistent wetting (drying) over the analysis period. A cross examination of results from greenness and precipitation trend analysis was conducted to distinguish any human- from nature-driven vegetation greening and browning. Using available very-high-resolution imagery from Google Earth Pro (Google Earth Pro 2020), the nature of LULC conversion was ascertained. Besides, the statistics of LULC change (including greening, browning pixels) were calculated.

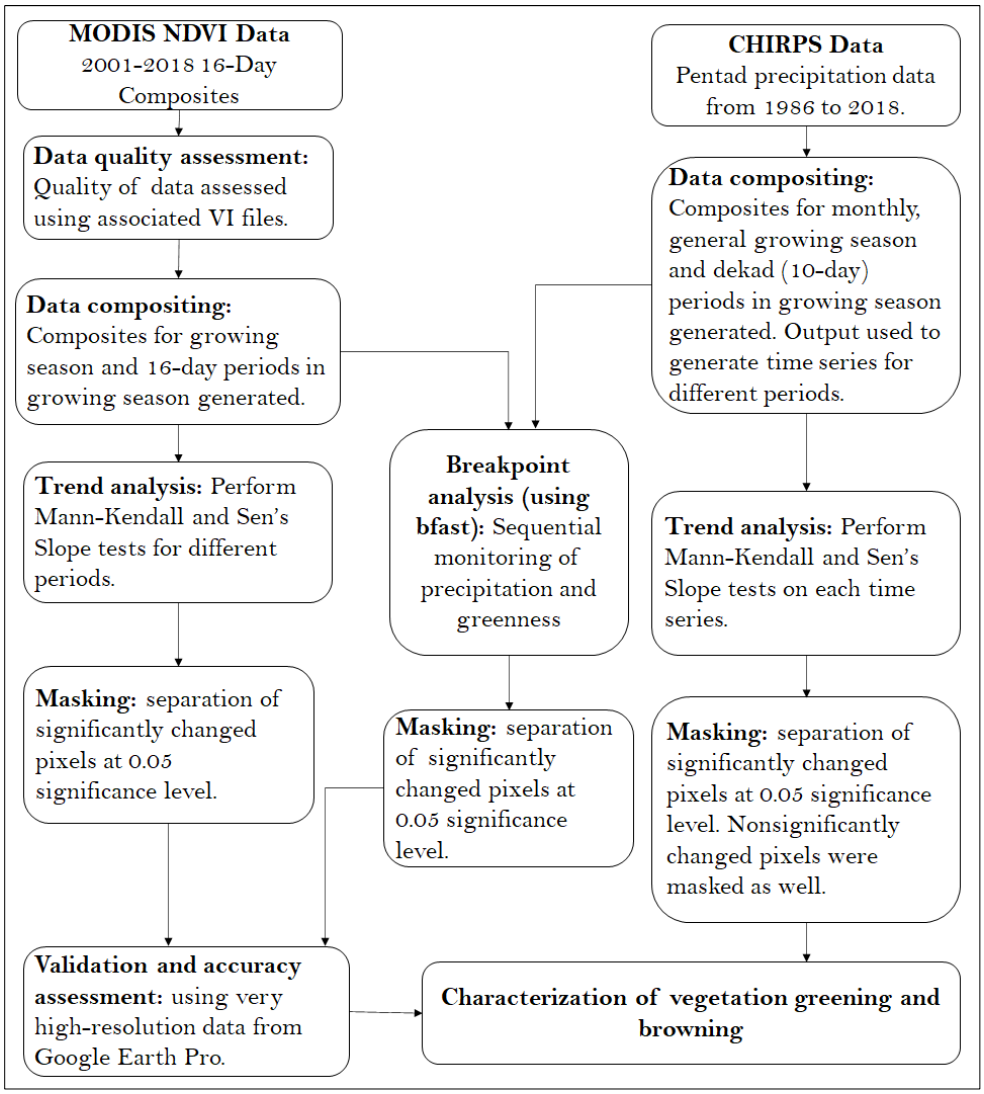

Figure 2.3. *Flowchart of analysis methods used in the study.*

2.3.2.2 Breakpoint Analysis: bfast

To further understand any temporal patterns in MEE greenness and precipitation, the bfast algorithm was applied using the 'bfastSpatial' package (http://www.loicdutrieux.net/bfastSpatial/). There exists a predictable annual cycle of greening an browning in vegetation, and these coincide with the occurrence of rainy and dry seasons (Morrison et al. 2018). bfast, created by (Verbesselt, Hyndman, Zeileis, et al. 2010) and (Verbesselt et al. 2012), creates a best-fit seasonal regression model with a trend component for the time series (Smith et al. 2019). This approach follows three main steps (i.) fitting a harmonic model based on a historical ('stable') period, (ii.) testing observations that follow the historical period for any structural breaks from the fitted model, and

(iii.) calculating the magnitude of change which is the median residual between observed and expected values in the monitoring period (DeVries et al. 2015; Morrison et al. 2018). While this approach has been applied on forested landscapes, the current study applied it to the whole of the MEE, whose LULC comprises forested, savanna, grassland, and cropland LULC (Figure 2.1). This was prompted by the unique LULC orientation in the MEE that makes it difficult to detect LULC changes via satellite image change detection analysis (Petursson et al. 2013). bfast breakpoint analysis can sequentially monitor vegetation change on a yearly basis, thus making it a suitable method for assessing changes in such LULC.

The models used in this part of the study were parameterized based primarily on the study by DeVries et al. (DeVries et al. 2015). First, the time series was divided into historical and monitoring periods. A minimum of two years for the historical period is recommended when using MODIS 16-day data (Verbesselt et al. 2012; Morrison et al. 2018). In this study, therefore, the period 2001–2004 was used as the initial historical period and was assumed to be generally stable before the start of the monitoring period. First-, second- and third-order harmonic models were fit on the NDVI data, the results were assessed, and the first-order model was finally selected as the suitable instance to use. The single-order model has been used previously with the assumption that vegetation phenology generally follows a similar trend (DeVries et al. 2015):

$$y_t = \alpha + \gamma \sin(\frac{2\pi t}{f} + \delta) + \varepsilon_t \quad (2)$$

where yt dependent variable
t independent variable
f temporal frequency
α model intercept
γ model amplitude
δ model phase
ε_t error term

As in the study by (DeVries et al. 2015), the trend component was excluded from the time series to reduce chances of yielding false breakpoints.

The change magnitude was calculated as the median of the residuals in the monitoring period. The median is thought of as a conservative measure, unlike the sum, that minimizes the chances of getting inflated magnitudes and therefore false breakpoints (DeVries et al. 2015). However, increasing the number of observations before and after a change event, by including long monitoring periods, yielded very high magnitudes and unrealistically numerous breakpoints. As such, this study elected to use sequential non-overlapping one-year-a-time monitoring periods. Here, the TS was trimmed to include the historical period plus one-year monitoring period. For monitoring the period from January to December 2005, for example, the TS for January 2001 to December 2005 was used, and the monitoring period was set to start in January 2005. This sequential monitoring approach is illustrated in DeVries et al. (DeVries et al. 2015). The approach is advantageous as it enables the assessment of subtle changes in vegetation within the MEE, especially alternating degradation and restoration that would go undetected using other methods. The default values for *h*, the minimal segment size between potentially detected breaks in the trend model given as a fraction relative to the sample size (Morrison et al. 2018), were used in this study.

Breakpoint analysis was also performed on the monthly total precipitation TS. The analysis was performed on both 1986–2018 and 2001–2018 time series, to understand any longer-term patterns as well as recent changes in the precipitation. Here, the third-order harmonic model with the trend term was the best fit. While there was no direct application on record of bfast for precipitation breakpoint analysis, it is noted that the algorithm can be used for this purpose (Verbesselt et al.; Verbesselt, Hyndman, Newnham, et al. 2010).

2.3.3 Validation of Results

A hybrid validation of analysis results was performed in this study. The collection of reference data borrowed from the methodology used previously by Landmann and Dubovyk (Landmann & Dubovyk 2014). The seasonal greening and browning map from Mann-Kendall and Sen's slope analysis (Figure 2.4) was linked to very-high-resolution imagery in Google Earth Pro and both qualitative and quantitative accuracy assessment of the results was performed. Locations of greening, browning and no change were investigated by visually interpreting historical imagery in Google Earth Pro. The selection of these testing points was based on the minimum size of detectable change (at least 250 m, the size of a MODIS NDVI pixel) and the availability of sufficient imagery to interpret change. As such, only locations with very-high-resolution imagery in one of the three initial and final years (2001–2003, 2016–2018, respectively) were used. By visually assessing historical imagery spanning these periods, vegetation change, or lack thereof, could be observed. A total of 153 visually interpreted points (51 browned, 50 greened and 52 no change) were used. Greenness change in pixels at these locations was first recorded. The seasonal greening and browning map from Mann-Kendall and Sen's slope analysis (Figure 2.4) was also reclassified into greened, browned and no change classes. The testing points were then compared to the reclassified raster and accuracy measures including overall, producer's, and user's accuracies were calculated. The final points were locations with pixels that indicated highly discernible change (like deforestation, reforestation etc.).

It was challenging to evaluate sequentially monitored vegetation change since it was not possible to gather testing points due to many temporal gaps in images in Google Earth Pro. In most instances, one can rarely find images for successive years, thus making it difficult to validate year-to-year change results. Since the bfast algorithm detects even subtle changes in vegetation greenness, changes could not be discerned with high confidence and therefore calculating accuracy assessment statistics would be misleading due to inconsistencies in testing data (Foody

2002). As such, these results were only visually and qualitatively assessed, and a general trend of change in the pixels was interpreted rather than year-to-year change. Evaluating such time series results has been found to be challenging previously (Kennedy et al. 2010; Gómez et al. 2016). In this study, inferences drawn from the field interviews were also qualitatively incorporated in this exercise to explain some of the trends detectable in both trend and breakpoint analyses.

2.4 Results

This study highlights and characterizes, using the Mann–Kendall, Sen's slope and bfast algorithms, recent vegetation greening and browning trends and patterns in the MEE at multiple time scales. The results highlight portions of the MEE that experienced persistent and significant changes in vegetation greenness, as indicated by changing NDVI. The results from similar analyses of precipitation TS are also presented and, together, attempt to disentangle nature- from human-driven changes observed over the MEE landscape.

2.4.1 Trend Analysis Results

2.4.1.1 Persistent Vegetation Greening and Browning in the MEE

Greening (browning) was defined as any significant increase (decrease) in NDVI as shown by either Kendall τ (Mann-Kendall and Sen's slope) or the magnitude of change (bfast). The results indicate various greening and browning patterns during the growing season (Figure 2.4) and near-half month (Figure 2.5) periods. During the growing season, greenness significantly increased in approximately 27% (3400 km^2) of the study area. Here, NDVI increased at rates up to 0.025 per year. These locations were concentrated mostly within croplands, grasslands, and savanna (Figure 2.1).

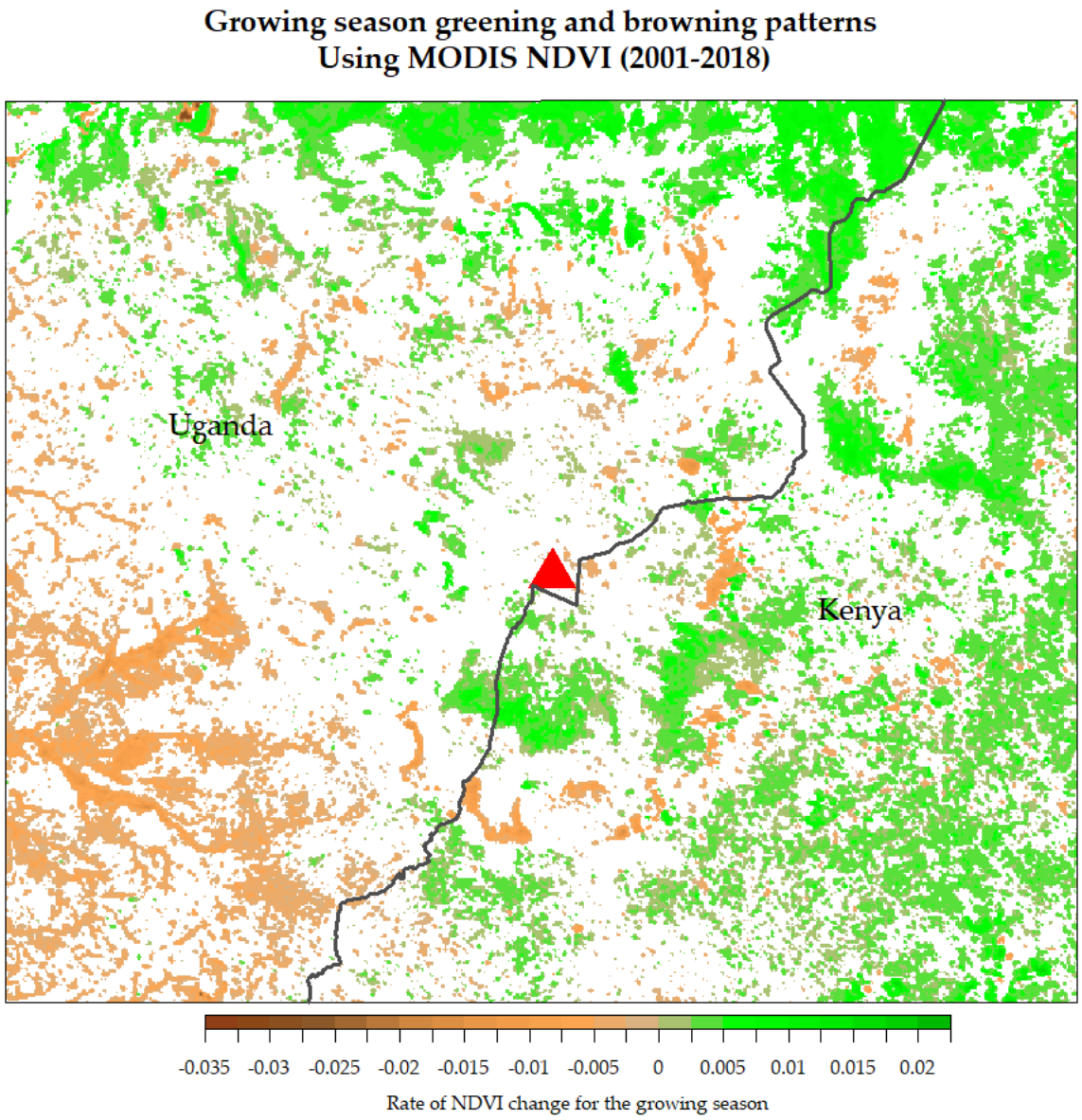

Figure 2.4. *Map of significant changed (greened and browned) locations during the growing season.* Slope values (Kendall τ), indicative of magnitude of change per time step, are shown here. White pixels indicate no significant change.

Significant browning was also evident, with NDVI in more than 1400 km^2 (about 11% of the total area) decreasing by up to 0.035 per year over the analysis period. These areas were mostly located in the southwestern part of the MEE in Uganda. This location includes the Namatala wetland, which has experienced intensive conversion to agriculture and settlement in the past years (Ministry of Water and Environment Uganda 2016). Browning was also evident in other locations around the Mount Elgon ecotone and elsewhere in the MEE. Based on our visual

assessment, most of these corresponded to areas where deforestation occurred over the analysis period. No significant trends were found in the rest of the MEE (62%, 7800 km^2).

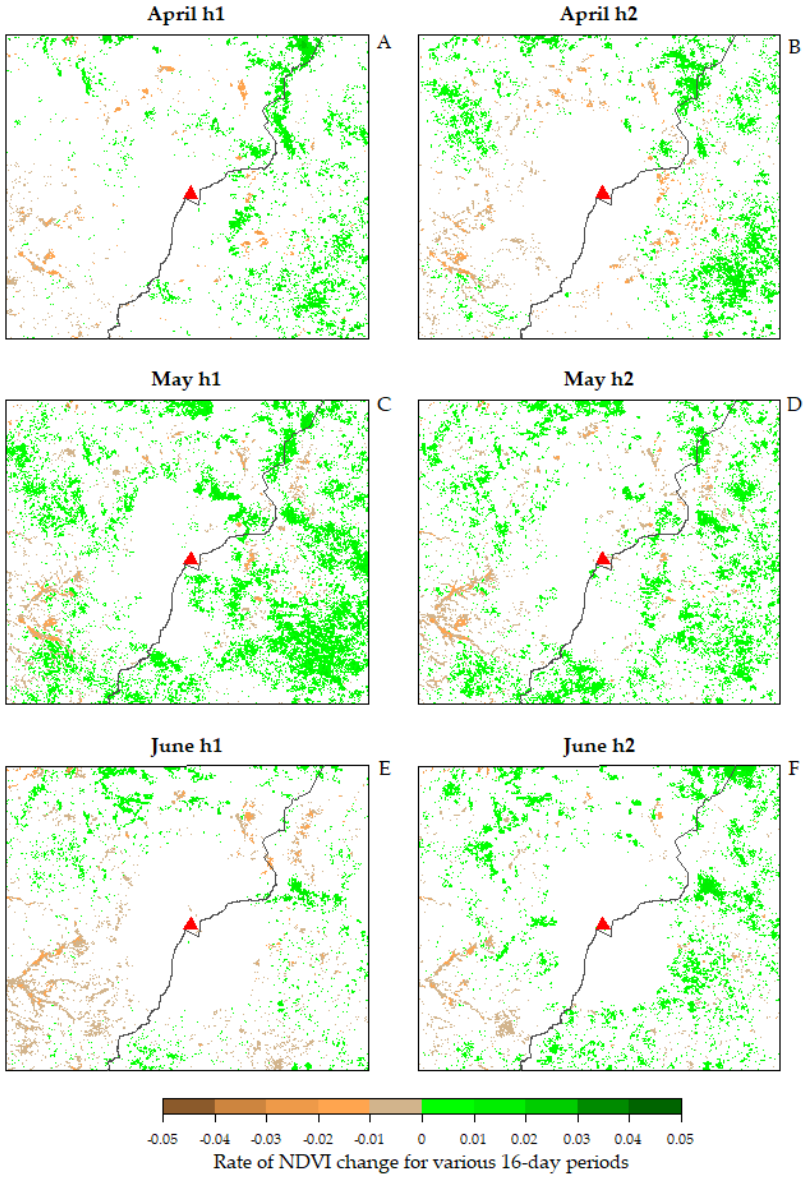

Figure 2.5. *Greening and browning trends in the Normalized Difference Vegetation Index (NDVI) for every 16-day period in the months of April, May and June for 18 years (2001–2018).*

Analysis of greening and browning trends in NDVI for every 16-day period in the months of April, May and June showed similar patterns; most browning occurred in the southwestern MEE and greening elsewhere. Most of the changed areas experienced greening and browning at rates of up to 0.03 and -0.04, respectively. The highest proportions of land where greening occurred

was found in the month of May, especially the May h1 period, in which about 20% (2400 km^2) of the MEE experienced significant greening (Figure 2.5). Greenness increased in more than 1600 km^2 (13%) of the study area during May h2. More greening was experienced in the June h2 and April h2 (9% of MEE greened during both periods). The greatest proportion of browned areas was observed in June h1, where about 600 km^2 (5%) of the MEE experienced vegetation greenness decline (Figure 2.5E). Most of the land within the MEE did not experience any significant change during these 16-day periods.

2.4.1.2 Precipitation Variability in the MEE

The test for monotonic trends in precipitation revealed various patterns of consistently increasing (wetting) and decreasing (drying) precipitation within the MEE (Figure 2.6). Most of the areas experienced increased precipitation over the years and only negligible proportions of the study area became drier. The greatest proportions of land during which consistently wetter conditions prevailed include 1999–2018, 1986–2018 and 2001–2018 (82%, 58% and 38%, respectively). The areas experiencing change covered approximately 10,300, 7200 and 4800 km^2, respectively. These periods also showed the greatest magnitude of change in precipitation amount. Here, precipitation increased by at least 13, 4, and 5 mm per year for 1999–2018, 1986–2018 and 2001–2018 periods. In addition, about 27% of the MEE also experienced wetter conditions during 2008–2018.

There were very small portions of the MEE with wetter conditions during the earlier years in the analysis; 1.61% of land (200 km^2) recorded wetter conditions in 1986–1996 while there was no significant increase in precipitation during the 1986–2005 and 1997–2007 periods. Consistently drier conditions were observed in two time periods (1986–1996 and 1986–2005). However, only negligible proportions of land (up to about 2%) experienced this change, although at substantial magnitudes of up to 9 mm per year. Different spatial patterns existed from 2000; significantly increasing precipitation in 2008–2018 was observed mostly on the Ugandan side,

and the mountain forest and wetland reserves seemed to be excluded (Figure 2.6B). In 2001–2018, the changed pixels were mostly found within the mountain area, in the north and some areas in the west (Figure 2.6E).

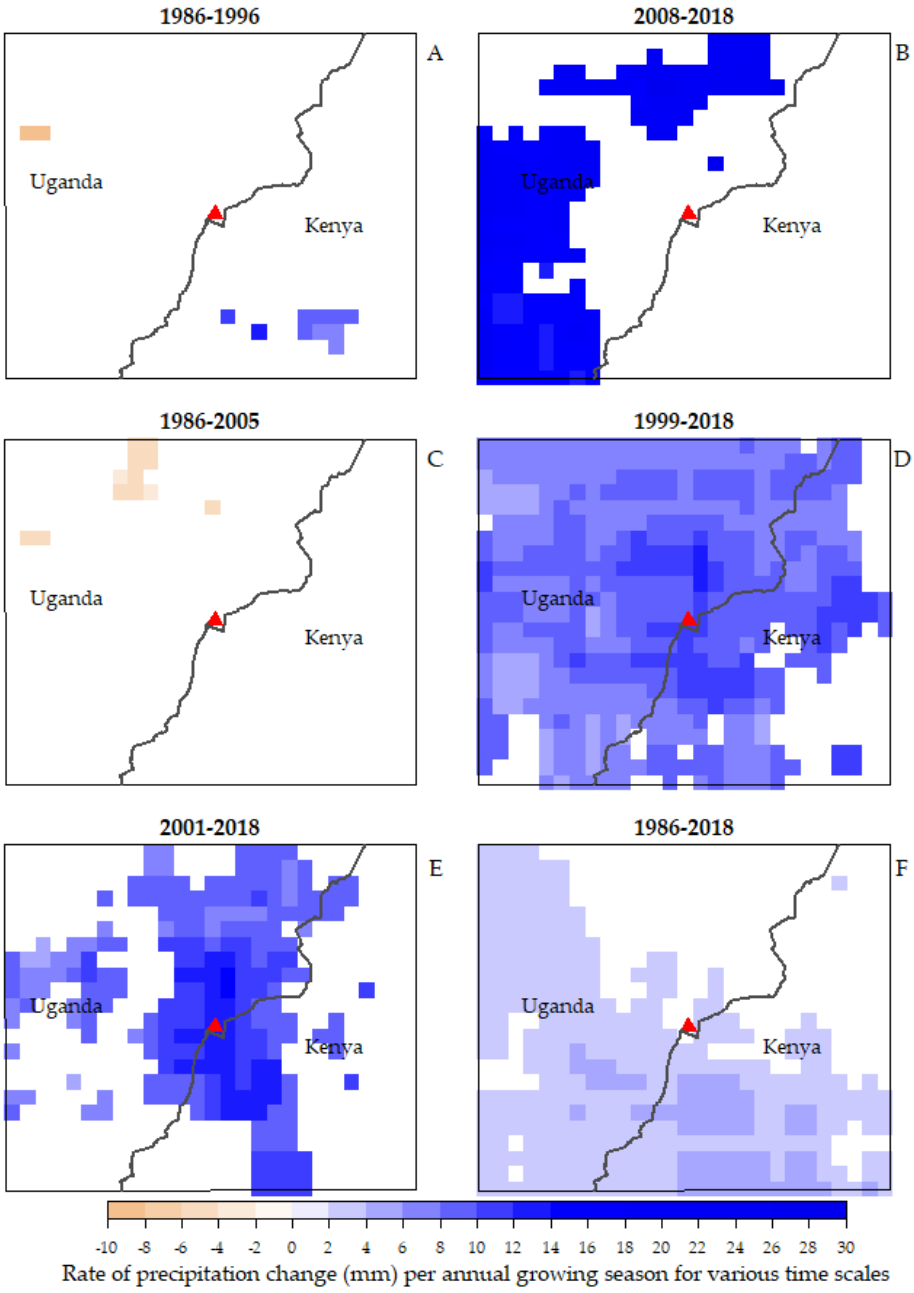

Figure 2.6. *Maps of precipitation change for each analyzed time period.*

On the other hand, areas in the northeastern portion of the study area did not experience changes in precipitation during the 1986–2018 period (Figure 2.6F). Lastly, the 1999–2018 period had

significant increases in total seasonal precipitation with an exception of a few eastern and southeastern portions of the MEE (Figure 2.6D). Overall, there was an increase in precipitation for most areas in the study area, with an increasing magnitude of change, especially in the post-2000 era.

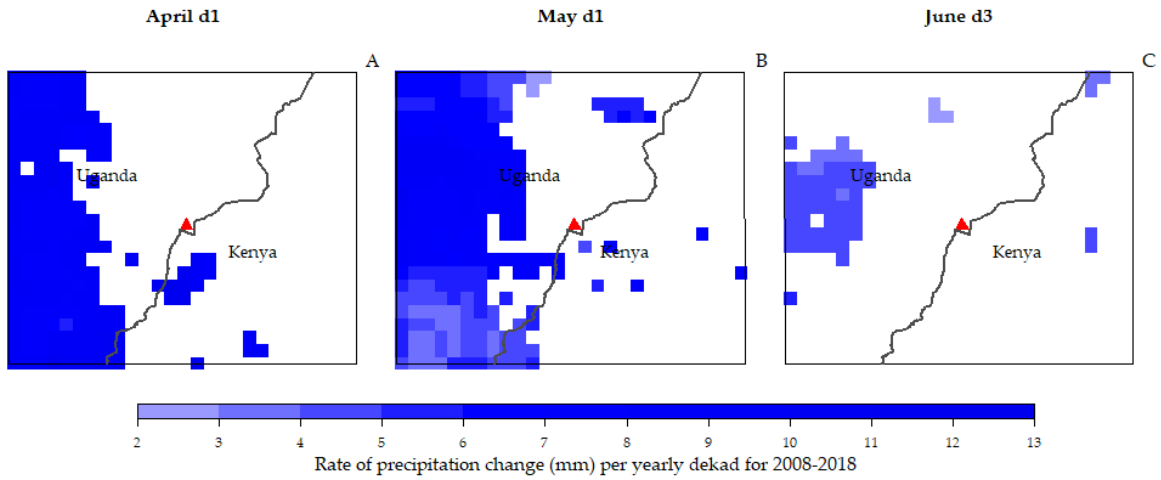

Figure 2.7. *Significantly changed precipitation for dekads in the period 2008 to 2018.*

The trend analysis for each dekad in the growing season found that, based on rates of change, the 2008–2018 period recorded the highest change in precipitation in April d1 and May d1, at rates of up to 13 mm per yearly dekad, see Figure 2.7). Areas where this change was experienced were located mostly in western MEE. An increase in precipitation was also recorded in April d2 in 2001–2018, June d3 in 1986–1996 and June d3 in 2008–2018. Negative trends in MEE precipitation were also observed in some dekads, mostly in 1986–2005. During this period, precipitation decreased in April d1, May d2 and June d1, at the rate of up to 3 mm per annual dekad.

Based on the proportions of land with significant change in precipitation, the study found that most of MEE precipitation significantly changed during May d1 in 1986–2018 (90%, 11,300 km^2) and May d1 in 1999–2018 (43%, 5400 km^2, Figure 2.8). From these results, some patterns are clear. For the months of May and June, annual dekad precipitation increased significantly for all time periods, although at varying rates and proportions. Precipitation in most of the MEE was

more stable in the earlier years in the study (as in 1986–1996) or generally depicted significant and consistently drier conditions (as in 1986–2005). Based on these results and those in Figure 2.6 above, it was necessary to conduct a breakpoint analysis to provide a better characterization of any specific spatio-temporal breaks in precipitation and greenness trends.

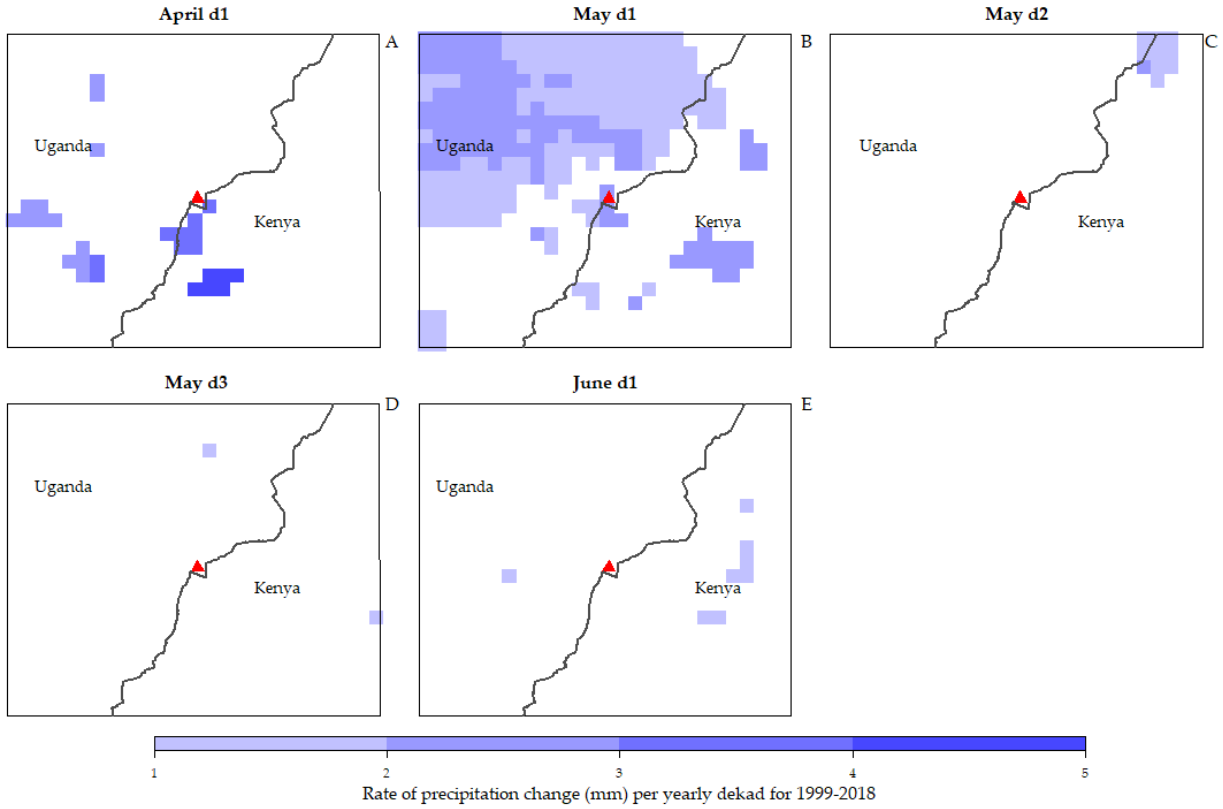

Figure 2.8. *Significantly changed precipitation for dekads in the period 1999 to 2018.*

2.4.2 Breakpoint Analysis Results: bfast

While breakpoint analysis was performed for both 1986–2018 and 2001–2018 precipitation TS, no significant breaks were found in the former. Therefore, results from 2001–2018 are presented in this study.

2.4.2.1 MEE Precipitation

The breakpoint analysis in bfast revealed no significant breaks in MEE average mean total monthly precipitation. However, breakpoints monitored for each pixel from January 2005 revealed very interesting patterns. In most configurations, the analysis revealed significant breakpoints in

2006 and 2007 for most of the MEE. To reduce the influence of post-change detection observations on change magnitude, the same analysis was performed for the period 2001–2008, with 2001–2004 set as the historical period. Therefore, change maps and statistics provided are based on this adjusted analysis. Precipitation changed significantly in the two years, with about 9800 km^2 (66% of the area) and 4800 km^2 (32%) of the MEE experiencing wetter conditions in 2006 and 2007, respectively (Figure 2.9). Most of the breakpoints in 2006 were detected in the months of July–October, while a great proportion of changes in 2007 were detected in March and April. Similar wetter conditions were detected in some locations in the months of May and June for both years. No drier conditions were detected. The magnitude of precipitation change ranged from approximately 10 to 53 mm during the monitored period (Figure 2.10A) and the bfast models used could explain up to 70% of the variance in the precipitation breakpoints (Figure 2.10B). Precipitation was also monitored sequentially for the period 2005–2018 and no breakpoints were detected except for a few pixels in 2005–2007.

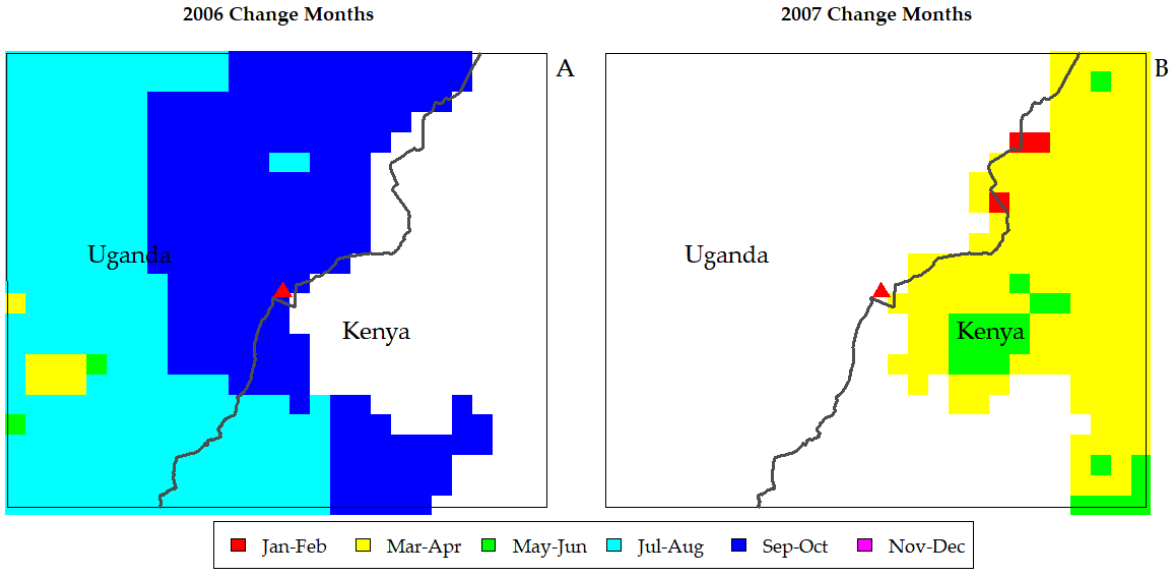

Figure 2.9. *Months when major breaks were detected in the precipitation time series (2001-2008) when the period 2005–2008 was monitored.*

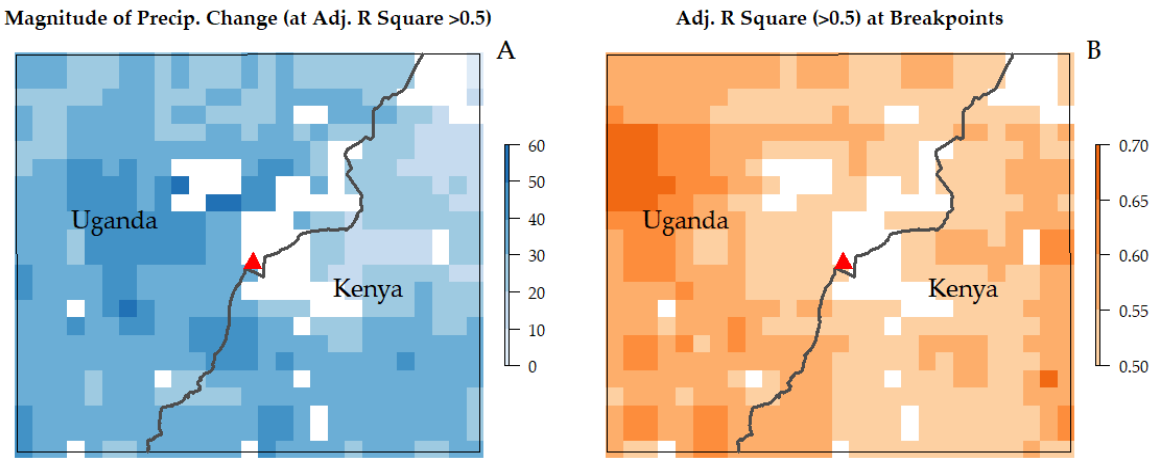

Figure 2.10. *Adjusted R^2 (greater than 0.5) and magnitude of change in the precipitation time series (2001–2008) using 2005–2008 as the monitoring period.*

2.4.2.2 MEE Greenness

The analysis of breakpoints revealed that some significant breaks existed in the NDVI time series for each year (2005–2018). Having been sequentially monitored, the results include, for each monitored year, months when the breakpoints were observed, the magnitude of change at the breakpoints, the length of historical data used and adjusted R^2. In this analysis, only highly statistically significant changes ($p < 0.05$) are reported. This decision was based on two reasons: (i.) There were no ground data for validating results from sequentially monitored bfast. To ensure that only accurate results are reported, breakpoints from models with less than 50% adjusted R^2 were excluded. Thus, only breakpoints from models with average to high explanatory power were reported. This 50% threshold has been used elsewhere by Landmann and Dubovyk (Landmann & Dubovyk 2014). (ii.) Vegetation greenness in the MEE showed significant interannual variability. As such, to ensure a long-enough historical period used by 'bfastSpatial', the study excluded any breakpoints from models using a historical period of less than two years.

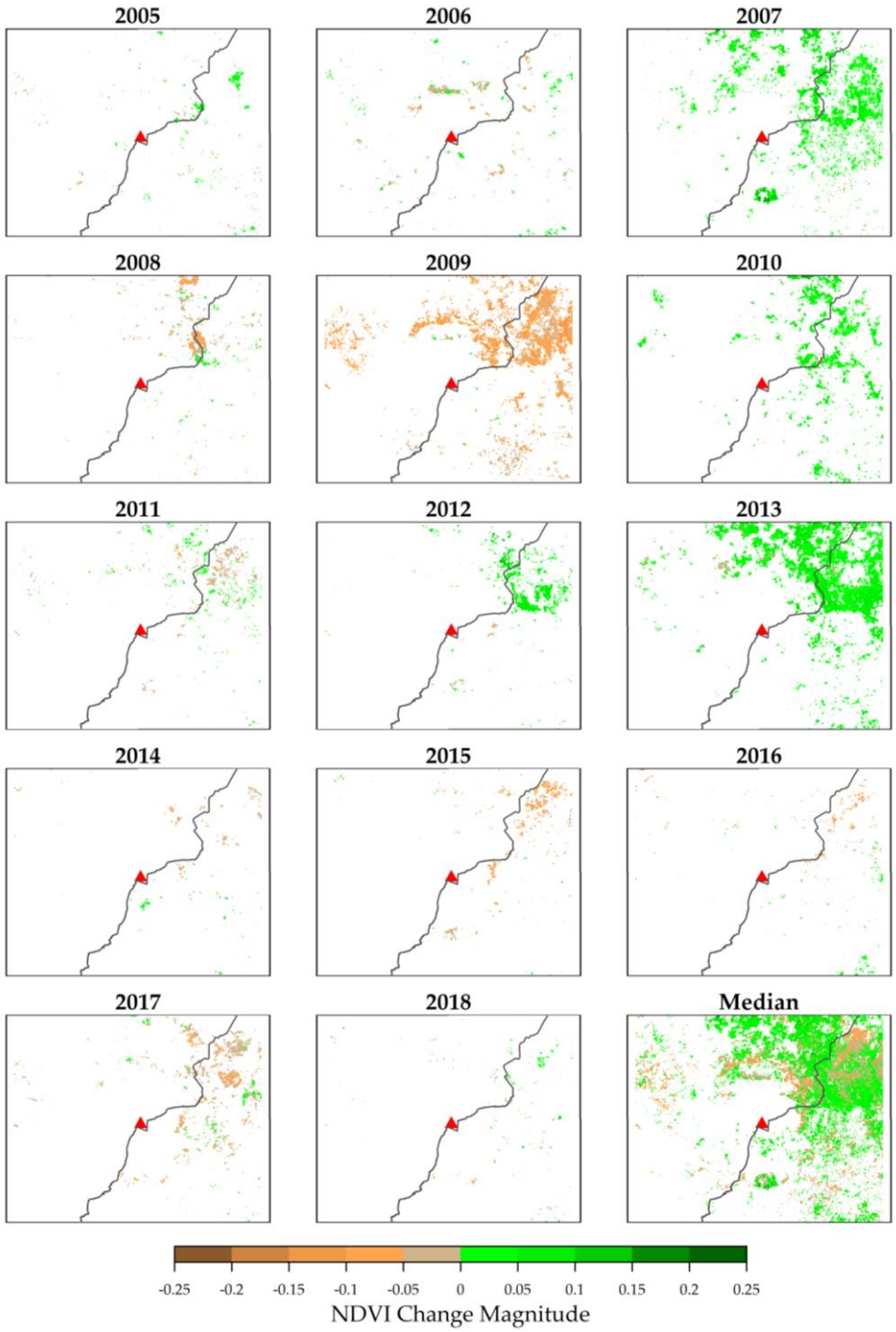

Figure 2.11. *bfast-detected greening and browning in the MEE.* These are results from bfastSpatial using NDVI time series (2001–2018) while sequentially monitoring each year in 2005–2018. These maps show magnitudes of change for pixels with significant breakpoints.

The 'bfastSpatial' model was able to detect changes in vegetation greenness, especially in the grasslands of the northeastern MEE (Figures 2.1 and 2.11). The observed changes could

be due to both natural factors (such as variability in precipitation) and/or human activities (for example, clearing of land for agriculture and settlement, deforestation for charcoal burning and construction etc.). The maximum magnitude of changes ranged from -0.24 and 0.21, thus indicating only subtle changes in the MEE vegetation. The breakpoints were detected in each of the years, but most of them were observed in 2013, 2007 and 2010 (greening) and 2009 and 2017 (browning), as shown in Figure 2.11. Overall, there were more areas where significant greening trends were detected compared to browning, with about 17% of the MEE (about 2500 km^2) and 10% (about 1500 km^2) showing greening and browning, respectively, over the monitoring period. These represent annual greening and browning rates of about 1.2% and 0.7%, respectively.

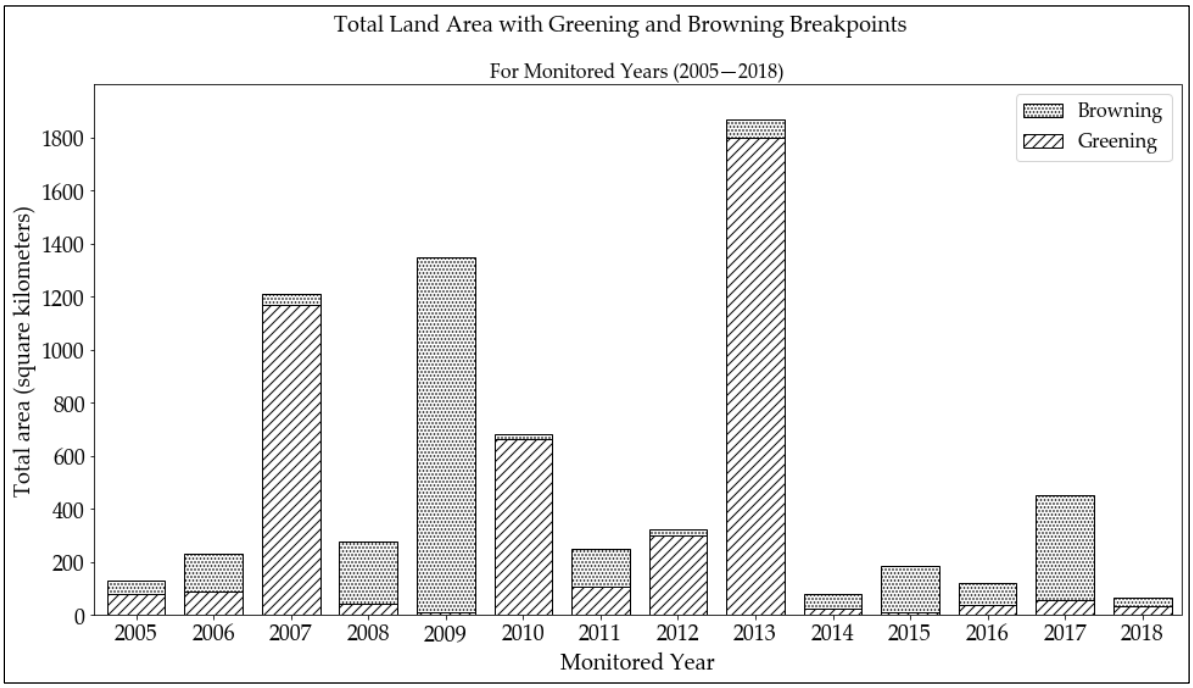

Figure 2.12. *Proportions of greening and browning areas in the MEE.* These are results from bfastSpatial using NDVI time series (2001–2018) while sequentially monitoring each year in 2005–2018. The graphs show the total area of land that experienced greening and browning for each monitored year.

Based on the yearly changes, differentiated greening and browning patterns were observed during the monitoring period. Cumulatively, the greatest proportion of land with changed greenness was in 2013 in which significant breakpoints were observed in approximately 13% of

the MEE (approximately 1850 km^2). This was followed by 2009 (1350 km^2), 2007 (1200 km^2) and 2010 (650 km^2) (Figure 2.12). For 2013, 2010 and 2007, the majority (over 95%) of the changed locations experienced greening. The year 2009 recorded browning in over 99% of the changed locations.

2.4.2.3 MEE Greenness vs Precipitation

There was an increase in precipitation in 2006 compared to previous years (Figure 2.13). There followed a steady decrease in 2007–2009 and finally an increase in 2010. Similar changes were observed in greenness during the five years. First, there was greening at most breakpoints in 2007 following the significant wetting in 2006. Significant browning followed, most of which occurred in 2009. This was also observable in an aspatial bfast breakpoint analysis performed on MEE mean NDVI, in which a sudden increase in NDVI was observed towards the end of 2006, followed by a consistently reducing trend until 2009/2010, in which another sudden increase was found (Figure 2.14). No significant breakpoints were found from a similar analysis using mean MEE precipitation. However, results from 'bfastSpatial' indicate that most of the MEE had very significant increases in precipitation in the second half of 2006 and the first half of 2007. Therefore, the corresponding changes in vegetation greenness can be attributed to this change in precipitation.

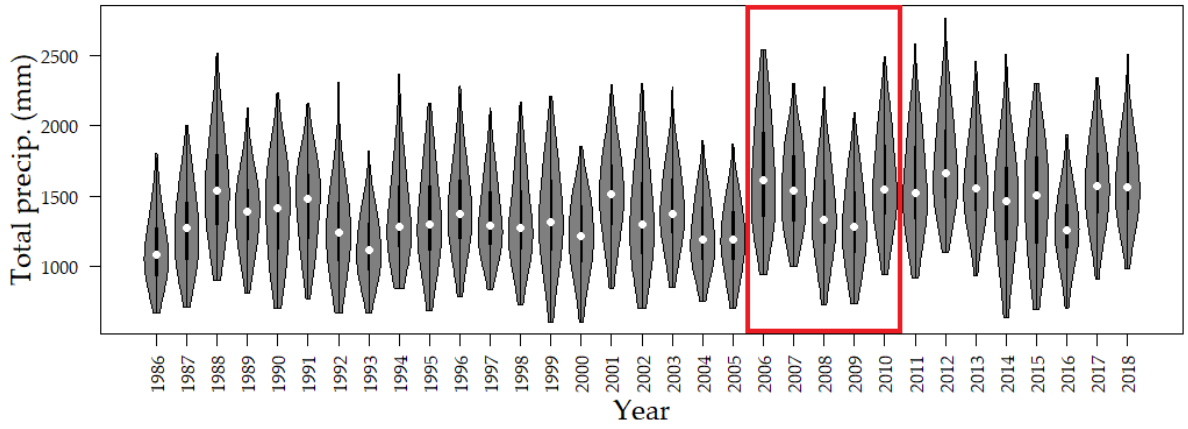

Figure 2.13. *Violin plot of average total annual precipitation in the MEE.* The red box highlights the period 2006–2010.

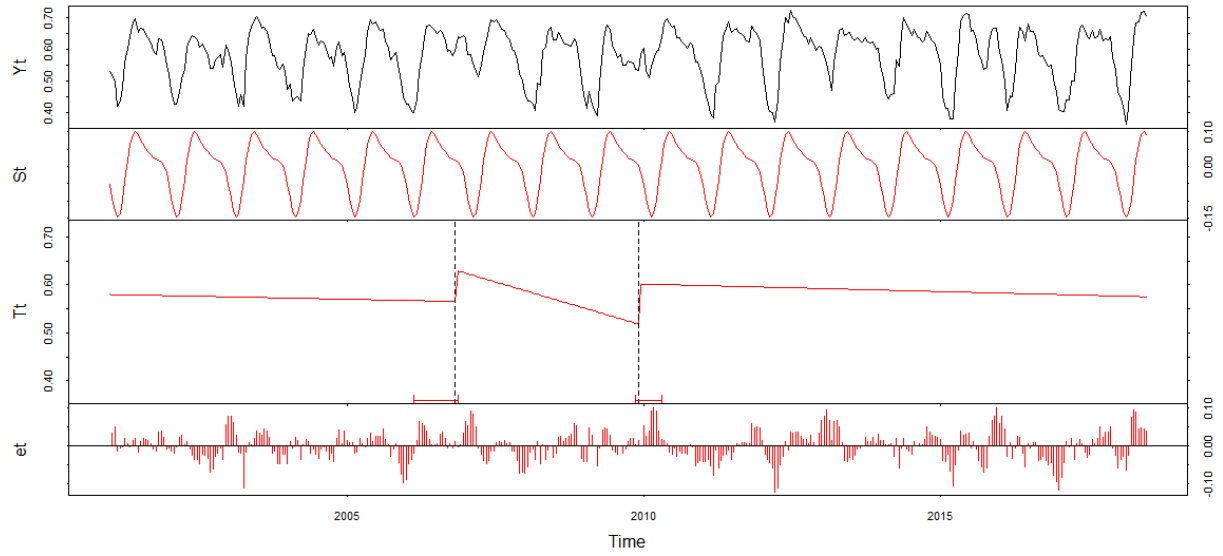

Figure 2.14. *bfast mean 16-day NDVI time series decomposition (2001–2018).* Breakpoints in trend were found between 2006 and 2010.

The significant and extensive browning observable mostly in 2009 (Figure 2.11) may be explained in terms of vegetation regaining its 'normal' greenness levels following sudden greening due to an above-normal precipitation. However, no significant breaks were found in precipitation around 2013, the year with the highest proportion of land with detected change in vegetation greenness. Thus, such browning and greening trends can be explained with regards to other factors, including temperature and anthropogenic activities that may have altered vegetation greenness during the monitoring period. The 'bfastSpatial' model did not find any significant breakpoints, in precipitation TS, in 2012. This may be due to the unstable historical data prior to the monitoring period. However, the violin plot (Figure 2.13) indicates that this year had some of the highest precipitation recordings. As such, there is a high chance that the greening following in 2013 was influenced by this increase in precipitation.

A visual inspection of these results in Google Earth Pro indicates that the subtle changes are indicative of various LULC changes. There was evidence of human settlement being introduced into the grasslands in the northeastern MEE. Information gathered from the field corroborates this finding and further explains the implications for landscape greenness. Inhabited

by nomadic pastoralist communities, this part of the MEE is susceptible to degradation, especially when these communities move, driven by rainfall patterns, to settle within the grasslands. Based on fieldwork and data from Google Earth Pro, reduced natural vegetation and tree density were evident in these locations. In other instances, the new inhabitants converted natural vegetation to agriculture and, although this would result in environmental degradation, some planted crops were greener than the natural vegetation, and, therefore, these areas were shown to exhibit greening trends. In other locations outside of the grasslands, visible greening trends were indicative of some afforestation practices. Data from the field revealed that this kind of greening was driven by the cultivation of evergreen early maturing blue gum (*Eucalyptus globulus*) tree species, sometimes together with and other times in the place of the maize crop. This was especially common in the eastern and southeastern parts of the domain and parts of Uganda.

2.4.3 Accuracy Assessment

Validation of Man-Kendall and Sen's slope results revealed an overall accuracy of 98.04% and user's accuracies of 100%, 98% and 96.2% for browned, greened, and unchanged locations, respectively (Table 2). Producer's accuracies of 98% (for both browned and greened locations) and 98.1% (no change) were also obtained. The visual inspection of bfast results using Google Earth Pro also revealed that most of the detected subtle changes occurred. However, no more detailed information like year of change could be discerned due to the lack of available high-resolution imagery.

Table 2.2. *Mann-Kendall and Sen's slope accuracy assessment statistics.*

	Browned	**Greened**	**No change**	**User's Accuracy**
Browned	50	0	0	100
Greened	0	49	1	98
No change	1	1	51	96.2
Producer's Accuracy	98	98	98.1	
Overall Accuracy				**98.04**

2.5 Discussion

2.5.1 Precipitation and Vegetation Change in the MEE

Climate change continues to affect economies in most developing nations, especially those relying heavily on natural processes for their livelihoods. Agriculture remains the backbone of many of these nations (Salami et al. 2010; FEWS Net 2013; NAAIAP & KARI 2014; Getachew Tesfaye Ayehu 2015; UNEP 2015; Wanyama 2017; Wanyama et al. 2019), yet agriculture's vulnerability to climate change effects cannot be contested. Climate-related natural hazards, including extensive flooding, extended droughts (Kotikot et al. 2018), landslides (Mugagga et al. 2012) among others, have significantly impacted agricultural production and endangered lives. The frequency of these events shows an increasing trend (C. Li et al. 2016; Ayugi et al. 2020), thus trapping many agriculture-dependent communities in an unending struggle for survival. Therefore, existing food insecurity in these developing nations can be attributed to their overreliance on rainfed agriculture (Kotikot et al. 2018). Moreover, the high population growth and densities in these nations and elsewhere have translated into need for more agricultural land (Mugagga et al. 2012). Coupled with political interference and corruption among forest park and reserve staff, this need for more land has resulted in forest encroachment and deforestation as ecologically fragile land is cleared for agriculture and settlement (Muhweezi et al. 2007; Bamutaze et al. 2010; Mugagga et al. 2012; Nakakaawa et al. 2015; EAC et al. 2016). Therefore, understanding the major drivers of landscape change is an important first step to inform better decisions to simultaneously conserve the natural environment and improve the livelihoods dependent on it. First, being able to separate nature- from human-induced landscape changes would be valuable in this endeavor.

Changes in the landscape occur at varying rates and magnitudes across space and time, from very subtle tree damages to forest clearings (Morrison et al. 2018). In this study, two major forms of landscape change – browning (areas of declining vegetation) and greening (areas of

increasing vegetation) (Murthy & Bagchi 2018) – were studied. The results show that MEE greenness exhibited substantial variability, and some form of the greening and browning change was recorded each year. As expected, these changes varied by scale, with the highest proportions of greened and browned locations observed over the growing season rather than any of the individual 16-day periods. Importantly, there was a lot of activity in areas bordering the mountain forest, as expected. Clearly, both greening and browning trends were observable, particularly on the Kenya side. Significant deforestation occurred as a result of encroaching fertile land on the high slopes of the mountain, for agriculture and settlement (examples in Figure 2.15). This finding has been reported in previous studies (Mugagga et al. 2012; Petursson et al. 2013).

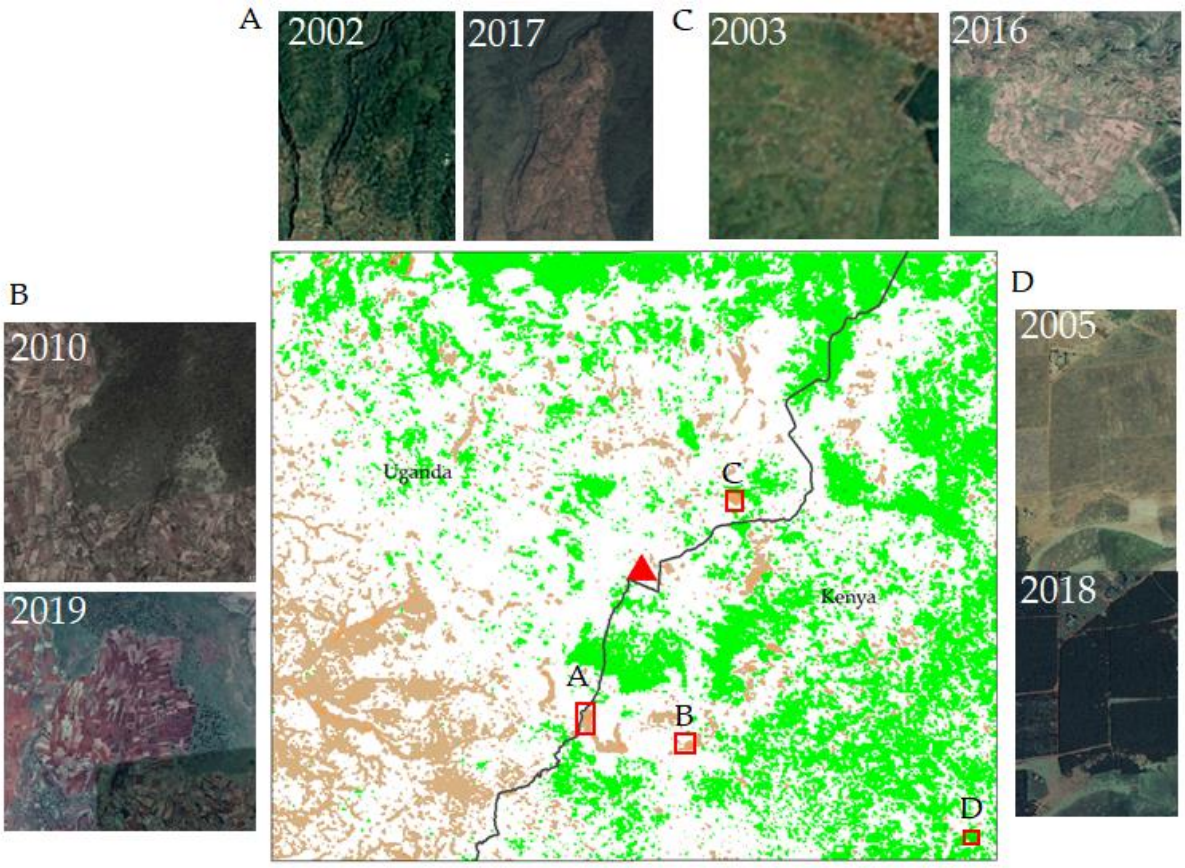

Figure 2.15. *Some of the greened and browned areas identified by Mann-Kendall and Sen's slope.* Images A, B and C indicate the conversion of natural vegetation (mostly forest) to cropland and settlement. Image D indicates afforestation. **Source:** Google Earth Pro (Google Earth Pro 2020).

The Shamba system, thought of as a win-win arrangement, enabled local communities to farm in protected areas while tending to the growing trees in their early stages of growth (Petursson et al. 2013). This was a government effort originally meant to convert native to plantation forests and later to replant trees on harvested forest land. However, the Shamba system farms overlap with plantation forest and bamboo vegetation thus making it more difficult to conclusively identify, characterize and quantify the nature and magnitude of LULC change, especially by the use of traditional classification and change detection methods (Petursson et al. 2013). The significant and consistent browning in the southwestern MEE are attributed to the conversion of the Namatala wetland to agriculture (mostly paddy rice farming) and settlement (due to the growth of Mbale town) (Ministry of Water and Environment Uganda 2016). Since the early 2000s, 80–90% of this wetland has been converted. The wetland area is an Important Bird Area (IBA) (BirdLife International) and therefore the reported LULC conversion caused many nature–human and human–human conflicts, including, respectively, bird poisoning and competition among people to own and utilize the wetland.

Disentangling nature- from human-induced vegetation change is an important yet complex task. In this study, patterns of change in precipitation varied with the TS duration (33-, 11-, 20- and 18-years) and resolution (dekad, seasonal). Previous studies indicated that precipitation in the area exhibited significant temporal variability, with both positive (Muthoni et al. 2019) and negative (Wanyama 2017) trends observed over time. It can be inferred that precipitation had changed more (increased) over the period after 2000 than earlier. This implies that some of the vegetation greening and browning should be linked to this MEE wetting. This is true for the period 2006–2010, where bfast reveals that greening and browning events in the MEE follow significant wetting and drying events. However, a visual interpretation of Mann-Kendall analysis maps for both MODIS NDVI and CHIRPS precipitation did not show much similarity. Besides, bfast did not reveal any breakpoints in precipitation around 2013, the year when most breakpoints in greenness

were detected. While this may be a fault in the bfast model used (because of, for instance, instability in historical data used), precipitation alone may not be a reliable predictor of vegetation change (Morrison et al. 2018). Davenport & Nicholson (1993) concluded that the NDVI–precipitation relationship varies both spatially and temporally, is not linear, generally exhibits a three-month lag, and depends on underlying LULC types. Therefore, it is likely that these complex relationships were not well revealed in both analyses in this study. Besides, the observed greening and browning patterns may be driven by other climate factors (such as temperature), which were not examined in this study, due in part to data unavailability for the MEE. Moreover, the spatial scale mismatch between the CHIRPS and MODIS data makes more quantitative comparisons challenging.

Visual inspections of the results from both analyses revealed the applicability of Mann-Kendall and bfast methods in detecting changes in vegetation greenness. Most people in the MEE are small-scale farmers, owning sometimes less than an acre (0.4 hectares) of land. This represents less than 10 percent of the pixel size used (250 by 250-meter MODIS), meaning that some subtle land conversions were missed. The choice to use these data was necessitated by the frequent availability of MODIS NDVI data. The ability of Mann-Kendall and bfast in delineating areas of change in the MEE using this coarse imagery is important, as free finer RS imagery like Landsat is limited by both cloud cover across tropical regions and their coarse temporal resolutions. Looking forward, combining Sentinel-2 and Landsat imagery may help address this issue, but this will not resolve the problem for historical studies like this one.

The use of Mann-Kendall and bfast algorithms proved to be a valuable integration. Mann-Kendall performed well in mapping locations that had experienced significant change in the entire TS (2001–2018). Consistently greened and browned locations were mapped with high confidence (95% significance level) and similar patterns existed for both 16-day and average growing season periods: significant and consistent browning in southwestern MEE and greening elsewhere. The

best and most accurate results were obtained using average growing season NDVI TS. Here, browned locations (especially around mountain boundaries and southwestern MEE) and greening elsewhere were clearly demarcated. This indicates that the growing season period, rather than the shorter 16-day period, is the best temporal scale for monitoring vegetation change in the MEE. bfast on the other hand performed well in mapping changed greenness locations for sequentially monitored periods from 2005 to 2018. This part of the analysis revealed only subtle changes in vegetation greenness in most locations, indicative of vegetation degradation rather than deforestation (DeVries et al. 2015). Importantly, areas with breakpoints across multiple years were effectively identified, a finding that would likely be omitted if using traditional post-classification change detection methods. These findings demonstrate that the process of vegetation greening and browning can be studied more thoroughly by fusing these two methods. Using Mann-Kendall and Sen's Slope, one can assess and quantify monotonic trends in their TS to get the general picture in the series. This can be complimented with an assessment of the temporal occurrence of significant breaks in the series using bfast. Using this integrated approach, vegetation greening and browning can be fully characterized and understood to provide more information for better decision making.

2.5.2 Sources of Uncertainty

Due to a lack of ground precipitation measurements, the present study did not validate the CHIRPS data over the MEE. The GHCN data (Global Historical Climatology Network - Daily (GHCN-Daily) 2012) would potentially be used, but only one data point existed in the study area and was therefore deemed insufficient for this task. While this is a potential source of uncertainty, these data have been used extensively in similar studies. Moreover, CHIRPS data are based on ground station data since they are created through "smart interpolation" procedures that incorporate both satellite information and gauge data (Funk et al. 2015) thus making daily CHIRPS imprecise, and reliable only at dekad or higher aggregations. Validation of bfast results

was also not possible due to a similar lack of data. Frequent, high-resolution imagery was not freely available to download and process, and the study relied on imagery from Google Earth Pro which had a lot of spatial and temporal gaps. While no accuracy statistics were calculated for these results, the results were interpreted based in part on data collected from the MEE field study.

2.6 Conclusions

The MEE of eastern Uganda and western Kenya was found to exhibit significant variability in vegetation dynamics and precipitation regimes. This variability was attributed to the existing LULC orientation especially in eastern MEE and climate change and variability. As such, it is highly probable that analysis of only a few images to ascertain MEE landscape change would yield inconsistent results. In this study, greening and browning in the MEE was examined using both TS trend and breakpoint analysis methods. The MEE had experienced significant and persistent greening and browning at different time scales and this change was attributed to both natural factors (including changing precipitation) and anthropogenic factors (especially the vegetation-to-cropland conversion). The southwestern MEE had consistently browned due to the conversion of the Namatala swamp to paddy rice farming and settlement. A lot of activity was also observed around the mountain forest boundary as people encroached and converted the forest LULC to agriculture and settlement. There were breakpoints in the vegetation greenness TS, particularly in the savanna and grassland land covers in northeastern MEE. The breakpoints were detected in each of the monitored years (2005–2018), but most of them were observed in 2013, 2007 and 2010 (greening) and 2009 and 2017 (browning). The study also concluded that MEE precipitation had significantly changed (increased) in the post-2000 era. More specifically, total precipitation significantly increased in 2006 and 2009–2010 with a consistently decreasing trend in between. We therefore concluded that these precipitation changes influenced significant greening and browning patterns observed in the same period. The greenness–precipitation relationship was weak in other periods as greening and browning changes were not strongly

influenced by changing precipitation. This may be attributed to the complex nature of the MEE landscape and/or the spatial and temporal scale mismatch between MODIS NDVI and CHIRPS precipitation data. The integration of Mann–Kendall, Sen's slope and bfast proved useful in comprehensively characterizing recent changes in vegetation greenness within the MEE. Having a comprehensive description of vegetation change is an important first step, especially for such a variable landscape, to effect policy changes aimed at simultaneously conserving the environment and improving livelihoods that are dependent on it.[2]

[2] This research was supported by funds from the 2019 and 2020 *Graduate Office Fellowship* (GOF) awarded by College of Social Science and Department of Geography, Environment, and Spatial Sciences at Michigan State University. It also received support from the 2020 *Research Enhancement Award* from The Graduate School at Michigan State University.

CHAPTER 3. QUANTITATIVE MULTI-FACTOR CHARACTERIZATION OF ECO-ENVIRONMENTAL VULNERABILITY IN THE MOUNT ELGON ECOSYSTEM[3]

3.1 Introduction

The natural environment continues to experience pressures from many factors, including climate change, economic development and human activities (He et al. 2018). Global environmental temperatures have increased since the 20th century, causing significant changes in the global climate (Guo et al. 2019). As a result, significant precipitation impacts have been observed (Nguyen et al. 2018), animal and plant species loss has intensified, and frequencies and magnitudes of environmental hazards have increased (Guo et al. 2019). In many parts of the world, populations and natural resource extraction have increased substantially, and the restorative abilities of ecosystems (especially food systems) have declined, thus rendering both human and natural systems more fragile (Zhong-Wu et al. 2006; Nandy et al. 2015; Guo et al. 2019). The world faces an unprecedented double challenge: "to eradicate hunger and poverty and to stabilize the global climate before it is too late" (FAO 2016). The big task, therefore, is to increase food production while fostering sustainability of Earth's environmental systems (Atzberger 2013). Assessing ecological and environmental (eco-environmental) vulnerability is key for examining ecological conditions; information drawn from vulnerability analysis can assist with targeted actions towards a sustainable environment and improved community livelihoods.

Vulnerability is challenging to measure. Several definitions of vulnerability have been proposed and, as Simane, Zaitchik, and Foltz (2016) noted, any attempt to quantify vulnerability depends on the definition and metrics used. Kelly & Adger (2000) defined vulnerability as a combination of the capacity of a community to cope with, recover from, or adapt to any external stress exerted on their livelihoods. The International Panel on Climate Change (IPCC) defined

[3] This is an accepted manuscript of an article published by Taylor & Francis in *GIScience & Remote Sensing* on 10 November 2021 available at https://doi.org/10.1080/15481603.2021.2000351. Reference: Wanyama D, Kar B, Moore NJ. 2021. Quantitative multi-factor characterization of eco-environmental vulnerability in the Mount Elgon Ecosystem. GIScience & Remote Sensing.

vulnerability, within the context of climate change, as the level of susceptibility to harmful effects caused by climate change (IPCC 2001). The IPCC further characterized a system's vulnerability to a hazard as a function of the hazard's characteristics (magnitude, rates of change) and the system's exposure, sensitivity, and adaptive capacity. Thus, the concept of vulnerability cross-cuts multiple disciplines (O'Brien et al. 2004) and is therefore viewed differently depending on context (Rama Rao et al. 2016). Vulnerability assessment is routine to many fields, which include livelihood vulnerability to hazards (Huong et al. (2019); Simane et al. (2016)), vulnerability to natural hazards (Han et al. (2019); Xiong et al. (2019)), vulnerability to climate change (Rama Rao et al. (2016); Torresan et al. (2012)), agricultural vulnerability (e.g. Aleksandrova et al. (2016); Baca et al. (2014); Parker et al. (2019)), groundwater (Duarte et al. 2015; Aydi 2018), and eco-environmental vulnerability (Sahoo et al. 2016; He et al. 2018; Zhao et al. 2018; Wei et al. 2020).

Eco-environmental vulnerability is closely associated with risk of damage to the natural environment (Nandy et al. 2015). As such, eco-environmental vulnerability assessment (EEVA) has been conducted to comprehensively evaluate natural resource systems that are impacted by both natural and anthropogenic activities (Fan et al. 2009). Many methods are used here, including fuzzy membership evaluation (Enea & Salemi 2001), analytical hierarchy process (AHP) (Wang et al. 2008; Nguyen et al. 2016; Liou et al. 2017; He et al. 2018; Venkatesh et al. 2020), entropy method (Zhao et al. 2018), spatial principal component analysis (SPCA) (Fan et al. 2009; Nandy et al. 2015; Wei et al. 2020), integrated approaches (e.g., multi-approach study and integration of environmental parameters (Teodoro et al. 2021), and combining pressure-state-response (PSR) method with either PCA (Boori et al. 2021) or AHP (Zhang et al. 2021). Due to recent developments in Earth observation technologies, spatio-temporally contiguous data have been produced and used in many environmental assessments including EEVA. As such, most EEVA studies are similar in their reliance on remote sensing (RS) data from satellites (e.g., MODIS, Landsat, GIMMS, Sentinel). More recently, EEVA has been conducted using Synthetic

Aperture Radar (SAR) due to its ability to work in cloudy, rainy and foggy conditions (Ji & Cui 2021) and Unmanned Aerial Vehicles (UAVs) (e.g., Teodoro et al. (2021). However, there is no rule of thumb as to how many variables should be used (Nguyen et al. 2016), and each EEVA study defines its variables based on contexts and available data. For instance, Venkatesh et al. (2020) and Nguyen et al. (2016) integrated 12 and 16 variables, respectively. In other studies, Liou et al. (2017) and Li et al. (2006) respectively used 12 and 9 variables in their EEVA studies. Commonly used variables in these studies include topography (elevation, slope, and aspect), vegetation variables (normalized difference vegetation index, normalized difference water index, land surface temperature) and some distance variables (distance to rivers and/or urban areas). EEVA reveals pertinent information about environmental quality, thus it is a critical step towards better formulations of environmental protection frameworks (Sahoo et al. 2016). This can aid attainment of ecological sustainability and restoration and ensure better environmental and resource management (Nguyen et al. 2016).

East Africa's highlands are significantly vulnerable. The East African region covers a wide range of ecological and climate regions exhibiting multiple land use and land cover (LULC) types and dynamics (Brink et al. 2014). People in this region rely heavily on rainfed agriculture, which, amid uncertainties in the climate system, threatens the region's food security and rural livelihoods (Guzha et al. 2018). Land is therefore a critical resource (Guzha et al. 2018), yet land holdings in East Africa are small and declining steadily (Maitima et al. 2009; Guzha et al. 2018). Additionally, populations continue to surge, necessitating expansion of food production systems (Wanyama et al. 2020). As a result, significant LULC conversions (especially natural vegetation to croplands and settlement) have widely been reported in many parts of East Africa, including Nech Sar National Park (Fetene et al. 2016), the Bale Mountain region (Hailemariam et al. 2016) (both in Ethiopia), and the Mara River Basin in Kenya and Uganda (Mwangi et al. 2017). These LULC changes have been observed in the Mount Elgon ecosystem (MEE), a major water tower in Kenya

and Uganda. The MEE is primarily agricultural, with savanna, grassland, and Afromontane forest as dominant land covers (Wanyama et al. 2020). Here, agricultural land has the highest population densities approximating 1,000 people per km^2 (Nakakaawa et al. 2015; Vlaeminck et al. 2016). The increasing fragmentation of small agricultural plots in the MEE signal mounting pressures on land and this has translated into increasing encroachment of ecologically fragile land (Nakileza & Nedala 2020) along with illegal access to protected areas (PAs) - for agriculture (Wanyama et al. 2020) and other extractive activities like timber production and charcoal burning (Mawa et al. 2020). This LULC change has, in part, modified local ecosystem functioning (Ongugo et al. 2017) which has resulted in more climate-related hazards (e.g., prolonged droughts, more frequent landslides and more extensive flooding (Nakakaawa et al. 2015; EAC et al. 2016)). Despite these trends, the broader eco-environmental vulnerability of the MEE has not been assessed comprehensively.

Previous studies related to EEVA in the MEE have mostly focused on landslide vulnerability in the Ugandan MEE. The Ugandan MEE is particularly vulnerable to landslide hazards which have become more frequent over time (Mumba et al. 2016). Broeckx et al. (2019) recently assessed landslide susceptibility and mobility rates for the area using a combination of logistic regression and Monte Carlo simulations. The study concluded that topography significantly affects landslide susceptibility. They attributed the larger landslide mobilization rates correlating highly with higher landslide susceptibilities to higher landslide quantity rather than magnitude. Ratemo & Bamutaze (2017) integrated qualitative data with geographic information systems (GIS) in analyzing risk elements and household vulnerability to landslides within Manafwa District in Uganda. This study found that 95% of the community was vulnerable to landslide hazards and the vulnerability was especially high in agricultural areas. In another study, landslide susceptibility was analyzed in terms of historical land use changes in eastern Uganda (Mugagga et al. 2012). The study reported that the encroachment onto critical slopes of the ecosystem resulted in a series of landslides in the area.

The Kenyan side of the MEE has been minimally studied. Mwangi & Mutua (2015) assessed climate change vulnerability for Kenya in terms of its exposure, sensitivity, and adaptive capacity characteristics. This study found that the Kenyan MEE was either moderately or highly vulnerable. The MEE landscape exhibits significant variability with vegetation greenness increase and decrease observed each year (Wanyama et al. 2020). This variability is attributed to the MEE's complex LULC orientation (Petursson et al. 2013), human activities (deforestation and forest degradation) and natural processes (changing climate regimes) (Wanyama et al. 2020), thus motivating a more comprehensive spatio-temporal assessment of the complex interrelationships in the area. While EEVA is not new, such a systematic study has not been conducted in the MEE. Besides, the current study does not focus on generation of eco-environmental vulnerability index (EEVI) surfaces as the only component; rather, it also explores changes in the time series of the variables used in an effort to explain the observed changes in the annual EEVI. As such, the study presents a systematic approach for comprehensively characterizing the nature and magnitude of eco-environmental vulnerability as well as factors influencing it.

This study assessed eco-environmental vulnerability for the MEE, a highly dynamic and significantly changing landscape. This study sought to quantitatively examine spatio-temporal patterns and trends in eco-environmental vulnerability, and factors driving the high variability observed in the MEE landscape. This study hypothesized that being mountainous, environmental vulnerability in the MEE varied significantly over distances as short as 5-10 km and was influenced greatly by multiple factors. Therefore, this study sought to answer the question: *how is environmental vulnerability distributed across the MEE, and what are the major factors driving these patterns?* To answer this question, the MEE was considered an integrated system, and its vulnerability was assessed using a novel combination of natural, environmental, and socio-economic data. With use of SPCA within GIS, this study effectively integrated variables computed

from remote sensing data (normalized difference vegetation index (NDVI)), digital elevation models (DEM), climate (precipitation and temperature), and socio-economic data (population density data) to compute an EEVI for the MEE. The final EEVI was categorized into five qualitative classes indicative of potential, slight, light, moderate, and severe vulnerability. This analysis highlighted the differentiated environmental vulnerability levels in the MEE and assessed, ranked, and identified areas where urgent action and the limited resources can be targeted. Additionally, spatio-temporal changes in precipitation concentration in the MEE were assessed using the precipitation concentration index (PCI). This was necessary to provide insights into the significant contribution of precipitation to overall vulnerability of the MEE. This analysis is a major step towards simultaneously conserving the natural environment and improving livelihoods that depend on it.

3.2 Materials and Methods

3.2.1 Study Area

The current study was conducted in the MEE located in western Kenya and eastern Uganda (Figure 3.1). The area is approximately 15,000 km^2 and extends from 1°37'42.82" N, 33°55'45.07" E to 0°42'15.76" N, 35°14'18.84" E. The mountainous area rises from a plateau that lies about 1,850-2,000 meters above mean sea level (amsl) in the east and 1,050-1,350 meters amsl to the west (Hamilton & Perrott 1981). Its vegetation is zoned by altitude (Petursson et al. 2013) and the montane Mount Elgon Forest (Doumenge et al. 1995) was gazetted in 1968 and 1992 in Kenya and Uganda respectively (Anseeuw & Alden 2010; Nakakaawa et al. 2015). The area is home to many important indigenous tree species (Petursson et al. 2013) including giant groundsel (*Senecio elgonensis*) and Elgon olive (*Olea hochstetteri*) (Wasonga & Opiyo 2018). There are two rainy seasons in the MEE. Most of the rain falls between April and October on the Ugandan side (with annual averages of 1,500-2,000 millimeters) (Mugagga et al. 2012).

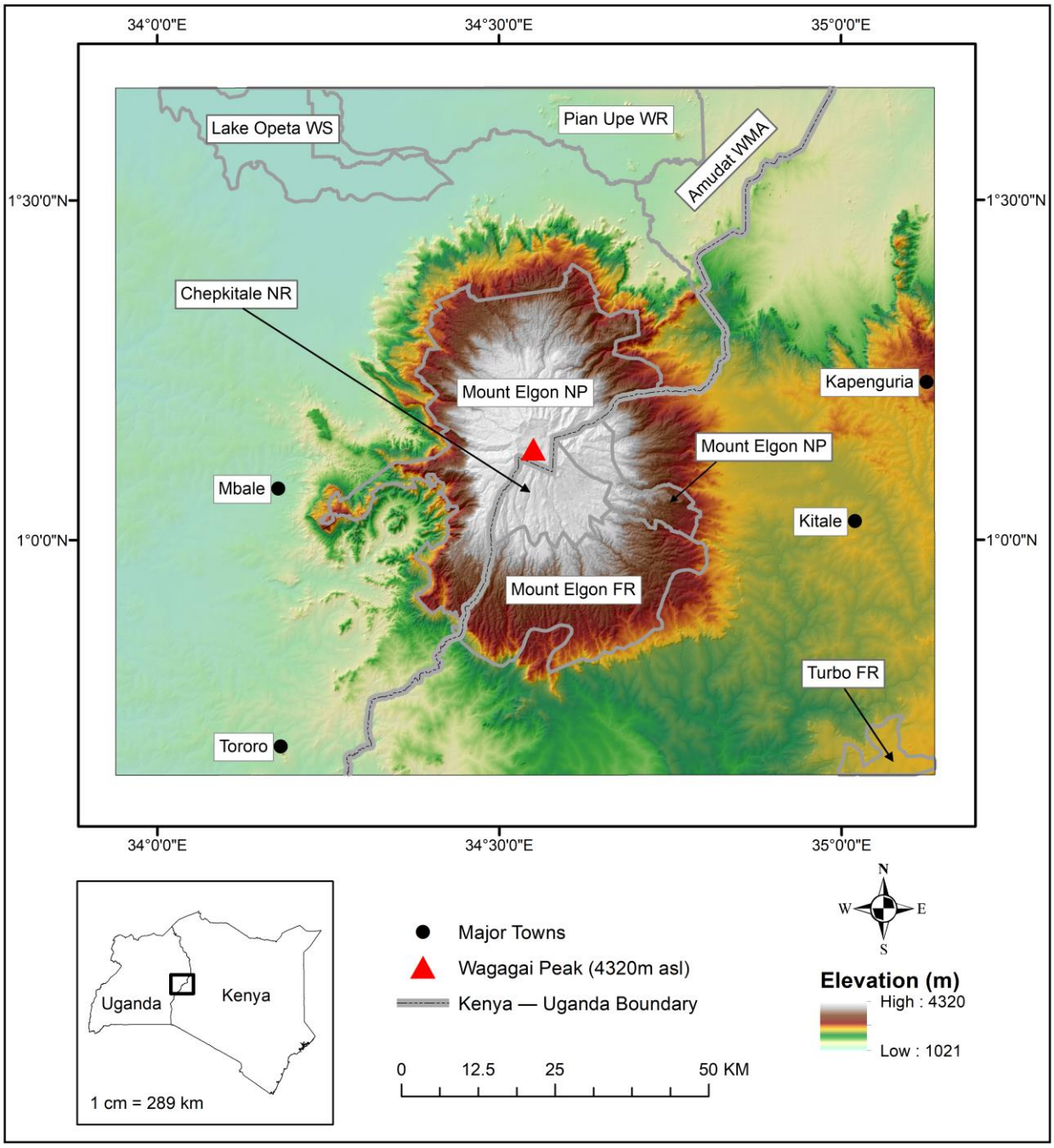

Figure 3.1. *Map of the MEE in eastern Uganda and western Kenya.* Elevation (meters amsl) and major protected areas are shown. Major towns are also shown for reference. It should be noted that FR is shorthand for forest reserve, NR is national reserve, NP is national park, WS is wetland system and WMA is wildlife management area.

The Kenyan side receives “long rains” between March and June – averaging 1,400-1,800 millimeters annually (Okello et al. 2010; Musau et al. 2015). The short rains, often received around

October-December, have become more erratic and largely unpredictable over time. There is marginal temperature variation for the area (15°C-23°C) on the Ugandan side (Mugagga et al. 2012) and 14°C-24°C on the Kenyan side (Musau et al. 2015)). For mountainous regions like this, however, temperature and precipitation vary significantly with changes in altitude and relative location of windward and leeward sides of the mountain (see, for example, Van den Hende et al. (2021)).

Significant interannual variability exists in the MEE landscape. This is attributed to various processes, including a substantial increase in post-2000's precipitation, agricultural expansion (Wanyama et al. 2020) and complex LULC orientations (Petursson et al. 2013). In addition, the MEE is composed of various microecosystems, thus some places have favourable climates (especially on higher altitudes) while others do not (at lower altitudes) (Mumba et al. 2016). This variability therefore impacts MEE livelihoods which are also threatened by increasing natural hazards (e.g., floods, droughts, landslides) resulting from changing climate regimes.

3.2.2 Data Sources

This study uses daily precipitation records from CHIRPS (Climate Hazards group Infrared Precipitation with Stations) (Funk et al. 2015), monthly maximum temperature records from CHIRTS (Climate Hazards Center Infrared Temperature with Stations) (Funk et al. 2019), 16-day NDVI from Moderate Resolution Imaging Spectroradiometer (MODIS) (Didan 2015), annual population density data from WorldPop (WorldPop Project 2020), and Shuttle Radar Topography Mission (SRTM) DEM from United States Geological Service (United States Geological Service 2000). CHIRPS data are available at 5 km spatial resolution and provide global daily and pentad records from 1981 to present. Daily records for the 1986-2018 period were obtained and preprocessed within Google Earth Engine (GEE) (Gorelick et al. 2017) and used to generate precipitation indices used in this study. CHIRTS data were created at the Climate Hazards Center (CHC) at University of California, Santa Barbara (Climate Hazards Center 2018), by blending

gridded thermal infrared data with station data to create a seamless, high resolution Tmax (maximum temperature) dataset that has been found to correlate very highly with observation data in the continent of Africa (Funk et al. 2019). This temperature dataset, for the 1986-2016 period, was used to compute temperature variables necessary for assessing the eco-environmental vulnerability of the MEE. NDVI data were obtained from MOD13Q1.V6, the 250-meter, 16-day MODIS composite. This dataset, extending over the period 2001-2018, was obtained through AppEEARS, https://lpdaacsvc.cr.usgs.gov/appeears/ (AppEEARS Team 2019). The WorldPop population density dataset (WorldPop Project 2020) is available at 1 km spatial resolution (at the Equator) and 2000-2020 temporal coverage. This dataset, for the period 2001-2018, was used to assess changes in population density and distribution within the MEE. The SRTM DEM data, available at 30-m spatial resolution, were downloaded from GEE (Gorelick et al. 2017) and used to assess the effect of topography on general eco-environmental vulnerability of the MEE.

Table 3.1. *Properties of datasets used in this study.*

Dataset	Spatial Resolution	Temporal Resolution	Source
Precipitation	5km	1986-2018	CHIRPSDaily (Funk et al. 2015)
Temperature	5km	1986-2016	CHIRTSMax Monthly (Funk et al. 2019)
SRTM DEM	30m	2000	United States Geological Service (United States Geological Service 2000)
NDVI	250m	2001-2018	MODIS (Didan 2015)
Population density	1 km	2001-2018	WorldPop (WorldPop Project 2020)

3.2.3 Generation and Justification of Variables Used

The choice of criteria for evaluating vulnerability is crucial and one should identify criteria that are both representative and adaptable (Hou et al. 2015). Also, for easier interpretation, variables used in the EEVA should have a directly proportional relationship with eco-environmental vulnerability. Since the environment is highly dynamic and significantly impacted by both natural processes (e.g., precipitation distribution, drought occurrence etc.) and human

impacts (e.g., deforestation, afforestation, agricultural practices etc.), a reliable EEVA should consider both natural and social system variables. In this study, eco-environmental vulnerability of the MEE was assessed using both agriculture- and general environment-related variables. These variables were selected based on literature (Nguyen et al. 2016; Sahoo et al. 2016; Simane et al. 2016; Parker et al. 2019), prior knowledge of the MEE, and insights from a 2019 field study in the area. Variables were selected to capture the effects of climate (precipitation and temperature), LULC change, population density and topography on the stability of an ecosystem that is heavily farmed, encroached and therefore experiencing significant interannual variability. All variables were normalized to range from 0 to 1 to allow for easier interpretation and comparison across variables. The variables were also resampled to 30-meter spatial resolution.

While agriculture remains the mainstay for most of East Africa, its dependence on natural processes makes the sector highly vulnerable to the impacts of climate change and variability (Wanyama et al. 2019), thus influencing food insecurity in the region (Kotikot et al. 2018). The effect that variability in precipitation has on the stability of the region cannot be contested. Precipitation, combined with temperature, drives important ecosystem processes. Significant variability in precipitation will lead to ecological degradation which will disrupt nature-dependent systems and practices, like rain-fed agriculture. For instance, under RCP 4.5 and 8.5, the 2070s climate will drive significant changes in spatial distribution of maize cropping in Kenya (e.g., some currently suitable areas in Narok and Siaya counties will become unsuitable for currently grown maize cultivars, while currently unsuitable areas in Nakuru and Kericho will become suitable) (Kogo et al. 2019). This shift in suitability therefore means that maize will replace some higher-value cash crops (e.g., tea in Kericho), thus amplifying the economic effects of climate change. Even with some projected increases in precipitation, the agricultural sector is unlikely to benefit because of other unfavourable aspects (e.g., timing and spacing of rainfall) (Bryan et al. 2013). In response to diminishing yields, and exacerbated by substantially increasing populations, many

people have expanded land under agriculture, often at the expense of natural vegetation (Maitima et al. 2009; Wanyama et al. 2020). Thus, variability in precipitation, coupled with significant warming trends, poses a substantial threat to the sustainability of both the environment and agricultural sector. In this study, eco-environmental vulnerability related to precipitation variability was assessed. Three precipitation variables were computed from daily records, including number of dry days (NDD), number of extreme events (NXE) and precipitation Z-scores during the growing season. Here, a dry day was defined as any day, between April 1 and June 30 (AMJ), when total precipitation amount was less than or equal to 2 mm. NDD was used to assess the influence of water shortage that occurs within the growing season, thus having negative influence on crop growth and yield. Therefore, the higher the NDD, the more vulnerable the area is. An extreme event was defined as any day within AMJ when precipitation exceeded 20 mm. NXE was used to evaluate the occurrence of extreme rainfall events within the growing seasons, events that likely induce flooding that destroys crops, property, and lives. The higher the NXE, the higher the vulnerability of the area. These two variables were defined following Haghtalab et al. (2019, 2020). Precipitation Z-scores were calculated by first computing total precipitation amounts for AMJ for each year from 1986 to 2018 and calculating a long-term mean (LTM) and standard deviation (LTSD). Then, the LTM was subtracted from each year's total precipitation and the result divided by the LTSD (Equation 1). 1986-2018 was used because the same period was used in the preceding study in the MEE (Wanyama et al. 2020), but also because 34 years are enough for an accurate estimation of climatology (Winkler et al. 2018).

$$Z_a = \frac{X_a - LTM}{LTSD} \quad (1)$$

where Z_a is the Z-score for year *a*; X_a is the AMJ total precipitation amount for year *a*; *LTM* is the long-term mean; and *LTSD* is the long-term standard deviation.

Precipitation Z-score was specifically meant to detect drying patterns in MEE precipitation, so all values with positive Z-scores were set to 0. To establish a directly proportional relationship with eco-environmental vulnerability, values were transformed to absolute non-negative values. As such, highest values were indicative of highest eco-environmental vulnerability.

Persistent warming has been reported in East Africa since 1960s (Githui 2008; Ongoma & Chen 2017; Musau et al. 2018) with a warming of 1.5-2.0 °C observed over the past 5 decades (Daron 2014). These high temperatures result in higher evapotranspiration rates (Seneviratne et al. 2012; Wanyama et al. 2019; Ayugi et al. 2020) and this has been linked to an observed or projected increase in frequency and intensity of droughts (Nguvava et al. 2019; Ayugi et al. 2020). Since the majority of the MEE depends heavily on rain-fed agriculture, such warming and intensified droughts have adverse impacts on farming practices and ultimately on local livelihoods. For example, higher evaporation reduces the amount of water available to the crops (Wanyama et al. 2019) and higher temperatures accelerate crop growth leading to lower yields due to reduced gap-filling (Hatfield & Prueger 2015). Therefore, to characterize the influence of the warming on eco-environmental stability, temperature Z-scores were calculated in a similar fashion as precipitation Z-scores above. However, the temperature data spanned 1986-2016 (CHIRTS data are currently available until 2016) and temperature means over AMJ were calculated. Since this variable was meant to detect warming patterns in MEE temperatures, all negative Z-scores were set to 0. As such, the highest values indicate locations of highest vulnerability.

Vegetation coverage and population changes are both important factors influencing eco-environmental processes. LULC change (driven by, among other factors, increasing populations and a changing climate) has far-reaching impacts ranging from ecological, physical and socioeconomic effects (Pellikka et al. 2013) (for instance, see Salazar et al. (2015), Feddema et al. (2005), Turner II et al. (2007), and Mugagga et al. (2015)). These changes can alter land-atmosphere interactions, hence modifying local and global climates. In heavily agricultural areas

with consistently increasing populations like the MEE, such changes present a significant threat to both the environment and people's livelihoods. In this study, changes in vegetation greenness were assessed using NDVI anomalies (deviations from LTM). First, AMJ seasonal means were calculated for each year (2001-2016). Then, anomalies were generated for each year using the 'anomalize' function in the 'remote' package in R (Appelhans et al. 2016). Since this variable was used to assess the effect of generally decreasing greenness due to major activities (like deforestation) and subtle changes (like vegetation degradation), all positive anomalies were set to zero. Values were then transformed to absolute (non-negative) values to establish a directly proportional relationship with eco-environmental vulnerability. Therefore, locations with little or no tree cover will have to cope with higher eco-environmental vulnerability compared to highly vegetated areas like forests.

Assessing changes in population was necessary in this study because many studies have linked population growth to major LULC changes (Metzger et al. 2006; Wu & Zhang 2012; Ayuyo & Sweta 2014) that greatly influence eco-environmental stability. For instance, regions with quickly increasing populations have experienced significant expansion of land under agriculture and settlement as communities strive to increase food production. Also, sparsely populated areas like savannas and grasslands generally experience less anthropogenic interference and are therefore more stable compared to overpopulated areas. In this study, several population density variables were generated and assessed; ultimately, raw values were found suitable. The existence of extreme values (mainly in urban areas) affected distribution of values in less densely populated areas, and therefore, population distribution patterns were hardly detectable. For this reason, a cutoff value was explored. To find outliers for each year, we used the 'boxplot.stats' function in 'grDevices' package (R Core Team 2016). Here, we computed boxplot statistics (minimum, lower quartile, median, upper quartile, and maximum values) and returned values of data points less than (greater than) the minimum (maximum). From these, we selected the

minimum value to create a series of “minimum extreme values” for 2001-2018, and the cutoff was calculated as the median value from this series. All pixel values greater than the cutoff were then set to this value (Equation 2). This variable was used to assess the contribution of population density to eco-environmental vulnerability of the MEE.

$$\text{IF } \mathrm{POP_n} > \mathrm{CUTOFF}, \text{then } \mathrm{POP_n} = \mathrm{CUTOFF}, \text{else PASS} \quad (2)$$

where POP_n is the population density for year *n*; $CUTOFF$ is the cutoff value; and *PASS* means “do nothing”.

Eco-environmental vulnerability is also strongly influenced by topographic variables (e.g., elevation, slope, and slope aspect). These variables play an important role in defining landscape conditions and determining the features of the land surface (e.g., potential for natural hazards, incoming solar radiation and LULC types (Eliasson et al. 2010; Nguyen & Liou 2019)). Elevation greatly influences regional climate regimes, evapotranspiration, and soils (Nguyen et al. 2016). Temperatures decrease with increase in altitude and some locations receive more rainfall than others, depending on their orientation relative to the mountain. Slope, on the other hand, influences various physical processes. For instance, magnitude of slope and general ‘hilliness’ of an area influence rainfall amounts received. Slope also influences soil erosion and landslides, with steeper slopes posing a higher risk for occurrence. Due in part to its topographic orientation, the MEE consists of various microecosystems, with higher altitudes generally exhibiting favourable climates compared to lower altitude areas (Mumba et al. 2016). Thus, two topographic variables (elevation and slope) were used to assess the effect of topography on eco-environmental vulnerability. For elevation, a cutoff value was first obtained at the 90th percentile. Higher values were then set to this cutoff (like population density above) since these generally represented stable mountain locations unpopulated by humans. Percent slope was also calculated, and values higher than 30 percent were excluded, because slopes higher than this

generally limit access and diminish land suitability for some socio-economic activities (e.g., maize farming) (Wang 2015; Wanyama et al. 2019).

3.2.4 Methods

This section describes the methods and analyses performed to characterize patterns of eco-environmental vulnerability in the MEE. The analyses included computing EEVI, assessing spatio-temporal patterns of change in multi-year variables, and characterizing precipitation concentration in the MEE. These analyses were performed in R (R Core Team 2018).

3.2.4.1 Spatial Principal Components Analysis

To compute an EEVI for the MEE, this study implemented principal components analysis (PCA), which has been applied in various studies (Li et al. 2006; Hou et al. 2015; Zou & Yoshino 2017). PCA reduces the dimensionality of data, increasing interpretability while minimizing loss of information (Pearson 1901). It linearly transforms original variables into a set of uncorrelated variables (called principal components, PCs), thus making it one of the simplest dimensionality reduction techniques (Jolliffe 1990). PCA can be expressed as follows:

$$Y = n_1x_1 + n_2x_2 + n_3x_3 + n_{\mathrm{m}}x_{\mathrm{m}} \quad (3)$$

where *Y* is the PC score; *n* is the component loading; *x* is the measured value of a variable; and *m* is the total number of variables (Hou et al. 2015).

The importance of a PC is ranked, denoted by eigenvalues, based on the amount of variance it captures in the original data (Hou et al. 2015; Zou & Yoshino 2017). For spatial data, SPCA is used and the technique transforms attributes in a multiband spatial dataset into a new multivariate space whose axes are rotated with respect to the original space (Hou et al. 2015; Zou & Yoshino 2017).

SPCA was used in this study to decompose climate, topography, population density and vegetation greenness variables to generate annual EEVI for the MEE (for 2001-2016). SPCA was

a suitable method since there was no clear understanding of the nature of patterns within these variables (Hou et al. 2015). The 'rasterPCA' function in the 'RStoolbox' package (Leutner et al. 2019) in R statistical software was used. SPCA results were assessed and for each year, the first five PCs were retained to compute EEVI using the equation below.

$$EEVI_i = n_1PC_1 + n_2PC_2 + n_3PC_3 + n_4PC_4 + n_5PC_5 \quad (4)$$

where $EEVI_i$ is the eco-environmental vulnerability index for year *i*; PC_1 is the first principal component; and n_1 is the contribution ratio of the first principal component (Hou et al. 2015).

The computed EEVI surfaces were reclassified into five qualitative groups indicative of different levels of eco-environmental vulnerability in the MEE. The equal interval classification scheme was applied, although other data classification schemes were explored. The scheme is useful when the objective is to put emphasis on the amount of an attribute value relative to another value (Torresan et al. 2012). Therefore, this method allowed for comparison of EEVI across years. This classification scheme has previously been used in similar studies (Torresan et al. 2012; Žurovec et al. 2017; Parker et al. 2019). Table 2 shows class ranges used in this study.

Table 3.2. *Value ranges for different levels of eco-environmental vulnerability in the MEE.*

Class	Range
Potential	0.383 - 0.586
Slight	0.181 - 0.383
Light	-0.022 - 0.181
Moderate	-0.225 - -0.022
Severe	-0.427 - -0.225

PCA was also performed on each of the original temporal series of NDVI, temperature, precipitation, and population density variables. This temporal PCA (TPCA) was necessary to identify persistent patterns of change in each variable over time. To do this, time series rasters of these variables (2001-2018 for precipitation, NDVI and population density, and 2001-2016 for temperature) were used, and only PCs explaining more than 1% of the variance were considered significant.

3.2.4.2 Precipitation Concentration Index

Given that significant changes in precipitation have been reported previously, especially post-2000 (Wanyama et al. 2020), this study assessed spatio-temporal changes in distribution of MEE precipitation over 34 years (1986-2018). Monthly precipitation totals for this period were used to compute the PCI (Oliver 1980; De Luis et al. 2011). PCI was preferred in this study because it is a powerful measure of precipitation distribution over time (De Luis et al. 2011). The index was calculated on two scales: annual and supra-seasonal. The supra-seasonal ranges were defined generally as wet (January-June) and dry (July-December). The annual and supra-seasonal PCI were computed according to Equations 5 and 6, respectively.

$$\mathrm{PCI}_{annual} = \frac{\sum_{i=1}^{12} p_i^2}{\left(\sum_{i=1}^{12} p_i\right)^2} * 100 \quad (5)$$

$$\mathrm{PCI}_{supraseasonal} = \frac{\sum_{i=1}^{6} p_i^2}{\left(\sum_{i=1}^{6} p_i\right)^2} * 50 \quad (6)$$

where p_i is the monthly precipitation in month *i* (De Luis et al. 2011).

PCI values range from 8.3 (uniform precipitation concentration) to 100 (irregular precipitation distribution) with increasing values denoting an increased monthly precipitation concentration (Oliver 1980). Oliver (1980) proposed that, on the annual and supra-seasonal scales, PCI values less than 10 indicate uniform precipitation distribution (lowest precipitation concentration), values between 11 and 20 show a seasonal distribution while values greater than 20 denote an irregular distribution. In this study, the PCI was used to show that distribution of MEE precipitation has significantly changed over time. As such, the Mann-Whitney *U* test, a non-parametric test, was applied to assess the statistical difference in precipitation concentration between the first 11 years (1986-1996) and last 11 years (2008-2018). The 11-year periods were used here because they were used in a previous study for the same study area (Wanyama et al. 2020). Such statistical comparison has been performed in previous studies (De Luis et al. 2011; Kibret et al. 2019). PCI change results were assessed at the 95 percent significance level.

3.3 Results

This study characterizes, using SPCA, TPCA and PCI, patterns of eco-environmental vulnerability in the MEE. The results highlight levels of eco-environmental vulnerability and areas of persistent changes in precipitation, NDVI, and population density. Results from PCI analysis are also presented and, together, attempt to comprehensively characterize eco-environmental vulnerability and the variability observed over the MEE.

3.3.1 Eco-environmental Vulnerability

3.3.1.1 SPCA Results

The first five PCs were retained to compute EEVI in this study. Together, these PCs explained more than 95% of the variance in the original eight variables included in the study. An example of the breakdown of variable loadings is shown in Tables 3, 4 and 5 for 2001, 2008 and 2016, respectively. Figures 3.2 and 3.3 show the five PCs in 2001 and 2016.

Table 3.3. *Loadings for the first five PCs in 2001.* Note that major loadings for each PC are shown in **bold**.

Variable	PC1	PC2	PC3	PC4	PC5
Elevation	**0.842**	0.051	**0.430**	**0.316**	0.005
Slope	**0.457**	-0.185	**-0.860**	-0.014	-0.128
Precipitation Z-scores	0.018	0.002	0.004	0.057	0.000
Temperature Z-scores	0.000	0.000	0.000	0.000	0.000
Number of dry days	0.155	0.174	0.157	**-0.661**	**-0.676**
Number of extreme events	**0.232**	-0.137	0.063	**-0.677**	**0.676**
NDVI	-0.045	-0.072	-0.030	0.037	0.163
Population density	-0.046	**-0.953**	0.212	-0.006	-0.207

Table 3.4. *Loadings for the first five PCs in 2008.* Note that major loadings for each PC are shown in **bold**.

Variable	PC1	PC2	PC3	PC4	PC5
Elevation	**0.841**	0.013	**0.322**	**0.280**	**0.241**
Slope	**0.449**	-0.101	**-0.777**	**-0.425**	-0.007
Precipitation Z-scores	0.084	-0.099	**0.423**	**-0.703**	**0.252**
Temperature Z-scores	-0.103	0.091	-0.039	-0.177	-0.159
Number of dry days	0.110	0.139	**0.324**	**-0.426**	**-0.517**
Number of extreme events	**0.241**	-0.060	0.029	0.183	**-0.763**
NDVI	0.003	0.019	-0.002	-0.005	0.001
Population density	-0.052	**-0.974**	0.083	0.031	-0.063

Table 3.5. *Loadings for the first five PCs in 2016.* Note that major loadings for each PC are shown in **bold**.

Variable	PC1	PC2	PC3	PC4	PC5
Elevation	**0.849**	0.055	**0.451**	**0.251**	0.064
Slope	**0.461**	0.107	**-0.878**	0.010	-0.072
Precipitation Z-scores	0.000	0.000	0.000	0.000	0.000
Temperature Z-scores	-0.000	0.002	0.002	-0.004	0.009
Number of dry days	0.012	-0.055	0.082	0.006	**-0.973**
Number of extreme events	**0.223**	0.057	0.113	-**0.966**	0.000
NDVI	0.072	0.005	0.045	0.038	**-0.204**
Population density	-0.110	**0.989**	0.068	0.041	-0.049

The amount of variance captured by each PC varied over time, and generally, the first PC averagely accounted for about 50%. This PC was heavily loaded on elevation, slope and NXE variables. The second PC, which explained about 25% of the variance, was loaded mostly on population density. Notice that the loading for this PC shifts between positive and negative (Tables 3, 4 and 5), thus introducing the visible changes in distribution of the PC values over the years (e.g., compare Figures 3.2B and 3.3B). The third PC (approximately 10% of variance) was mostly

a linear function of slope and elevation, as well as climate variables in some years (see Table 4). Loadings of the fourth and fifth PCs exhibited major changes from year to year, but climate variables (NXE and NDD) together with elevation were common components. These two PCs explained about 10% of the variance in the original data.

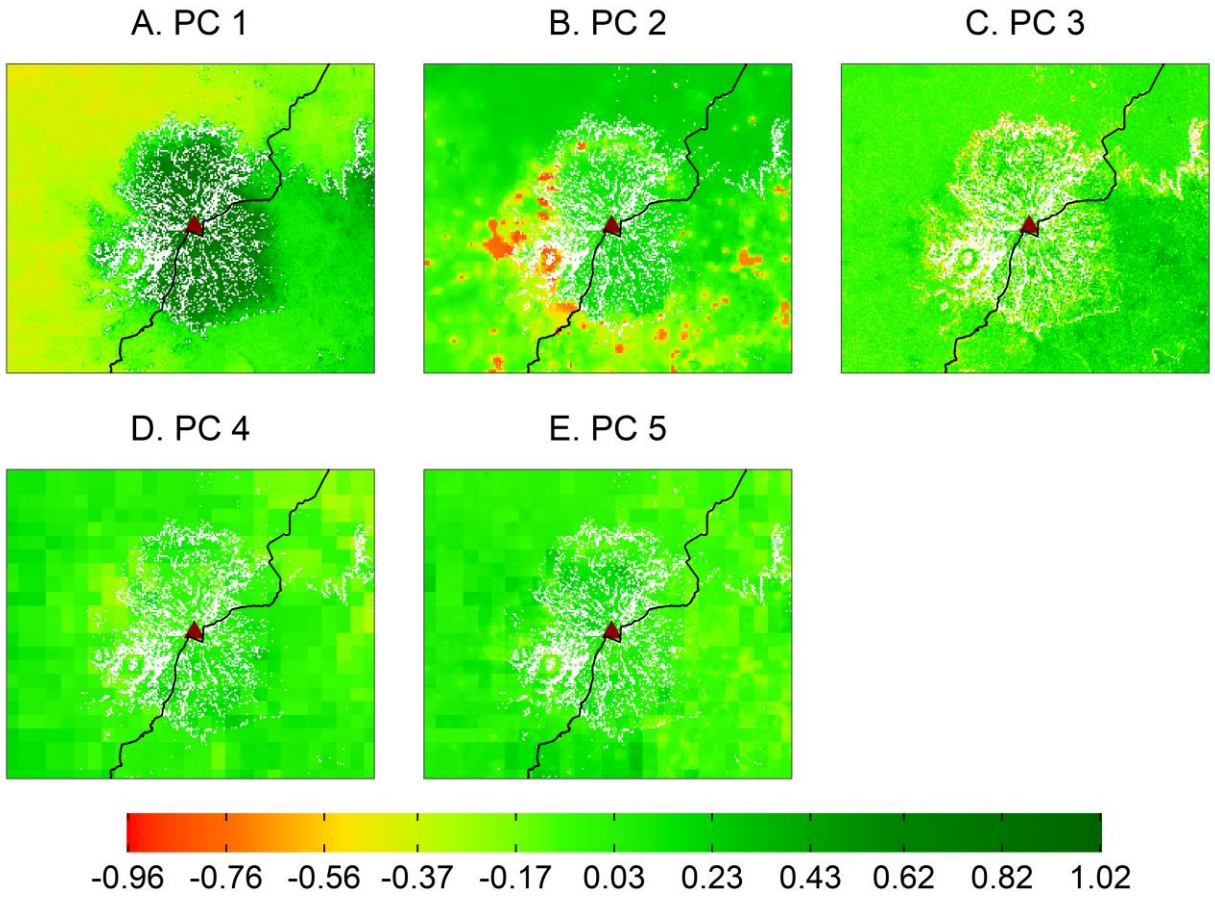

Figure 3.2. *The first five PCs used to compute EEVI for 2001.*

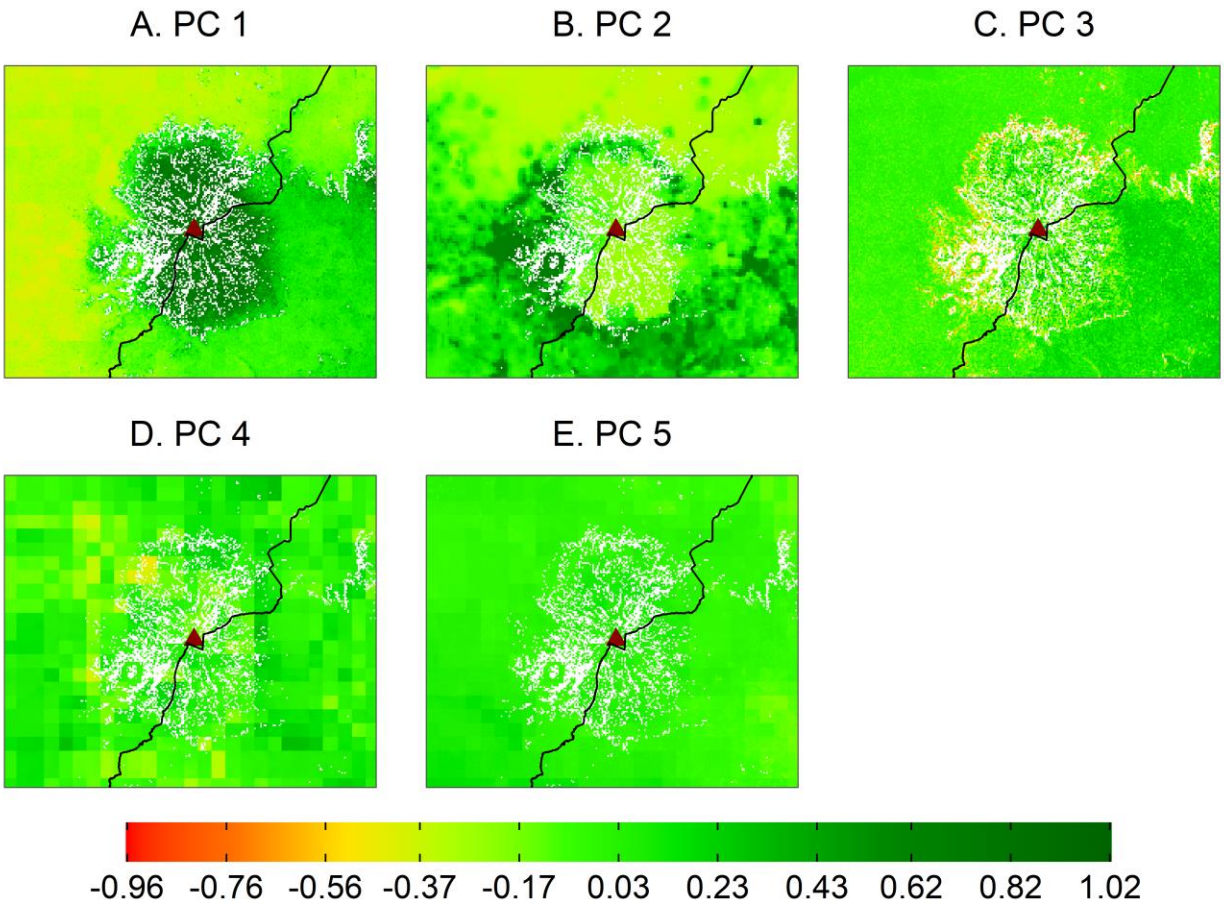

Figure 3.3. *The first five PCs used to compute EEVI for 2016.* It should be noted that the scale in this figure is same as in Figure 3.2.

3.3.1.2 Eco-environmental Vulnerability Index

In this study, eco-environmental vulnerability was defined as the risk of damage to the natural environment (Nandy et al. 2015). As such, this study was conducted to evaluate the natural resource system affected by both natural and human activities within the MEE. Results show that 38% of the MEE (5,700 km^2) is moderately vulnerable (Figure 3.4). These areas are mostly grasslands and agricultural land in the northwestern and western parts of the MEE, respectively. Highest proportions of this vulnerability level were observed in 2005 (52%), 2008 (50%), 2001 (47%), 2012 (45%) and 2014 (43%) when most of the savannas were also moderately vulnerable. The second highest proportion of the MEE was lightly vulnerable, and these areas majorly included areas in the southeastern MEE, which are primarily composed of mixed land uses (cropland, shrubland, grassland). This vulnerability class was the most static of

all, as no major changes in proportion and locations were observed across the 16-year period (with percent proportions ranging from 24 to 29%).

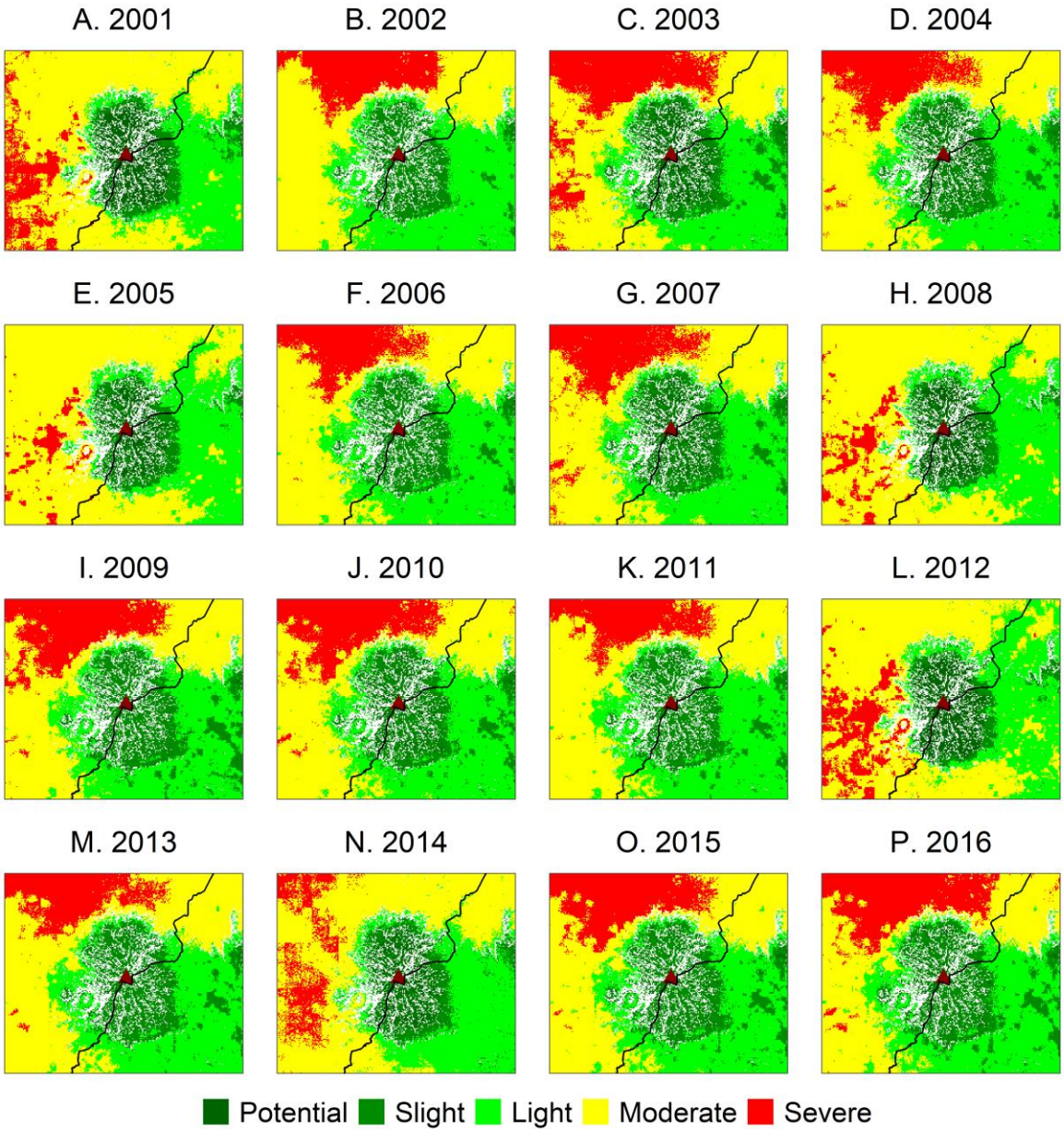

Figure 3.4. *EEVI for each year from 2001 to 2016.* Notice that eco-environmental vulnerability varies over time, but persistent patterns exist in space. EEVI increases with decrease in elevation.

There was generally an equal proportion of land in the severe and potential vulnerability classes (both averaging 12% (1,800 km^2) over the 16 years). High elevation (>2,000 m amsl) locations on the Afromontane forest constituted the slight vulnerability class, and these generally

remained stationary throughout the study period. On the other hand, savannas in northern MEE represented most of the land under the severe class, although some agricultural lands in eastern MEE were also found in this class, especially during 2001, 2003, 2008, 2012 and 2014. Some of the high elevation areas of Mount Elgon fell into the smallest class (proportions ranging from <1 percent to about 8%). Land under this class was highest in 2001, 2012 and 2008 (1,200 km^2, 1,200 $km^2$and 1,000 km^2, respectively) and least in 2009, 2011 and 2013 (approximately 20 km^2, 30 km^2 and 30 km^2, respectively). It is worth mentioning that the proportion of land under the potential and moderate vulnerability classes exhibited a generally decreasing trend over time (Figure 3.5A and D), while a positive trend was observed in the slight, light, and severe vulnerability classes (Figure 3.5B, C, and E).

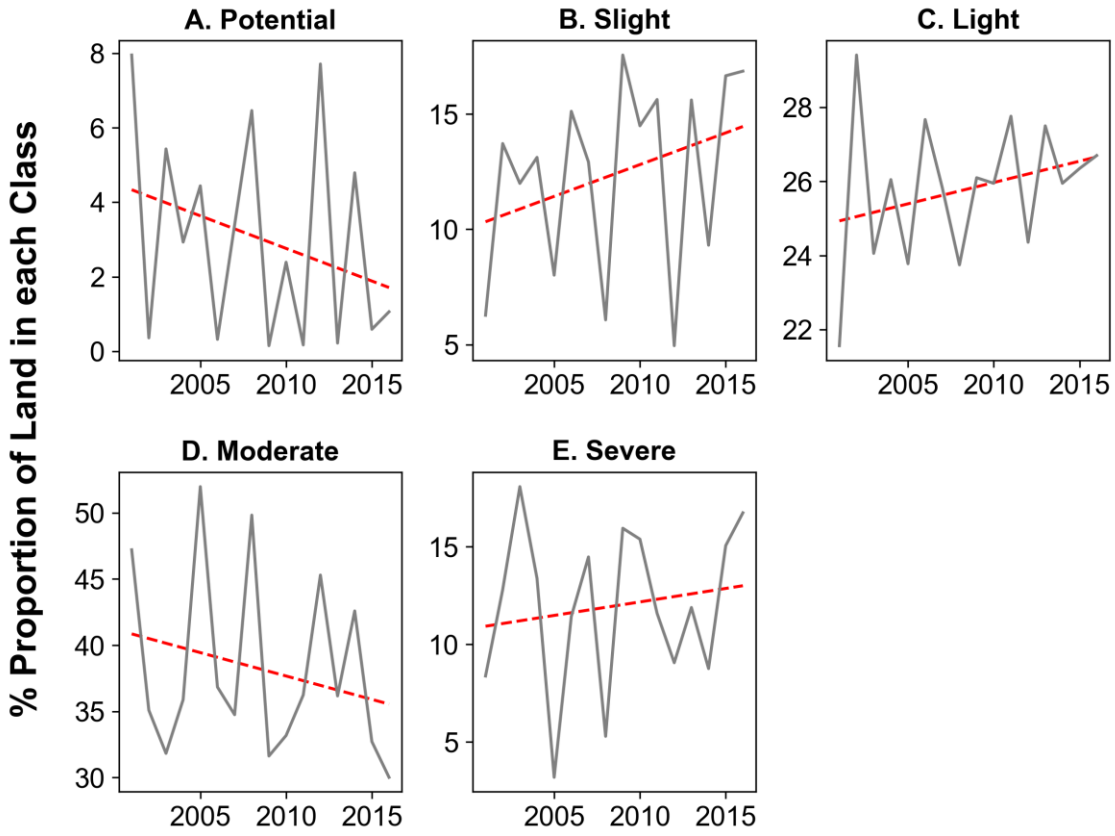

Figure 3.5. *Percent proportion of land under each EEVI class from 2001 to 2016.* The red lines represent fitted linear trends for each series.

3.3.1.3 TPCA Results

Results from decomposing the temperature time series (2001-2016) are not provided because no significant patterns in MEE temperatures were found. For precipitation time series (2001-2018), each of the first three PCs explained more than 1% of the variance. PC1 revealed the general spatial distribution of precipitation in the MEE (Figure 3.6A). Savanna and grasslands in northeastern MEE are the driest while the Afromontane forest and parts of southern MEE are the wettest. The second and third PCs (Figures 3.6B and C) showed varying trends in precipitation possibly related to topography. Such persistent changes in precipitation may be responsible for major changes in eco-environmental vulnerability over the years (Figure 3.4).

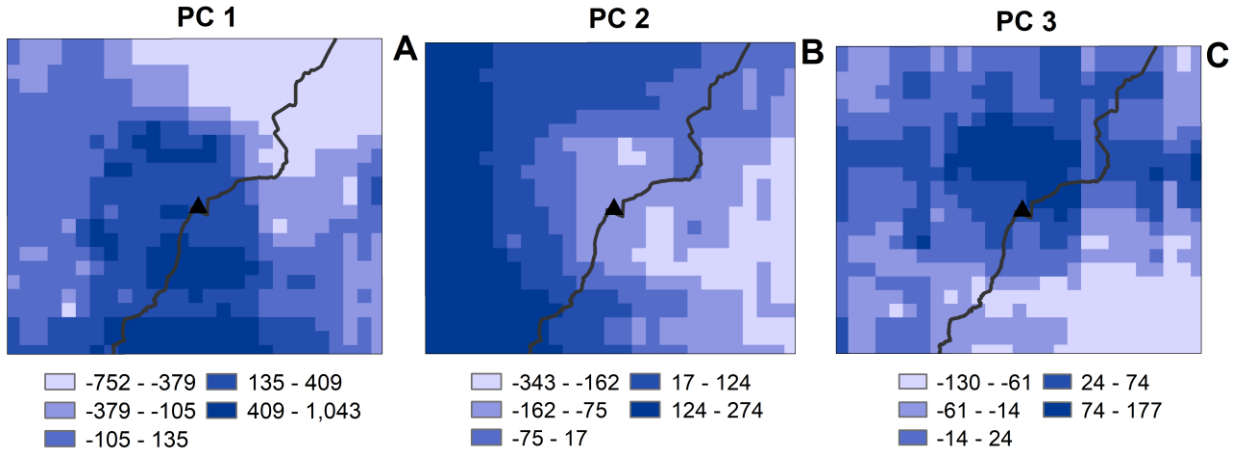

Figure 3.6. *Important PCs obtained from the precipitation time series (2001-2018) using TPCA.*

The first two PCs from the NDVI time series (2001-2018) decomposition contained important information. PC1 captured the distribution of major LULCs in the MEE (Figure 3.7A). Here, the Afromontane forest in central MEE, savanna and grasslands in north and northeast, and agricultural land were all identified. Equally interesting is PC2 (Figure 3.7B) which delineated locations of major greening (in the northern MEE and high elevation areas of the mountain) and browning (especially in southwestern MEE and the edges of the mountain forest). Results from decomposing the population density time series (2001-2018) revealed the general distribution of the population in the MEE (Figure 3.7C). Here, urban centers and other highly populated areas

(mostly agricultural lands) were identified. Least populated areas were found in most of the savannas and grasslands as well as high elevations.

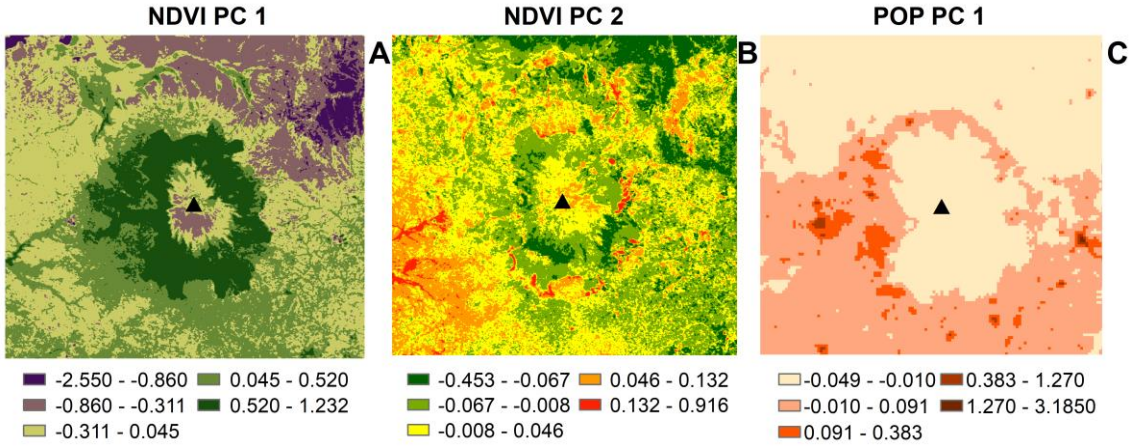

Figure 3.7. *The first two PCs from NDVI time series (A and B) and the first from population density time series (C).*

3.3.2 Precipitation Concentration in the MEE

Assessment of PCI over the dry period yielded only a few locations in southwestern MEE with significantly different precipitation concentration between 1986-1996 (first 11 years) and 2008-2018 (last 11 years). This result is not provided in this study. Figure 3.8 shows locations where PCI values for 2008-2018 were greater than 1986-1996 for both the annual (Figure 3.8A) and wet season (Figure 3.8B) periods. In these locations, there is a more than likely probability ($p<0.05$) that precipitation concentration was greater in the later period than the previous. This is especially true for western MEE (on the annual scale) and the west-to-northeastern stretch of the MEE (for the wet season).

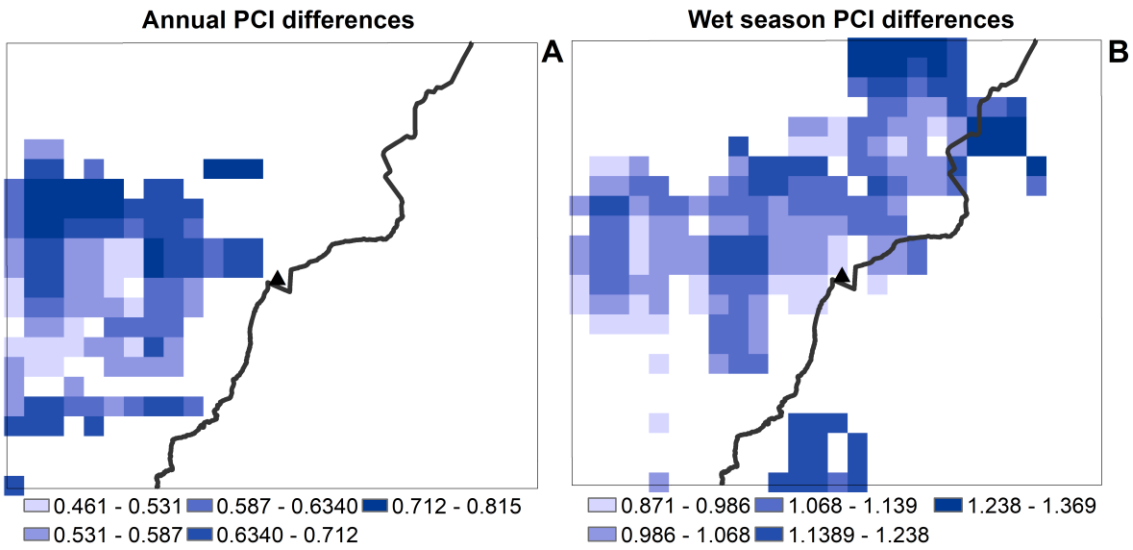

Figure 3.8. *Locations where precipitation concentration in last 11 years (2008-2018) was significantly ($p<0.05$) greater than the first 11 years (1986-1996).*

3.4 Discussion

3.4.1 Eco-environmental Vulnerability in the MEE

Climate change continues to affect most developing nations, especially those relying on rainfed agriculture (Wanyama et al. 2020). The vulnerability of the agriculture sector is worsened by the intensifying and more frequent natural disasters coupled with significant environmental change. In the MEE, a largely agricultural area, populations have increased to approximately 1,000 people per km^2 in some areas (Nakakaawa et al. 2015; Vlaeminck et al. 2016). Here, farm sizes are consistently shrinking as populations increase, and this signals mounting pressure on land (Nakakaawa et al. 2015; McKinney & Wright 2021). The need to increase food production has fueled encroachment on ecologically fragile land (Nakileza & Nedala 2020) and illegal access to PAs (McKinney & Wright 2021). As a result, this LULC change has, in part, modified local ecosystem functioning (Omwenga et al. 2019), intensified climate-related hazards (Nakakaawa et al. 2015; EAC et al. 2016) and introduced and/or increased significant interannual variability (Wanyama et al. 2020). Moreover, precipitation concentration is amplifying notably in the wet season (Figure 3.8), thus adding another layer of risk for agriculture and ultimately for local

community livelihoods. These complex human-environment interactions in the MEE therefore underpin the region's eco-environmental vulnerability. Yet characterizing this vulnerability is marred by the absence of data at appropriate spatial and temporal scales and inadequacies in practical methodologies.

Representing vulnerability as a single index provides important information about the degree of vulnerability, and helps identify most vulnerable regions (Žurovec et al. 2017) where action can be targeted. Outputs from these analyses are maps which generally reflect the kind of datasets and methods used, as well as decisions about data aggregation, variable weighting and resolution of the analysis (Abson et al. 2012). PCA has commonly been used in these studies, especially when no prior knowledge exists about patterns in the variables (Hou et al. 2015). PCA doesn't weight original variables; rather, it provides relative vulnerability relating to how individual drivers of vulnerability co-vary in space (Abson et al. 2012; Defne et al. 2020). It is therefore a good source of information about how multiple variables interact, aggregate and affect a given location (Defne et al. 2020). This is important, as human-environment systems are known to have complex interactions and therefore intricate interrelationships among biophysical and socio-political factors. By aggregating these variables into a single vulnerability index, therefore, locations experiencing highest cumulative vulnerability can be delineated. This does not mean that important underlying information about the variables is lost; policymakers can assess the retained PCs and identify, based on their knowledge, drivers or types of vulnerability that are most important in their context (Abson et al. 2012).

The present study found that majority of the MEE (comprising savannas, grasslands, and most of the agricultural land in Ugandan MEE) was moderately vulnerable based on the analysis methods and variables used. A majority of the savannas and grasslands were severely vulnerable, and this has also been reported elsewhere by Jiang et al. (2018). Eco-environmental vulnerability also varies in time with increases in the 'slight', 'light' and 'severe' categories. This

temporal dependence means that eco-environmental vulnerability is a function of multiple local factors, often operating at a range of space and time scales. This dynamism constrains the validity of vulnerability scores to specific scales (Aretano et al. 2015). The temporal variability in eco-environmental vulnerability over the 2001-2016 period was related to multi-year variables derived from precipitation (NDD, NXE, precipitation Z-scores), temperature (temperature Z-scores) and population density. Therefore, it can be inferred that the MEE will continue to experience significant interannual variability in eco-environmental vulnerability as the climate system changes and populations increase particularly in the northwestern part of the domain (Figure 3.4). It should also be noted that, being mountainous, topographic variables (elevation and slope) also had a substantial influence on the vulnerability of the MEE - with EEVI markedly increasing with decrease in elevation. Previous studies have also found that topographic characteristics and precipitation significantly influence eco-environmental vulnerability (Nguyen et al. 2016; Jiang et al. 2018; Li et al. 2021).

Atzberger (2013) stated that, under climate change, society is tasked with increasing food production while fostering sustainability of Earth's environmental systems. Results from this study are aimed at steering action towards achieving this goal in the MEE, by providing policymakers and development practitioners with valuable and comprehensive knowledge of the varying levels of eco-environmental vulnerability in the MEE and identifying areas that require immediate conservational attention. As seen over the years, savannas and grasslands are mostly severely or moderately vulnerable. This is not shocking, as these areas (i) are increasingly being inhabited by humans who introduce major LULC changes (e.g., natural vegetation to agriculture) (Wanyama et al. 2020), (ii) receive the least amounts of rainfall (Figure 3.6A), and (iii) are uncharacteristically warming over time. The erratic rainfall in these areas means that rainfed agriculture is not a reliable source of livelihood and the increasing temperatures make pastoralism a risky venture. Most agricultural areas in the west and southwestern MEE exhibit moderate eco-environmental

vulnerability. This may be driven by a significantly changing and/or varying climate, although the intensifying human activities in these areas are also to blame. For instance, the expansion of land under agriculture at the expense of natural vegetation has a long-term effect of modifying ecosystem processes and accelerating climate change and variability. These areas include some of the most populated areas in rural Africa - meaning that majority of the MEE population is substantially vulnerable to climate change and related environmental change, and that this vulnerability is likely to rise with rising populations.

Despite its socio-ecological importance and the complex human-environment interactions influencing its stability, the MEE has been understudied. This is due in part to the acute data inadequacies in this area and the rest of East Africa. In some cases, data (e.g., from national census) are available but only at mismatched spatial and temporal scales and/or in aspatial formats that limit their usage. Through recent developments in Earth observation technologies and modeling techniques, valuable spatio-temporally contiguous data have been produced and are now being accessed freely and used to conduct important environmental assessments including EEVA. This study leverages globally available multi-decadal data (MODIS NDVI, CHIRPS, CHIRTS, and WorldPop) and open-source software (R and GEE) to assess eco-environmental vulnerability. This is a demonstration that this analysis can easily be translated to regions with similar characteristics (e.g., other mixed forest and agriculture landscapes like the Mau Complex in Kenya, Mount Kilimanjaro in Tanzania, among others). Additionally, using these datasets enables important ecosystem properties like EEVI to be characterized and monitored over time, thus ensuring better planning and decision making for environmental conservation and local livelihood improvement.

This study found that areas surrounding PAs are at great risk of deforestation and forest degradation (e.g., see Figure 3.7B), corroborating results by Wanyama et al. (2020). MEE PAs have also been influenced by activities such as overexploitation of forest resources by logging

companies and post-independence political changes, mainly due to institutional deficiencies (Petursson & Vedeld 2017). This result shows that there is a spatial structure to eco-environmental vulnerability, and this is key as it can inform policymakers about factors driving ecosystem vulnerability in the MEE. The amplifying precipitation concentration (Figure 3.8) also means that the MEE climate is significantly changing and consequently diminishing MEE's ability to support rainfed agriculture, a major source of livelihood for majority of the local population. Conservation of this ecosystem is therefore imperative, and this study recommends that areas in the moderate and severe vulnerability classes should especially be targeted. To achieve this, policies aimed at protecting PAs and other natural lands should be better enforced. One such way is the adoption of the bottom-up approach in which local community members' opinions are considered in conservation and resource management decision making. As Tadesse et al. (2017) note, this approach is key to mobilizing local community participation in conservation of common-pool natural resources. The approach provides a great avenue to (i) gather important indigenous knowledge systems from the people, (ii) boost ownership and garner the support of communities, and (iii) ultimately ensure successful implementation of projects and policies. Gashu & Aminu (2019) concluded that natural resource management is impossible without proper involvement of local communities. The study also found that EEVI is significantly driven by human activities either directly (e.g., increasing populations, clearing forests for agriculture) or indirectly (e.g., changing precipitation patterns due to deforestation). Therefore, acknowledging that people are major players in this ecosystem is an important step towards simultaneously conserving the environment and improving livelihoods. Against this background, this study recommends that positive behavior change should be encouraged and funded among local communities. This includes adopting lifestyles and habits that foster more sustainable use of natural resources. Efforts aimed at curbing the widespread conversion of natural vegetation to croplands and settlement are especially encouraged. On the same account, the role of natural vegetation in regulating the local climate system should be emphasized.

3.4.2 Sources of Uncertainty

There is no rule of thumb as to how many variables should be used in EEVA (Nguyen et al. 2016), and each study defines its variables based on contexts and available data. Data unavailability is a widely known problem in East Africa. Due to this shortcoming, data used in this study were available at multiple and mostly very coarse spatial resolutions: the DEM was obtained at 30 m, population density at 1 km and CHIRPS and CHIRTS at 4 km. This scale mismatch introduced some uncertainties in the EEVA results. Additionally, the present study would have benefited from census data for Kenya and Uganda. From these, more specific demographic variables associated with eco-environmental vulnerability would have been computed and incorporated in the study to produce a more detailed picture of eco-environmental vulnerability. However, the census is conducted once every 10 years in these countries and therefore would mismatch the temporal scale of analysis (annual) used in this study. It is also worth noting that even this decadal data was not available. In its place, population density data from WorldPop, which have been used in previous studies in Africa (Kibret et al. 2019; McNally et al. 2019; Helman & Zaitchik 2020), were used. Further, the study design and interpretation of the results were based in part on prior knowledge of the MEE, and insights from a 2019 field study in the area.

3.5 Conclusions

The present study found that the majority of the MEE (comprising savannas, grasslands, and most of the agricultural land in Ugandan MEE) was moderately vulnerable based on the analysis methods and variables used. EEVI showed a marked increase in vulnerability with decrease in elevation. EEVI is most severe in the savannas of the northwestern part of the domain. Savannas and grasslands constituted the majority of the severe vulnerability class. Eco-environmental vulnerability varied from year to year, indicating that it is a function of multiple factors operating at numerous scales (local to coarse scale). Eco-environmental vulnerability in the MEE is strongly associated with multi-year variables based on precipitation, temperature, and

population density. With fast increasing populations and intensifying climate change and variability, eco-environmental vulnerability in the MEE will continue to experience significant interannual variability. Moreover, precipitation concentration is amplifying especially in the wet season, thus adding another layer of risk for agriculture and ultimately for local community livelihoods.

To achieve sustainability in the MEE ecosystem and the livelihoods it supports, areas in the moderate and severe vulnerability classes need prioritized conservation. It is recommended that environmental conservation policies be implemented and enforced in these areas by adopting the bottom-up approach in which local community members' opinions are incorporated in decision making. In addition, more data must be collected and used. Communities can be encouraged to adopt lifestyles and habits that foster more sustainable use of natural resources, and international donors can use this information to target conservation activities.[4]

[4] This research was supported by funds from the 2019 and 2020 *Graduate Office Fellowship* (GOF) awarded by College of Social Science and Department of Geography, Environment, and Spatial Sciences at Michigan State University. It also received support from the 2020 *Research Enhancement Award* from The Graduate School at Michigan State University.

CHAPTER 4. SIMULATION OF FUTURE LAND USE CHANGE IN A DATA-SCARCE BUT RAPIDLY CHANGING MOUNT ELGON ECOSYSTEM[5]

4.1 Introduction

Land use and land cover (LULC) changes have been recognized both locally and globally as important factors driving anthropogenic changes in the environment (Guan et al. 2011; Mishra & Rai 2016; Gibson et al. 2018; Hasan et al. 2020). Since the last ice age, about 75% of natural vegetation has been altered due to human activities (Ellis & Ramankutty 2008; Uddin et al. 2015). Anthropogenic landscape modification is therefore not a new phenomenon, but rates, intensity and extents of these changes have been the highest in recent decades (Ellis 2007). For instance, it is estimated that about 420 million hectares of forested areas have been lost via conversion to other LULC types since 1990s alone (FAO & UNEP 2020). This LULC change is influenced greatly by fast increasing populations (Metzger et al. 2006), exacerbated by effects of climate change and/or variability, which have increased demand for more food, water and shelter (Foley et al. 2005), and therefore necessitated rapid expansion of agricultural, pastural and urban lands (Foley et al. 2005; Lambin & Meyfroidt 2011). LULC changes have been linked to various ecological, socioeconomic impacts (Pellikka et al. 2013) including regional climate modifications (Salazar et al. 2015) such as cooling temperatures (for instance, Feddema et al. (2007)) and decreasing precipitation (for example, see Turner II et al. (2007)). The changes have also been associated with declines in biodiversity (Foley et al. 2005; Newbold et al. 2015) due to habitat fragmentation and loss (Halmy et al. 2015), and diminishing ecosystems' regulatory functioning such as carbon sinks (e.g. Mugagga et al. (2015)), among other effects. Persistent LULC changes can alter land-atmosphere interactions thereby modifying local and global climates. Coupled with a significantly changing climate, LULC changes threaten major ecological processes (e.g., biodiversity conservation) and socio-economic practices (e.g., rainfed agriculture). Thus, a comprehensive

[5] This is an unpublished manuscript. Reference: Wanyama D, Moore NJ, Bunting EL. 2021. In Preparation. Simulation of future land use change in a data-scarce but rapidly changing Mount Elgon Ecosystem.

understanding of historical, present, and future changes in LULC is necessary for planning and implementing programs aiming to simultaneously conserve the natural environment and improve local livelihoods and processes dependent on it.

East Africa's highlands are significantly vulnerable to the effects of climate change and variability. Here, 'short rains' have become highly variable and unpredictable with time. Further, 'long rains' have shown significant within-season shifts, and more extreme natural events (e.g., droughts, floods, and landslides) have become more common. On the other hand, land is a critical resource in this region (Guzha et al. 2018) as a majority of the inhabitants derive their livelihoods from subsistence agriculture. Yet land holdings per household have steadily reduced over time (Maitima et al. 2009; Guzha et al. 2018). Thus, the heavy reliance on rainfed agriculture in East Africa continues to threaten the region's food security and rural livelihoods (Guzha et al. 2018; Wanyama et al. 2020). Additionally, the fast increasing populations have necessitated expansion of food production systems (Wanyama et al. 2020) and as a result, significant LULC changes (particularly loss of natural vegetation to cultivated land and settlement) have widely been reported in many parts of East Africa (Fetene et al. 2016; Hailemariam et al. 2016; Mwangi et al. 2017).

The Mount Elgon ecosystem (MEE), a major water catchment area in western Kenya and eastern Uganda has experienced similar LULC changes. The MEE is dominated by agricultural land, savanna, grassland, and an Afromontane forest (Wanyama et al. 2020). Cultivated areas in the MEE are among the highly populated areas in rural Africa, approximating 1,000 people per km^2 (Nakakaawa et al. 2015; Vlaeminck et al. 2016). Existing extractive activities like charcoal burning and timber production (Mawa et al. 2020), increasing encroachment of ecologically fragile land on the high slopes of the mountain (Nakileza & Nedala 2020), and illegal access and cultivation of protected areas (PAs) (Wanyama et al. 2020) all point to the mounting pressure on land resources in the MEE. Deforestation and degradation of natural vegetation have been

blamed for the intensifying occurrence of climate-related natural hazards (for instance, prolonged droughts, more frequent landslides and more extensive flooding (Nakakaawa et al. 2015; EAC et al. 2016)) which have threatened lives and property and diminished the ecological and environmental (eco-environmental) stability of the area (Wanyama et al. 2021). The MEE landscape is known to be highly variable, with observed greening and browning patterns across multiple temporal scales primarily related to the significant increases in post-2000 precipitation and agricultural expansion (Wanyama et al. 2020). Long-term trends over the growing season (April-May-June, AMJ) generally show deforestation and reforestation at the edges of the protected forest while land degradation has been detected (especially in the savannas and grasslands) over shorter-term periods. Such dynamics make it difficult to accurately estimate future LULC changes for better land use planning and conservation. Remote sensing (RS) and Geographic Information Systems (GIS) have been invaluable tools in such analyses.

RS and GIS are important tools in conservation and management of natural resources. The use of RS data has increased significantly over the last decade due to the opening of the Landsat archive (Woodcock et al. 2008; Morrison et al. 2018), the launching of the higher-resolution Sentinel satellites, and significant improvements in geospatial data analysis methods. Satellite RS poses several advantages including the ability to collect and provide spatiotemporal data in a manner that is timely and cost-effective to the user. On the other hand, GIS allows for efficient handling and manipulation of this ‘big data’ to provide important information for policy and decision-making. This is especially important for highly variable landscapes like the MEE, because analyses of LULC change for these areas require large amounts of data at fine spatial and temporal scales (e.g., 30 m and daily, respectively). Satellite RS data and GIS capabilities are key in land use change (LUC) models that comprehensively characterize historical and current LULC changes and predict future LULC changes.

LUC modeling refers to the simulation of a socio-ecological system over space and time in a manner that relates to measured LULC change (Paegelow et al. 2013; Gibson et al. 2018). LUC models serve two purposes: to identify factors or proxies that explain LULC change and to predict possible future scenarios of LULC based on the factors (Overmars et al. 2003; Eastman & He 2020). Change analysis in these models is performed using historical LULC data to determine patterns, transitions and past LULC changes (Halmy et al. 2015). The transitions are then integrated with environmental variables to estimate future LULC changes (Pijanowski et al. 2002; Halmy et al. 2015). Several LUC models have been developed including Cellular Automata (CA) (Vaz et al. 2012), CA-Markov (Halmy et al. 2015; Huang et al. 2015; Lu et al. 2019; Aburas et al. 2021), logistic regression (Das et al. 2019) and model combinations (Shafizadeh-Moghadam et al. 2017; Gharaibeh et al. 2020). Example applications of LUC modeling include; an assessment of the impact of future grassland cover change on catchment water and carbon fluxes in South Africa (Gibson et al. 2018), monitoring and predicting landscape dynamics within Iran's Meighan Wetland and surrounding areas (Ansari & Golabi 2019), predicting growth and changes in urban areas (Shafizadeh Moghadam & Helbich 2013; Aburas et al. 2021), and assessing deforestation in Thailand (Waiyasusri & Wetchayont 2020), among others. LUC models provide information beyond traditional LULC change analyses, and therefore allow for better policy- and decision-making that is necessary to simultaneously conserve the natural environment and improve local livelihoods and processes dependent on the natural environment. The complex MEE landscape is currently understudied and LULC change prediction has only been done on the Ugandan side. Two LUC modeling studies exist for the Ugandan MEE and none for the Kenyan side. The study by Mwanjalolo et al. (2018) found that subsistence agricultural land and protected grasslands in Uganda experienced highest gains and that LULC patchiness was associated with the increasingly high demand for agriculture and settlement land. The expansion of agricultural land was also estimated to continue in 2040. J. Li et al. (2016) used an agent-based model (ABM) to analyze historical LULC change (1996-2013) and later simulated possible

changes in agricultural land in Uganda under business-as-usual and deforestation scenarios. The study reported that agricultural land increased from 8.98 million ha in 1996 (37%) to 10.31 million ha in 2013 (43%). Agriculture was projected to increase further in 2025 to 12.10 m ha (50%) and 12.39 m ha (51%) in the business-as-usual and deforestation scenarios, respectively. The two studies were conducted at the national scale, meaning that localized environmental relationships and patterns were not emphasized. There is therefore need for an ecosystem-wide simulation of LULC change which will inform positive environmental conservation and livelihood improvement actions within the MEE.

The goal of this study was to simulate possible future land use changes in the MEE based on existing remote sensing LULC products and TerrSet's Land Change Modeler (LCM). Here, the main objectives were (1) to forecast possible future LULC changes for the MEE using LCM; and (2) to assess the accuracy of the simulated LULC surfaces in relation to observed persistent changes in the MEE. It is argued that accelerated climate change and significant vegetation-to-cropland conversion have led to an unpredictable and rapidly changing landscape making it difficult to accurately characterize future LULC trajectories using historical change transitions. The present study first combined data from GlobeLand30 and Regional Centre for Mapping of Resources for Development (RCMRD) to generate improved LULC data for 2001, 2009, and 2017. The study then examined spatial and temporal distribution of LULC change and identified areas of major LULC changes in the periods 2001-2009 and 2001-2017. Projections to 2025 and 2033 were then developed to estimate how LULC will potentially change over time. Accuracy of the simulations (for 2017) was assessed first against the 2009 and 2017 LULC maps, and then against greening and browning surfaces over the growing season for 2001-2018. Such a comprehensive analysis of future LULC changes can support decision- and policy-making efforts towards a conserved environment and improved local livelihoods.

4.2 Materials and Methods

4.2.1 Study Area

The MEE covers approximately 15,000 km^2 in western Kenya and eastern Uganda (Figure 4.1). This mountainous area extends from 1°37'43" N, 33°55'45" E to 0°42'16" N, 35°14'19" E. The Mount Elgon Forest was classified as a montane forest (Doumenge et al. 1995) and was designated as a protected area in 1992 and 1968 in Uganda and Kenya, respectively (Anseeuw & Alden 2010; Nakakaawa et al. 2015). Rainfall in the MEE is bimodal with most of the rain ("long rains") falling in March-June (Kenyan side) and April-October (Ugandan side) (Okello et al. 2010; Mugagga et al. 2012; Musau et al. 2015). "Short rains" often fall around October-December, but these have become very unpredictable over the years. While marginal temperature and precipitation variation exists in the MEE, these weather elements vary significantly with changes in altitude and relative location of windward and leeward sides of the mountain.

The MEE landscape exhibits significant variability due in part to the large increase in post-2000's precipitation, significant conversion of natural vegetation to cropland (Wanyama et al. 2020) and complex orientation of LULC in the area (Petursson et al. 2013). As a result, eco-environmental vulnerability in this area varies significantly as well (moderately or severely vulnerable in the savannas, grasslands, and some agricultural areas) (Wanyama et al. 2021). Higher altitude areas of the MEE are known to have more favorable growing conditions compared to lower altitudes (Mumba et al. 2016), thus explaining the increasing encroachment of higher elevation areas by local communities.

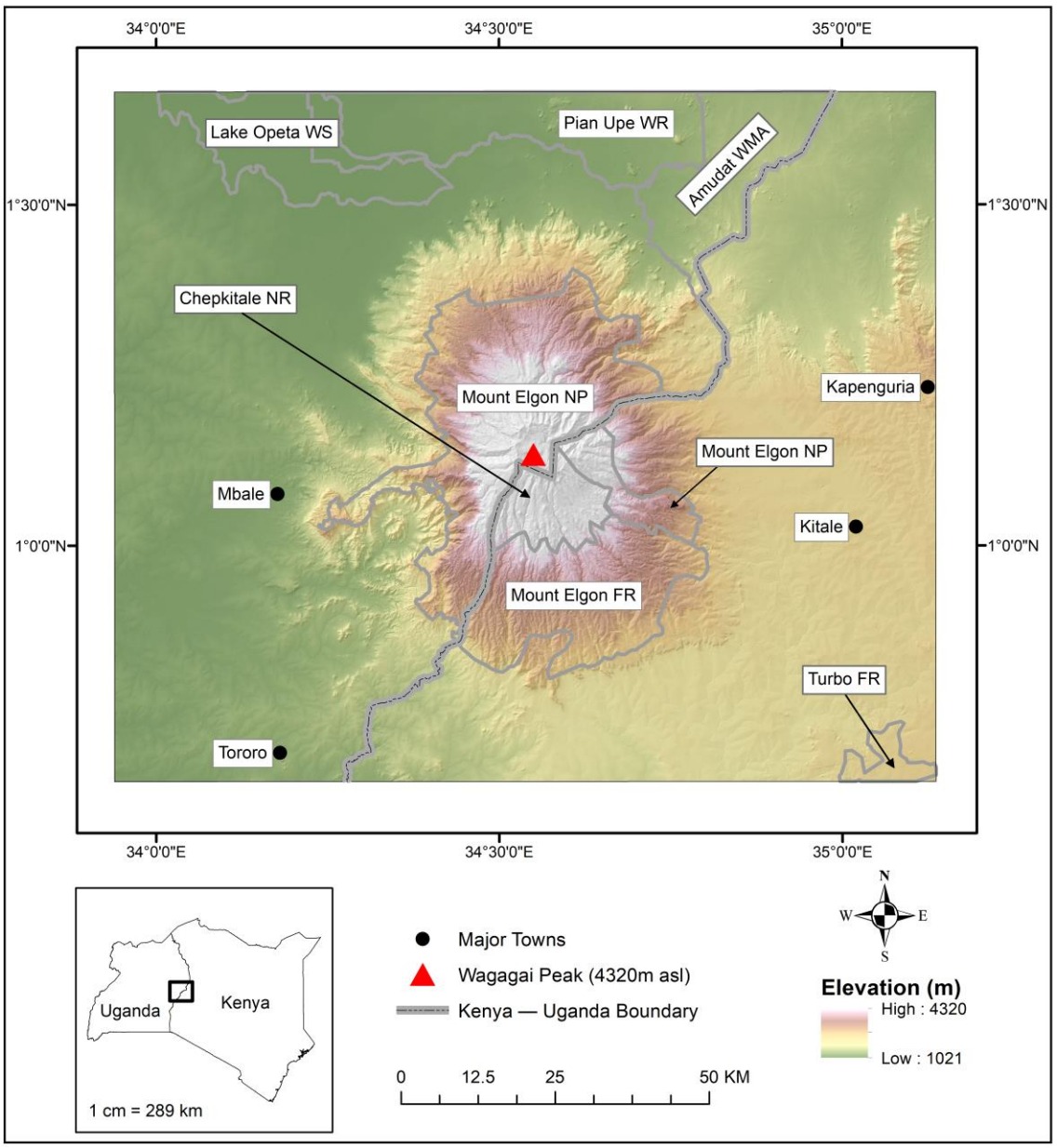

Figure 4.1. *The Mount Elgon Ecosystem (MEE) in eastern Uganda and western Kenya.* Elevation (meters amsl) and major protected areas are shown. Major towns are also shown for reference. FR is forest reserve, NR is national reserve, NP is national park, WS is wetland system and WMA is wildlife management area.

4.2.2 Data Sources, Pre-processing, and Variable Generation

This study used LULC products from GlobeLand30 and RCMRD to generate improved LULC data used in LCM simulations. The GlobeLand30 data (Jun et al. 2014; Liao et al. 2014) for 2000, 2010 and 2020 were acquired through the GlobeLand30 website (Chinese Ministry of

Natural Resources 2019). These data are available at 30-meter spatial resolution and initially contain 10 land cover classes. The data for 2010 and 2020 have respectively been found to be approximately 84% and 86% accurate (Chinese Ministry of Natural Resources 2019). The RCMRD LULC data (RCMRD 2020) was obtained from RCMRD's Eastern and Southern Africa Land Cover Viewer. This dataset contains annual LULC data for the period 2000-2017 for eastern and southern African nations. The data were developed from Landsat time series using the Continuous Change Detection and Classification (CCDC) algorithm in Google Earth Engine (GEE) (Gorelick et al. 2017). Initial LULC classes (forest land, grassland, cropland, wetlands, settlement, and other land) in these data corresponded with International Panel on Climate Change (IPCC) categories necessary for reporting greenhouse gas emissions (Iversen et al. 2014).

RCMRD's LULC data for 2001, 2009 and 2017 were used together with GlobeLand30 data to generate an improved LULC dataset for 2001, 2009, and 2017. First, LULC classes for the two datasets were reclassified to include only forest, mixed vegetation, wetland, cropland, urban, and open grassland classes. Mixed vegetation composed of savannas and grasslands while grasslands found near the mountain top were mapped as open grasslands. The RCMRD data was passed through a majority filter twice, to approximate the level of detail in the GlobeLand30 data. To assess the accuracy of these two datasets, the accuracy of the 2017 (for RCMRD LULC) and 2020 (for GlobeLand30) datasets was assessed. Here, reference points were first generated through visual interpretation of high-resolution imagery in Google Earth Pro (Google Earth Pro 2020) for the period 2017-2020. A total of 346 validation points (101 for forest, 86 for mixed vegetation, 13 for wetlands, 96 for cropland, 16 for urban areas, and 34 for open grasslands) were randomly generated in this exercise. These validation points were compared to the reclassified rasters and producer's and user's accuracy measures for each LULC class were calculated. The accuracy statistics for each LULC class in GlobeLand30 were then compared with those in the RCMRD classes. In addition, the spatial distribution of each LULC class was

assessed visually to identify areas that were correctly (or incorrectly) classified. From these, most accurately classified areas were selected from each of the two LULC datasets and mosaicked to generate an improved LULC dataset for 2017. As a result, the final LULC dataset composed of cropland, forest (around the mountain), wetlands and urban classes from GlobeLand30 and mixed vegetation and open grassland from the RCMRD data. LULC datasets for 2001 and 2009 were similarly generated. The accuracy of these fused datasets was iteratively compared to historical imagery in Google Earth Pro and manually improved where necessary. This was done especially for cropland and urban classes in the 2001 LULC data. The final dataset in 2017 was also compared with the 346 validation points to generate accuracy assessment statistics reported in this study. Final LULC data for 2001 and 2009 were used in LCM to respectively represent baseline LULC conditions and to compute LULC transition potentials. The LULC surface in 2017 was used to validate LCM simulations for that year.

Table 4.1. *Datasets used in the present study.*

Dataset	Spatial Resolution	Years	Source
LULC data	30 m	2001, 2009, 2017	Regional Centre for Mapping of Resources for Development (RCMRD 2020)
LULC data	30 m	2000, 2010, 2020	GlobeLand30 (Chinese Ministry of Natural Resources 2019)
Precipitation	5 km	1986-2018	CHIRPS (Funk et al. 2015)
SRTM DEM	30 m	2000	United States Geological Service (United States Geological Service 2000)
Rivers	-	-	DIVA-GIS and World Resources Institute (DIVA-GIS; World Resources Institute)

Variables representing drivers of LULC change were obtained from multiple sources. Pentad (5-day) precipitation records from CHIRPS (Climate Hazards group Infrared Precipitation with Stations) (Funk et al. 2015) were used to generate variables related to precipitation variability. The CHIRPS data, available at 5 km spatial resolution, provide global daily and pentad records from 1981 to present. In this study, pentad records for the 1986-2018 period were obtained from GEE and used to compute long-term mean (LTM) and standard deviation (LTSD) for 1986-2018 at both annual and seasonal (AMJ) scales. The 30 m Shuttle Radar Topography Mission (SRTM)

DEM dataset from United States Geological Service (United States Geological Service 2000) was downloaded from GEE. The DEM was used to generate topographic variables (elevation and slope) associated with LULC change in the MEE. Euclidean distance from rivers was computed using a major rivers datasets acquired from World Resources Institute (World Resources Institute) and DIVA-GIS (DIVA-GIS). More proximity variables included distance from urban areas (based on the urban LULC class in 2001) and distance from known anthropogenic disturbance (defined here as the distance from all pixels that converted to cropland in the 2001-2009 period).

4.2.3 Land Use Change Modelling

The current study used LCM in TerrSet (Eastman 2016a; Eastman 2016b) to simulate future LULC change in the MEE. This model generates LULC surfaces based on artificial neural networks (ANN), Markov chains, and transition potential maps obtained by training either logistic regression, modified K-nearest neighbor, or multilayer perceptron (MLP) algorithms (Eastman 2016a). LCM does this in the following three stages.

4.2.3.1 Change Analysis

In this study, change analysis in LCM involved an evaluation of trends of change in LULC classes for three sets of years: 2001 – 2009, 2009 – 2017, and 2001 – 2017. Here, LCM provided important statistics (including gains and losses, net changes, and contributors of change in each LULC class). In addition, maps of transitions, gains and losses, LULC class exchanges, and persistence could be created.

4.2.3.2 Transition Potential Modelling

In this step, LCM identifies the potential of each pixel to transition by linking the LULC changes to underlying spatial drivers of change. By doing this, LCM groups LULC transitions based on driving factors that best explain each transition. Since this study was interested in the interaction among forest, mixed vegetation, and cropland classes which led to the observed increase (decrease) in cropland (forest and mixed vegetation), only cropland expansion from

forest and mixed vegetation was modelled (forest-to-cropland and mixed-to-cropland were grouped and modelled using the same driver variables – since both transitions result from the same underlying environmental interactions).

In LCM, spatial driver variables can either be static (i.e., unchanging over the simulation period e.g., distance to rivers) or dynamic (i.e., changing over time e.g., proximity to current agricultural land). In this study, cropland expansion was modelled using a suite of topographic, climate, and proximity variables selected based on literature, prior knowledge of the MEE, and insights from the 2019 field study in the area. These variables included LTSD for both annual and AMJ periods (mm), distance from rivers (m), elevation (m amsl), slope (%), distance from 2001 urban pixels (m), and distance from pixels that converted to cropland during the 2001-2009 period (m). All variables were set as static except for distance from 2001 urban pixels.

The latest version of TerrSet (TerrSet2020) allows transition potentials to be modelled using MLP neural network, logistic regression, or SimWeight K-nearest neighbor algorithms. In this study, the MLP algorithm was used since it has been enhanced to work well without user intervention (Eastman 2016a). In addition, the MLP can model multiple transitions in a single sub-model. Output from transition potential mapping is a map of levels of vulnerability for each pixel to transition (transition potentials) which is a necessary input in predicting future LULC change. In this study, two transition potential surfaces were generated, one using 2001-2009 transitions (M0109) and another using 2001-2017 transitions (M0117).

4.2.3.2 Change prediction

At this modelling stage, a future LULC change scenario is generated based on rates of change in historical LULC and transition potentials (Eastman 2016a). LULC predictions can be made for a specified year either through Markov chain analysis or other external models. Results include a hard prediction map (map showing spatial distribution of LULC classes) and a soft prediction (a map showing vulnerability of each pixel to change). Soft predictions are often

preferred. In this study, simulations were generated for 2017 (using 2001-2009 transition potentials), and 2025 and 2033 (using both 2001-2009 and 2001-2017 transition potentials).

4.2.4 Model Validation

To assess validity of the model in simulating future LULC change in the MEE, accuracy of the prediction surface for 2017 was assessed in two ways. First, a 3-way cross tabulation was conducted between the 2009 map, the predicted LULC surface for 2017 and the real LULC surface for the same year. Output from this was a map of hits (pixels which changed as the model predicted), misses (pixels which changed although the model predicted no change) and false alarms (pixels that did not change although the model predicted change) (Eastman 2016a). Second, the hits, misses and false alarms surface was compared to a map of persistent greening and browning over the growing season (Figure 4 in Wanyama et al. (2020)) to identify any similar patterns.

4.3 Results

This study characterizes past and simulates future LULC change in the MEE based on existing remote sensing LULC products and LCM. The results highlight patterns of change especially in the forest, mixed vegetation, and cropland LULC classes as well as possible future LULC trajectories for 2025 and 2033. Results from validating improved and simulated LULC surfaces are also presented and, together, attempt to comprehensively characterize possible future LULC change in the MEE.

4.3.1 Improved LULC Maps and Patterns of Change

Accuracy assessment of the improved LULC dataset in 2017 found that the dataset was about 96.8% accurate overall with a Kappa statistic of 0.95. User's and producer's accuracy was above 90% except for the urban class. Most improved classes include wetland and urban and these were mostly misclassified in the RCMRD dataset. In the three periods, similar LULC

compositions existed in the MEE. Dominant LULC classes included cropland, mixed vegetation, and forest (60%, 24% and 11% of the total area in 2017, see Figure 4.2).

Table 4.2. *Accuracy assessment statistics for the improved LULC dataset (A), RCMRD dataset in 2017 (B) and GlobeLand30 dataset in 2020 (C).* Improved accuracies are underlined.

LULC	Forest	Mixed vegetation	Wetland	Cropland	Urban	Open Grassland
A. Improved LULC						
Users	97.1	96.6	92.9	95.7	100	100
Producers	100	100	100	92.7	75	100
B. RCMRD LULC (2017)						
Users	98.1	86.3	65	97.7	90.9	100
Producers	100	95.3	100	89.6	62.5	85.3
C. GlobeLand30 LULC (2020)						
Users	96.2	97.7	92.9	97.9	100	100
Producers	99	97.7	100	97.9	93.8	91.2

Forested areas were mostly located within protected areas (Figures 4.1 and 4.3). The open grasslands were located at high elevation areas of the MEE and generally remained unchanged over time, as expected (Figure 4.3). Mixed vegetation was found mostly in the north and northeastern parts of the domain. This study found that mixed vegetation persistently reduced across the years, decreasing from 390,000 ha (26%) in 2001 to 364,500 ha (24%) in 2017. Forest cover showed an increase in 2001-2009 (+0.3%) and a decrease in 2009-2017 (-0.9%). These decreases in forest and mixed vegetation were compensated mainly by significant gains in the cropland class (Figure 4.4). Over the 2001-2017 period, croplands expanded by 31,500 ha (+2.1%). More specifically, about 22,000 ha and 8,900 ha of mixed vegetation and forest respectively changed to cropland between 2001 and 2017. Over 2009-2017, more than 14,000 ha of mixed vegetation and about 11,000 ha of forested areas were converted to cropland. The least change in cropland was observed in 2001-2009 in which only 6,000 ha of new croplands were identified (mostly from mixed vegetation).

Distinct spatial patterns existed in the occurrence of change in the cropland class. Gains, losses, and net expansion in cropland were mostly observed within fringe areas of the protected

forest and transitional zones connecting existing mixed vegetation and cropland (see Figures 4.3 and 4.4). These patterns were observed more in 2009-2017 and 2001-2017 periods compared to 2001-2009.

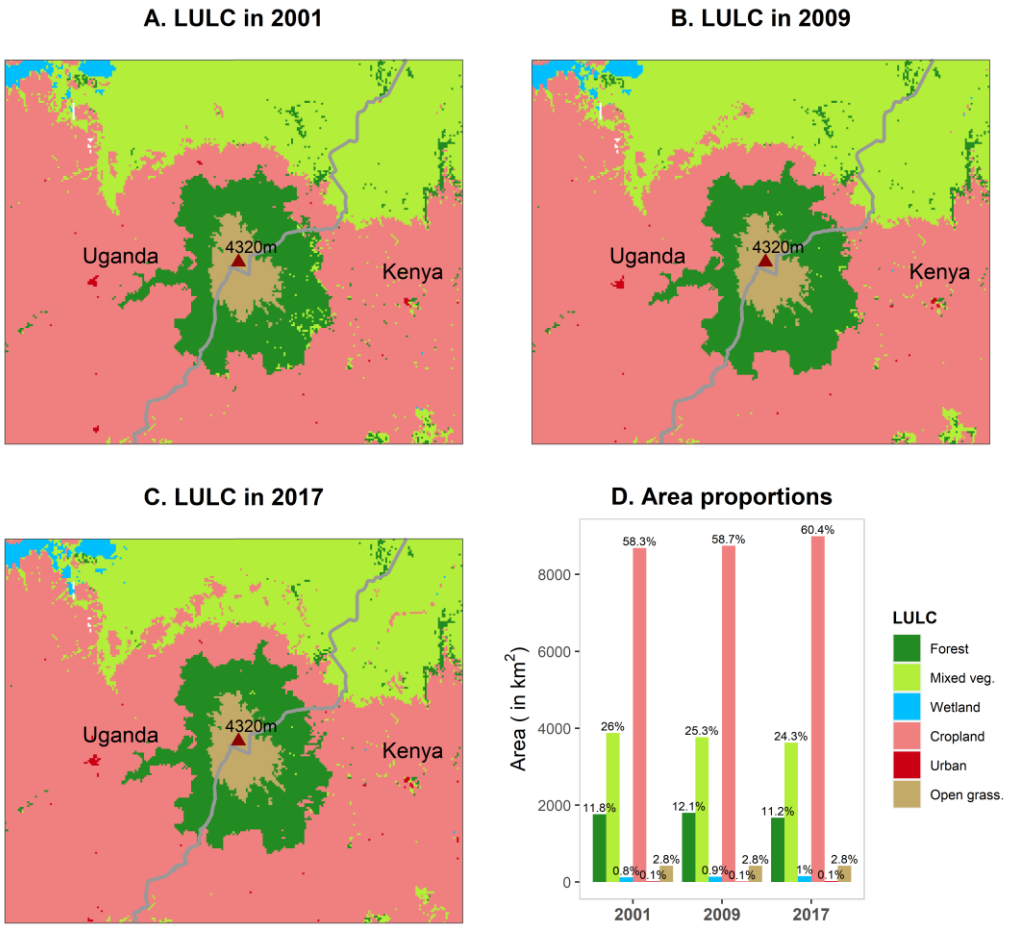

Figure 4.2. *Improved LULC surfaces for 2001, 2009 and 2017.* Figure D shows the percent proportion of each LULC class per year.

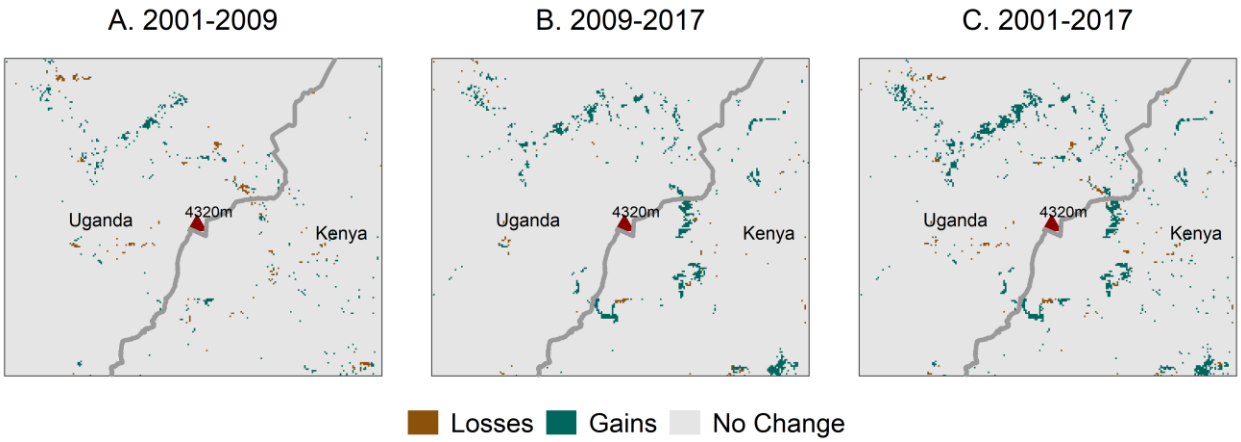

Figure 4.3. *Gains and losses in the cropland class for the periods 2001-2009 (A), 2009-2017 (B) and 2001-2017 (C).*

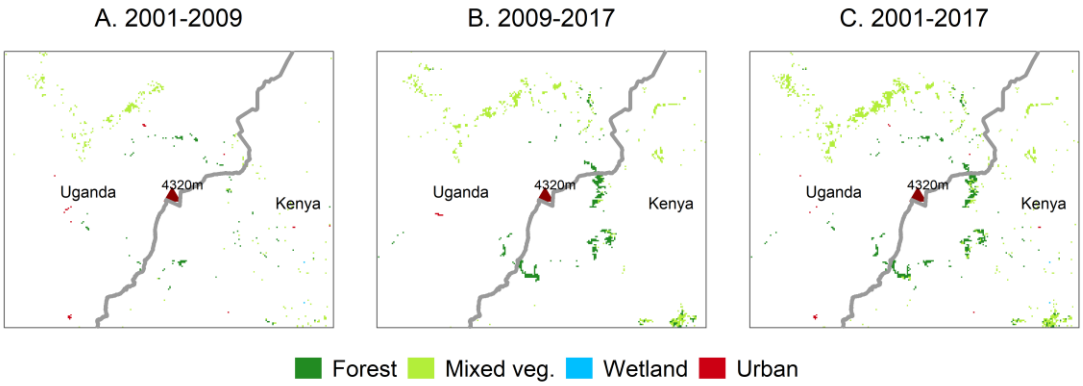

Figure 4.4. *LULC classes that changed to cropland for 2001-2009 (A), 2009-2017 (B) and 2001-2017 (C).*

4.3.2 Transition Potential Modeling

The MLP model used to compute transition potentials found that elevation, slope, and distance from cropland areas were the most important factors influencing LULC change in the MEE (see sensitivity analysis results from MLP in Appendix B). For example, a model for simulating LULC transitions in 2001-2009 using elevation (slope) alone achieved an accuracy rate of 63% (57%) and a skill measure of 0.51 (0.43). Using distance from 2001-2009 cropland areas as the only driver of LULC change, the MLP model achieved an accuracy of 48% and a skill measure of 0.31. The next influential drivers included distance from urban areas in 2001 and distance from rivers. LTSD at both annual and AMJ scales were the least important factors

influencing LULC change in the MEE. Similar results were found in modeling 2001-2017 transitions, generally with lower accuracy rates and skill measures.

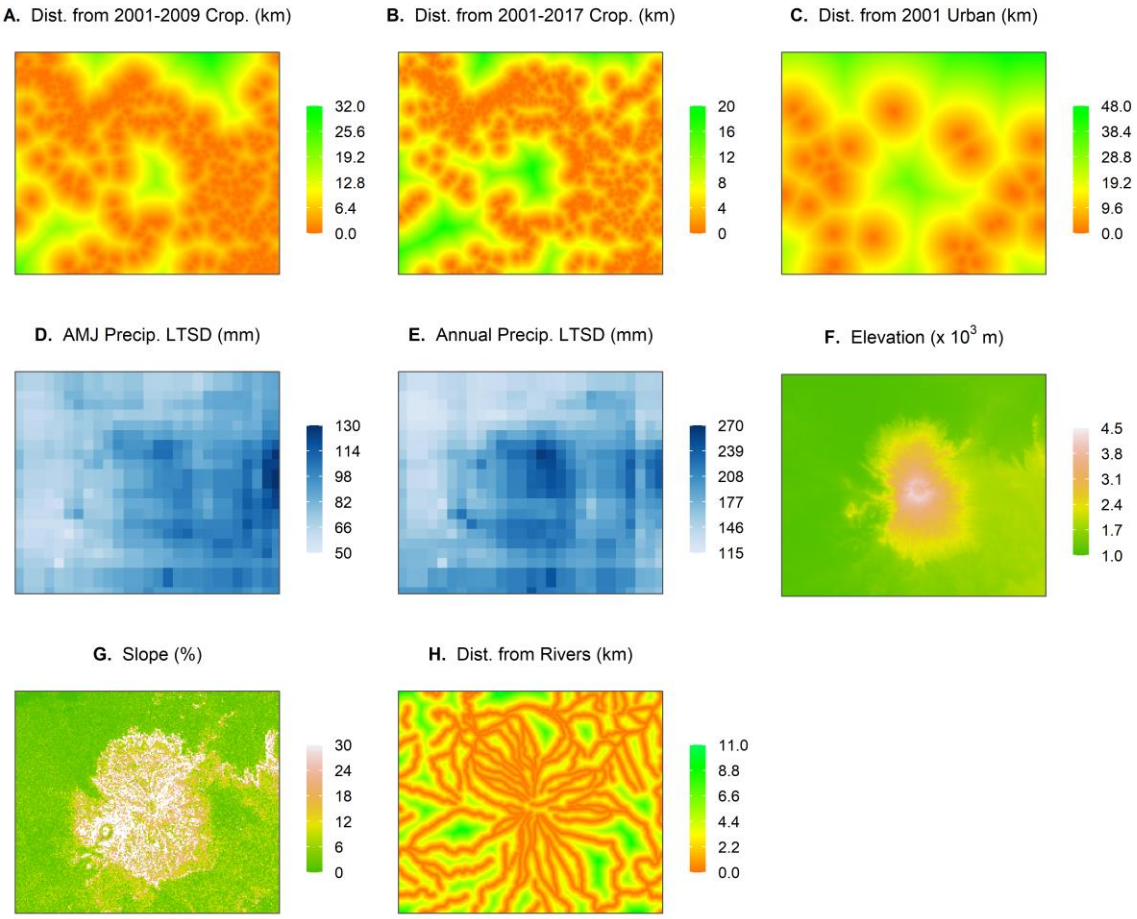

Figure 4.5. *Spatial drivers of LULC change used in final LCM models.* It should be noted that distance from 2001-2009 croplands (A) was used in M0109 while distance from 2001-2017 croplands (B) was used in M0117.

Overall, the MLP models were highly skillful. The M0109 model achieved an accuracy rate of 92.8% and a skill measure of 0.9 in modeling transitions between 2001 and 2009. Slightly lower values were obtained for the M0117 model (an accuracy rate of 88% and a skill measure of 0.84). In terms of individual transitions, M0109 performed best in modeling persistence of both mixed vegetation and forest classes and transition of mixed to cropland (skill measures of 0.96, 0.88, and 0.94, respectively). The model was only averagely accurate in modeling forest to cropland transitions (skill measure of 0.68). There was an increase in accuracy when modeling forest to

cropland transitions using the M0117 model (skill measure of 0.72). However, this model's accuracy was slightly reduced in modeling transitions from mixed vegetation to cropland (skill measure of 0.85).

Outputs from LCM change prediction are maps showing both hard and soft prediction surfaces. Maps of future change in 2025 and 2033 are shown in Figure 4.7 (using M0109) and Figure 4.8 (using M0117). Greater LULC changes were observed when using 2001-2017 transitions compared to 2001-2009 transitions. While using these transitions yielded a similar change in mixed vegetation (decrease), the two showed contrasting patterns in forest and cropland classes especially in the 2025 simulation. The M0109 model showed an increase in forest cover and a slight decrease in cropland while the LULC simulation from M0117 revealed a persistent decrease (increase) in forest (cropland). The two models yielded similar LULC patterns for 2033, but final proportions of each class were quite different. For instance, the final proportion of cropland in 2033 (Figure 4.6C) was 60.7% (using M0109) compared to 62.4% (using M0117).

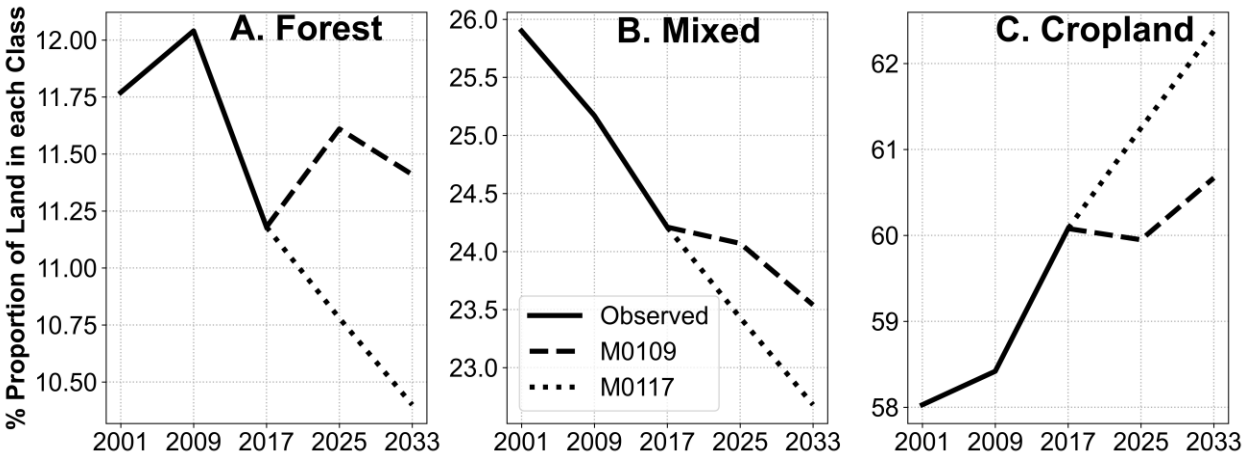

Figure 4.6. *Proportion of major LULC classes observed in 2001, 2009, 2017 (solid lines), and simulated for 2025 and 2033 using 2001-2009 and 2001-2017 transitions (dashed and dotted lines, respectively).*

Clear spatial patterns were observed in the distribution of LULC change vulnerability using both models. Areas around edges of the mountain and transitional zones between mixed vegetation and cropland (Figures 4.7A2, 4.7B2, 4.7C2, 4.7A2 and 4.7B2) had higher probabilities

for conversion. However, levels of this vulnerability were slightly higher when using M0117 compared to M0109. The amount of forest land under threat was more in Kenya compared to Uganda especially using 2001-2017 transitions (Figures 4.8A2 and 4.8B2). On the other hand, the amount of mixed vegetation at risk was more on the Ugandan side. Most of the vulnerable areas were generally located within or near protected areas (Figures 4.1, 4.7 and 4.8).

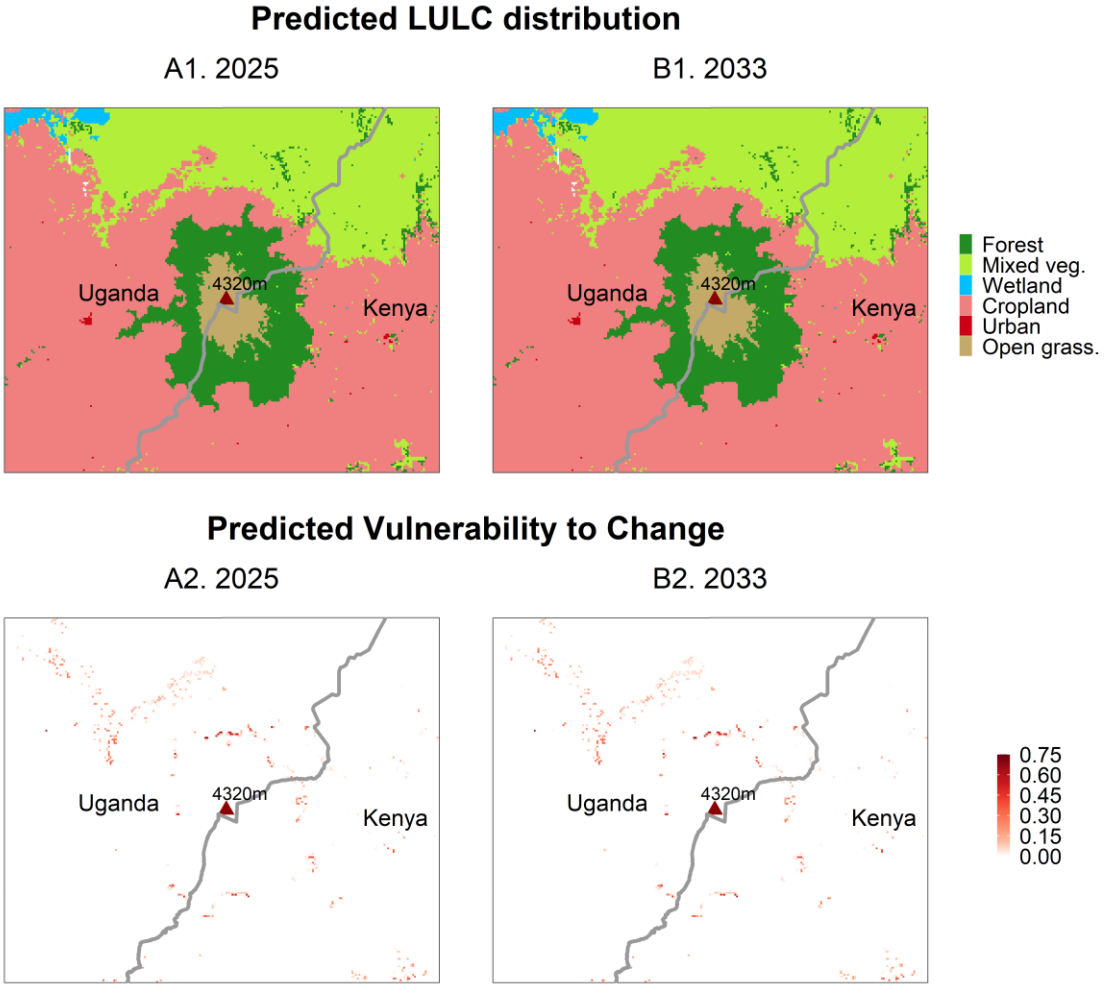

Figure 4.7. *Predicted spatial distributions of LULC classes and change vulnerability for 2025 and 2033 based on 2001-2009 LULC transitions.*

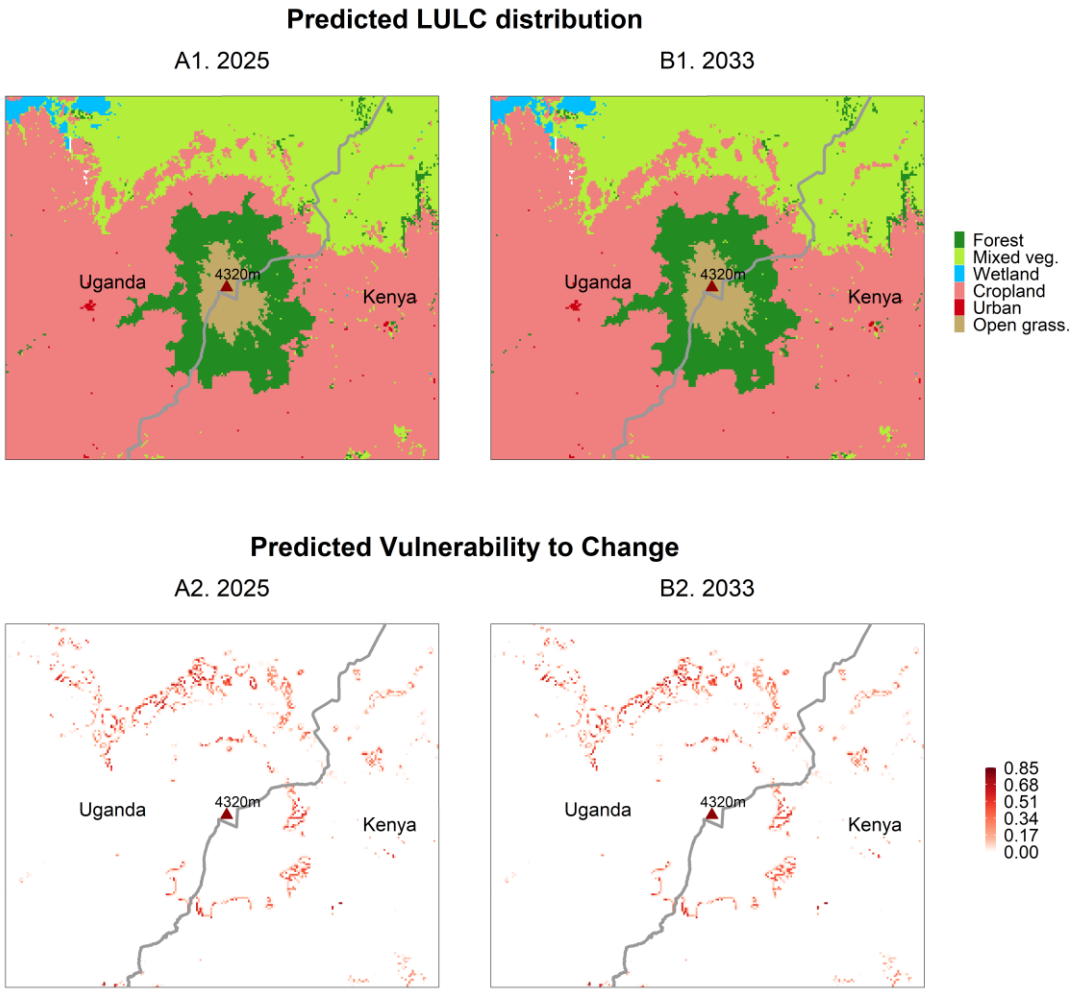

Figure 4.8. *Predicted spatial distributions of LULC classes and change vulnerability for 2025 and 2033 based on 2001-2017 LULC transitions.*

The MEE landscape has been found to be dynamic as shown by its persistently greening and browning patterns especially during the growing season (Wanyama et al. 2020). The majority of this landscape either greened or browned over the 2001-2018 period, and these changes were related to both human activities (e.g., deforestation) and natural processes (e.g., significant increases in post-2000 precipitation). The M0109 simulation for 2017 was compared against Mann-Kendall and Sen's Slope trends for the AMJ period over 2001-2018. Results indicated similar patterns of LULC change. For instance, LULC change was detected around forest fringe areas in both cases. Furthermore, more forest cover change was detected on the Kenyan side, and both analyses show that most of the LULC changes were experienced within or near

protected areas. It should be noted, however, that only 40% of the areas of LULC changes detected by M0109 were also found to have changed by Mann Kendall and Sen's Slope. In addition, most of the greening and browning identified by Mann-Kendall and Sen's Slope were not detectable using the M0109 model, indicating that LULC change analyses using only a few LULC images in time are not well suited for the variable MEE.

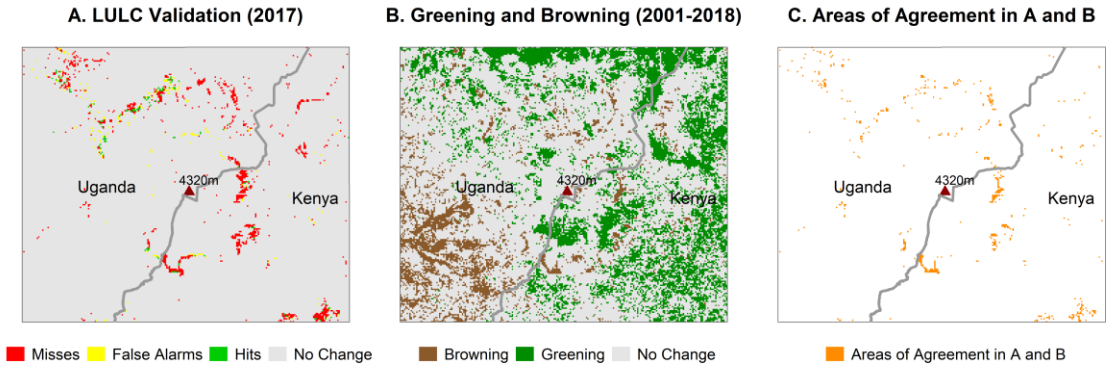

Figure 4.9. *Validation results for the 2017 simulation.* (A.) Validation map for 2017 obtained by comparing the LCM prediction for 2017 with observation data for that year (Figure C). (B.) Areas with persistent greening and browning in NDVI during the 2001-2018 period (adapted from Wanyama et al. 2020). (C.) Areas of change detected in both (A) and (B).

4.4 Discussion

The conversion of natural vegetation to new cultivated land and settlement is a common LULC trend reported in Africa (Ordway et al. 2017; Arowolo & Deng 2018; Mwanjalolo et al. 2018; Rukundo et al. 2018). In the present study, agriculture was estimated to expand from approximately 58% in 2001 to more than 64% in 2033, at the cost of mixed vegetation and natural forests. This loss of natural vegetation has been associated with various environmental issues like biodiversity loss (Foley et al. 2005; Newbold et al. 2015), intensifying natural hazards (for example, prolonged droughts, more frequent landslides and more extensive flooding (Nakakaawa et al. 2015; EAC et al. 2016), changing and/or varying climates, and diminishing ecosystems' regulatory functioning (e.g., carbon sequestration (Mugagga et al. 2015; Rukundo et al. 2018)), among others. LULC change has therefore been recognized as an important factor driving anthropogenic changes in the environment (Guan et al. 2011; Mishra & Rai 2016; Gibson et al.

2018; Hasan et al. 2020). There has been an uptick in the number of studies dedicated to characterizing LULC change made possible by the increasing availability of improved satellite RS data and advancement in geospatial analysis methods and computational capabilities. The opening of the Landsat archive (Woodcock et al. 2008), the launching of more satellites like the Sentinel missions, and expansion of data storage and computer processing capabilities have made it possible for a more complete characterization of LULC change. This is especially important for highly variable landscapes, because analyses of LULC change for these areas require large amounts of data at fine spatial and temporal scales.

In this study, LCM was implemented to characterize LULC change in the MEE and to simulate possible future scenarios of LULC based on identified environmental and social variables. LCM is an inductive model (Gibson et al. 2018), meaning that it seeks to statistically link observed LULC change to its potential driving factors (Overmars et al. 2007; Gibson et al. 2018). LCM therefore uses historical LULC maps to assess past LULC changes and transitions (Halmy et al. 2015). The transitions are then integrated with environmental variables to estimate future LULC changes (Pijanowski et al. 2002; Halmy et al. 2015). Such a methodology is therefore prone to errors related to both algorithms and input data used (Gibson et al. 2018). The improved LULC data used in this study achieved an overall accuracy of 96.8% and a Kappa statistic of 0.95 for 2017. All individual classes achieved accuracies greater than 90% except for the urban class. While these are great accuracy levels, data for 2001 and 2009 were not validated beyond visual comparisons against Google Earth Pro, and therefore caution should be taken when interpreting results from this study.

LCM works under the assumption that rates of change are constant and therefore the relationship between LULC change and driving factors is constant too (Gibson et al. 2018). However, LULC change is influenced by complex processes that are associated with non-linear and dynamic human-environment interactions that can be difficult to characterize using models

and variables (Kolb et al. 2013; Camacho Olmedo et al. 2015; Gibson et al. 2018). For significantly variable landscapes, this characteristic defies the assumption, and LUC models may yield unreliable LULC simulations. A comparison of LULC changes in the MEE revealed dissimilar rates of change between 2001-2009 and 2009-2017 (for instance, compare gains and losses in cropland in Figures 4.3A and B). Further, there was an increase in forest cover in 2001-2009 and a decrease in 2009-2017 and 2001-2017 (Figure 4.6A). These changes are attributed to various activities within the MEE, including the existence of the Shamba System on the Kenya side. The Shamba System enables local communities to farm in protected areas while tending to the growing trees in their early stages of growth (Petursson et al. 2013). This is the Kenyan government's effort meant to accelerate native-to-plantation forest conversion (initially) and reafforestation (later). Other factors include changes in political regimes which may have the negative effects of increased instances of corruption among forest management staff, relaxed enforcement of forest protection legislations, and increased illegal access to and cultivation of PAs. Inferences from a 2019 field study in the area and prior analyses also revealed that the climate in the MEE has changed significantly over recent decades. Grasslands in the northeastern MEE have warmed significantly in recent years (Wanyama et al. 2021), and post-2000 precipitation increased substantially – thus driving persistent greening and browning in the area (Wanyama et al. 2020). Such LULC complexities often manifest in LULC simulation results. For example, due to the unsystematic LULC transitions in the MEE, the M0109 model was highly accurate in modeling mixed-to-cropland conversion (skill measure of 0.94) and only averagely accurate for forest-to-cropland conversion (skill measure of 0.68). Additionally, validation of the 2017 simulation revealed a lot of misses and false alarms compared to hits, majority of which were located at the edges of the forest. Further comparisons showed that most of the reported LULC changes were actual changes which could better be characterized by trend analysis methods like Mann-Kendall and Sen's Slope, linear regression, among others. As such, decisions to use LUC models should involve an assessment of the kind of information that the models

provide against the uncertainties associated with them, especially when working with highly dynamic landscapes. In addition, an integration of these methods can provide a more comprehensive assessment of historical, present, and future LULC change.

Rapid population growth continues to pressure food production systems. In the majority of the MEE, land is handed down to sons when they are ready to start their own families. Formal education is not emphasized in most of these areas, and therefore cases are high of early marriages resulting from youth dropping out of schools early. As such, land holdings generally reduce four- or five-fold every 15 years. Significantly varying climates, on the other hand, have led to diminishing land suitability for agricultural production. For parts of the MEE and many other places reliant on agriculture, this means an accelerated conversion of available forests and natural vegetation to cropland, which threatens the eco-environmental stability and ecosystem services provision. Yet, socio-economic systems in Kenya and Uganda are not efficient to allow for local farmers to sell their produce at a profit. Generally, the number of 'middlemen' increase substantially around harvesting times, and these people buy produce from farmers (when it is very cheap), store it, and resell it to the same farmers later (when it is very expensive). In the long term, these three aspects compound and leave local people trapped in an endless struggle to survive.

Through LUC modeling, important information can be generated about factors or proxies that explain LULC change and possible future change trajectories (Overmars et al. 2003; Eastman & He 2020). Such information is necessary for better planning and policymaking. For example, the present study demonstrates that if business-as-usual persists into 2030s, croplands will possibly keep increasing while forests, savannas and grassland will continue to shrink. Policymakers should therefore focus on interventions aimed at making agriculture more sustainable, so that food production will be less detrimental to the sustainability of other land uses and land covers. First, sustainable intensification (SI) of agriculture is proposed as a possible win-

win for both the local people and the environment. SI targets currently unimproved land and aims to optimize its use to produce more food per unit area of land while conserving the natural environment (Pretty 1997; Gunton et al. 2016; Struik & Kuyper 2017), thus negating the need to expand land under agriculture (Gunton et al. 2016; Struik & Kuyper 2017). There exist debates about the definition of SI and what it entails, with some arguing that the 'sustainable' nature of SI is only vaguely defined and that SI is not too different from current agricultural practices (Petersen & Snapp 2015). Others have proposed ecological intensification as a better option to guide agricultural systems management (Petersen & Snapp 2015; Gunton et al. 2016; Mungai et al. 2020). SI has been demonstrated in parts of the Kenyan MEE with the involvement of One Acre Fund, a non-governmental organization that finances and trains local farmers on modern farming techniques (One Acre Fund). Crop diversification is another approach to increase food production without harming the environment. This involves growing more than one crop, to reduce the risk of crop failure especially during these climate change times. This framework also gives people a chance to test and switch to other crops that may do better in the 'new' climates, thus increasing production without expanding land under agriculture. The main challenge here is the lack of knowledge about the kind of crops that would do well in current climates. For this to be successful, therefore, there is need for systematic analyses such as land suitability for different crops (based on climate, soil, and topographic factors).

The main limitation of this study was data availability. Precise multi-year LULC data for the MEE were not readily available and therefore this study used data obtained from an integration of LULC data from GlobeLand30 and RCMRD. While these datasets were thoroughly assessed against Google Earth Pro imagery and improved where necessary, some inaccuracies may have been undetected. However, the LULC data were interpreted in part based on prior knowledge of the MEE, and insights from prior studies (Wanyama et al. 2020; Wanyama et al. 2021) and the field study conducted in the MEE in 2019. Further, the 2017 LULC simulation was validated first

against the real LULC data for that year and then against a map of persistent greening and browning over AMJ during 2001-2018. Selection of explanatory variables used in this study was also based on insights from previous studies (Wanyama et al. 2020; Wanyama et al. 2021) which found that climate and topographic variables are important in the MEE. This, coupled with data unavailability, constrained the analysis to the seven explanatory variables. This study may therefore benefit from additional social variables This is important, as landscape change is significantly impacted by both environmental and social processes.

4.5 Conclusions

This study simulated possible future land use changes in the MEE based on existing remote sensing LULC products and LCM. The study projected that agriculture will possibly expand from approximately 58% in 2001 to more than 64% in 2033 if current and future LULC transformation follows rates in 2001-2017. These new croplands will occur mostly around edges of the protected forest and zones of transition between mixed vegetation and existing croplands. The vulnerability for land to be converted to agriculture was significantly influenced by elevation, slope, and distance from cropland areas. Due to the unsystematic LULC transitions in the MEE (associated with the Shamba System, political changes, and climate change, among others), simulating forest-to-cropland conversion was only averagely accurate compared to mixed-to-cropland conversion. As such, decisions to use LUC models should involve an assessment of the kind of information that the models provide against the uncertainties associated with them, especially when working with highly dynamic landscapes. In addition, an integration of time series analysis methods (e.g., Mann-Kendall and Sen's Slope) with LUC modeling can provide a more comprehensive assessment of historical, present, and future LULC change – which is necessary to instigate policy changes aimed at simultaneously conserving the environment and improving livelihoods that are dependent on the natural environment.

CHAPTER 5. IMPORTANT INSIGHTS FROM THE FIELD STUDY

5.1 Introduction

While RS and geospatial technologies provide an invaluable opportunity to study historical, present, and future landscape change, these tools fail to provide contextualized explanations of landscape change and other environmental processes. Data from field studies can be handy in filling these gaps – to provide a comprehensive characterization of landscape change and related human-environment interactions. This section therefore documents information about the field study conducted in 2019 in the MEE, whose insights were important in designing studies and explaining results presented in this dissertation.

5.2 Field Study

The field study conducted in July-September 2019 involved the administration of semi-structured interviews to local community members and government officers working in the MEE. More environmental data was collected via direct observation. Most of the interviewees were from significantly changing landscapes (areas showing significant changes in vegetation greenness, Figure 2.4). To identify specific areas to visit, random points were first generated (60 in significantly greened areas, 60 in significantly browned areas and 80 in areas of no significant change). Participants closest to a random point were selected for interviews. A total of 81 people were interviewed including 24 in the Ugandan MEE and 56 in the Kenyan MEE. Of these, 70 were local community members, while the rest were officers working in different government institutions e.g., Kenya Agricultural and Livestock Research Organization (KALRO), Kenya Plant Health Inspectorate Service (KEPHIS), Kenya Farmers Association (KFA), Kenya Forest Service (KFS), and Kenya Seed (Kitale and Bungoma). The participants in this study were interviewed about perceptions of climate change and land-use change, and historical patterns of agriculture and land-use change (see questionnaire in Appendix A). Interviews were conducted and written responses recorded using Qualtrics software (Qualtrics 2019).

5.3 Insights from the Field Study

Changes in precipitation revealed by Mann-Kendall, Sen's Slope and bfast were corroborated by results from the field. All interviewees reported perceptions that precipitation had significantly changed over the last decade. Key observations included delays in the start of the rainy season (reportedly by almost a month on average), increased precipitation intensities, increased occurrences of extended droughts, and flooding. These changes were directly linked to worsening agricultural practices and yields due to increased instances of failed germination, more pest attacks, drying of crops, and stunted crop growth. These perceptions are consistent with the observed changes.

Greening and browning trends observed in grasslands in the northeastern MEE were related to the introduction of new human settlements in the area. Information gathered from the field supports this finding and further explains the implications for landscape greenness. Inhabited by nomadic pastoralist communities, this part of the MEE is susceptible to degradation, especially when these communities move, driven by rainfall patterns, to settle within the grasslands. There was evidence of reduced natural vegetation and tree density in these locations. The fieldwork also revealed that persistent greening observed in the grasslands was associated with conversion of natural vegetation to croplands (which are generally greener than grasslands). In other locations outside of the grasslands, visible greening trends were indicative of some afforestation practices. Data from the field revealed that this kind of greening was driven by the cultivation of evergreen early maturing blue gum (*Eucalyptus globulus*) tree species, sometimes together with and other times in the place of the maize crop. This was especially common in the eastern and southeastern parts of the domain and parts of Uganda.

Variables influencing eco-environmental vulnerability were defined in part based on prior knowledge of the MEE and insights from the field study. Communities in the MEE rely heavily on rainfed agriculture, and therefore changes in environmental conditions (e.g., precipitation and

temperature) can significantly influence their livelihoods. The proportion of land under forest and natural vegetation is shrinking as populations increase. Against this basis, the eco-environmental vulnerability study incorporated climate and population variables in computing EEVI. Results indicated that savannas and grasslands are mostly severely or moderately vulnerable. The field study revealed that these areas (i) are increasingly being inhabited by humans who introduce major LULC changes (e.g., natural vegetation to agriculture), and (ii) are uncharacteristically warming over time. In addition, models for computing EEVI revealed that EEVI was significantly influenced by multi-year variables based on precipitation, temperature, and population density.

By incorporating insights from the field with RS and GIS analyses presented in this study, this study ensures that landscape change and related human-environment interactions are comprehensively characterized, at multiple scales. Scales of analysis in this study included 10-day, 16-day, monthly, seasonal, annual, and household scales. This approach therefore makes it possible to make policy recommendations at appropriate scales that would allow easier implementation of the recommendations. This is important, as successful implementation of environmental conservation and livelihood improvement plans heavily depends on scales at which environmental problems occur, and those at which action is recommended and implemented.

5.4 Internal Review Board Determination

On March 26, 2019, this study (IRB Number: STUDY00002404) was determined to be exempt under 45 CFR 46.104(d) 2(ii). Exempt studies do not need to be renewed.

CHAPTER 6. CONCLUSIONS

6.1 Overall Contributions

This LCS-PE study examines, across multiple scales (10-day, 16-day, monthly, seasonal, annual, and household), human-environment interactions and landscape change under climate change – to comprehensively characterize processes in the highly variable MEE. The focus is on how nature- and human-related factors and practices interact to influence landscape dynamics, drive eco-environmental vulnerability, and eventually threaten nature-dependent livelihoods in the MEE. Historical landscape change was comprehensively characterized, and possible future change was projected. Ultimately, this study seeks to identify avenues to simultaneously improve the agricultural system and livelihoods and enhance environmental conservation within the study area.

6.1.1 Landscape Change Related to Human Activities and Natural Processes

Study 1 characterized comprehensively, over multiple time scales, recent patterns and trends in MEE vegetation greening and browning. The study first assessed and quantified the nature and magnitude of change in greenness for the period 2001–2018. To disentangle nature- versus human-driven vegetation greening and browning, the study similarly characterized trends and variability in MEE precipitation for the period 1986-2018. The study combined trend (Mann-Kendall and Sen's slope) and breakpoint (bfast) analysis methods to comprehensively examine recent vegetation greening and browning in Mount Elgon at multiple time scales. The study used both 16-day NDVI composites from MODIS and 5-day CHIRPS precipitation data and attempted to disentangle nature- versus human-driven vegetation greening and browning.

The MEE was found to exhibit significant variability in vegetation dynamics and precipitation regimes. This variability was attributed to the existing LULC orientation especially in eastern MEE and climate change and variability. As such, it is highly probable that analysis of only a few images to ascertain MEE landscape change would yield inconsistent results. The MEE

had experienced significant and persistent greening and browning at different time scales and this change was attributed to both natural factors (including changing precipitation) and anthropogenic factors (especially the vegetation-to-cropland conversion). The southwestern MEE had consistently browned due to the conversion of the Namatala swamp to paddy rice farming and settlement. A lot of activity was also observed around the mountain forest boundary as people encroached and converted the forest LULC to agriculture and settlement. There were breakpoints in the vegetation greenness TS, particularly in the savanna and grassland land covers in northeastern MEE. The breakpoints were detected in each of the monitored years (2005–2018), but most of them were observed in 2013, 2007 and 2010 (greening) and 2009 and 2017 (browning). The study also concluded that MEE precipitation had significantly changed (increased) in the post-2000 era. More specifically, total precipitation significantly increased in 2006 and 2009–2010 with a consistently decreasing trend in between. We therefore concluded that these precipitation changes influenced significant greening and browning patterns observed in the same period. The greenness–precipitation relationship was weak in other periods as greening and browning changes were not strongly influenced by changing precipitation. This may be attributed to the complex nature of the MEE landscape and/or the spatial and temporal scale mismatch between MODIS NDVI and CHIRPS precipitation data. The integration of Mann–Kendall, Sen's slope and bfast proved useful in comprehensively characterizing recent changes in vegetation greenness within the MEE. Having a comprehensive description of vegetation change is an important first step, especially for such a variable landscape, to effect policy changes aimed at simultaneously conserving the environment and improving livelihoods that are dependent on it.

6.1.2 Study 2: Environmental Vulnerability Related to Social and Natural Factors

The second study examined eco-environmental vulnerability for the MEE using freely available RS, topographic and socio-economic data. This study sought to quantitatively examine

spatio-temporal patterns and trends in eco-environmental vulnerability, and factors driving the high variability observed in the MEE landscape. The study found that the majority of the MEE (comprising savannas, grasslands, and most of the agricultural land in Ugandan MEE) was moderately vulnerable based on the analysis methods and variables used. EEVI showed a marked increase in vulnerability with decrease in elevation. EEVI is most severe in the savannas of the northwestern part of the domain. Savannas and grasslands constituted the majority of the severe vulnerability class. Eco-environmental vulnerability varied from year to year, indicating that it is a function of multiple factors operating at numerous scales (local to coarse scale). Eco-environmental vulnerability in the MEE is strongly associated with multi-year variables based on precipitation, temperature, and population density. With fast increasing populations and intensifying climate change and variability, eco-environmental vulnerability in the MEE will continue to experience significant interannual variability. Moreover, precipitation concentration is amplifying especially in the wet season, thus adding another layer of risk for agriculture and ultimately for local community livelihoods.

To achieve sustainability in the MEE ecosystem and the livelihoods it supports, areas in the moderate and severe vulnerability classes need prioritized conservation. It is recommended that environmental conservation policies be implemented and enforced in these areas by adopting the bottom-up approach in which local community members' opinions are incorporated in decision making. In addition, more data must be collected and used. Communities can be encouraged to adopt lifestyles and habits that foster more sustainable use of natural resources, and international donors can use this information to target conservation activities.

6.1.3 Study 3: Possible Future Landscape Changes in the MEE

This study simulated possible future land use changes in the MEE based on existing RS LULC products and LCM. The study examined spatial and temporal distribution of LULC change and identified areas of major LULC changes in the periods 2001-2009 and 2001-2017. Projections

to 2025 and 2033 were then developed to estimate how LULC will potentially change over time. Accuracy of the simulations (for 2017) was assessed first against the 2009 and 2017 LULC maps, and then against greening and browning surfaces over the growing season for 2001-2018. The study projected that agriculture will possibly expand from approximately 58% in 2001 to more than 64% in 2033 if current and future LULC transformation follows rates in 2001-2017. These new croplands will occur mostly around edges of the protected forest and zones of transition between mixed vegetation and existing croplands. The vulnerability for land to be converted to agriculture was significantly influenced by elevation, slope, and distance from cropland areas. Due to the unsystematic LULC transitions in the MEE (associated with the Shamba System, political changes, and climate change, among others), simulating forest-to-cropland conversion was only averagely accurate compared to mixed-to-cropland conversion. As such, decisions to use LUC models should involve an assessment of the kind of information that the models provide against the uncertainties associated with them, especially when working with highly dynamic landscapes. In addition, an integration of time series analysis methods (e.g., Mann-Kendall and Sen's Slope) with LUC modeling can provide a more comprehensive assessment of historical, present, and future LULC change – which is necessary to instigate policy changes aimed at simultaneously conserving the environment and improving livelihoods that are dependent on the natural environment.

6.2 Broader Contributions

This dissertation integrates LCS-PE theories and methods from multiple disciplines to comprehensively analyze human-environment interactions that drive observed landscape changes in the MEE. This study is important in various ways. First, it provides a more complete explanation of the underlying complex human-environment interactions shaping the MEE landscape. This includes valuable knowledge about (i.) persistent patterns of vegetation greening and browning related to changing precipitation and human activities, (ii.) levels and factors influencing eco-environmental vulnerability of the area, and (iii.) possible future changes in LULC

in the MEE. Knowledge of the complexities within the MEE can inform identification of avenues for streamlining environmental conservation and livelihood improvement efforts in the area. For instance, past LULC conversions have occurred in areas around edges of PAs and forests. EEVI significantly increases with decrease in elevation, and this vulnerability is expected to worsen with intensifying impacts of climate change. Further, grasslands and savannas have been shown to be moderately or severely vulnerable. These areas are therefore recommended for prioritized conservation. In addition, land under agriculture is projected to keep expanding into 2040 if current and future LULC follows change transitions observed in the previous two decades. Refocusing efforts to produce more food more sustainably without further expansion of agricultural land is therefore recommended.

6.3 Future Research Directions

6.3.1 Vulnerability Envelope Mapping

Future research will involve mapping the evolution of historical, present, and future environmental vulnerability in the MEE based on results from this dissertation. Areas of historical, present, and future greening and browning will be mapped and assessed against EEVI surfaces. This will establish whether persistence in greening and browning is associated with patterns of eco-environmental vulnerability. Further, these will be compared to future LULC change scenarios developed in this study – to evaluate how future vegetation change and eco-environmental vulnerability will coevolve, thus threatening the stability of the ecosystem and dependent livelihoods. This study will also factor in future climate change scenarios to develop a vulnerability envelope - to predict areas with highest eco-environmental vulnerability in future. Such an analysis can provide more information about the complex human-environment interactions in the MEE, and therefore aid in legislation of better environmental conservation and livelihood improvement policies.

6.3.2 Agent-based Modeling of Farmers Decisions

An ABM will be developed to analyze the interrelations among farmers, other actors (e.g., businesses, government among other actors), and their immediate environment, how farmers make decisions on the extent and type of farming practice to adopt, and how these decisions shape the MEE agroecological landscape. The study will focus on how these interactions enable or restrict farmers from expanding land under agriculture hence driving landscape change and dynamics studied in this dissertation. Model inputs will include internal (including family characteristics and land ownership), external (such as government legislation, businesses, and local civil society organizations, CSOs) and natural factors (including variables used in eco-environmental vulnerability and land use projections). Analysis at this fine scale will enable an exploration of cross-scale discrepancies in human-environment interactions in the highly dynamic MEE.

6.4 Closing Remarks

Fast-increasing populations and the resultant need for more land for agriculture and settlement are the primary drivers of landscape change in agroecosystems. As a result, persistent greening and browning trends are observed especially around protected areas. Such dynamics in vegetation greenness are detectable at multiple scales (e.g., 16-day, monthly, and seasonal), but can be characterized more comprehensively at the seasonal scale. Due to the high variability in these landscapes, such an analysis should integrate trend analysis and breakpoint detection methods as opposed to the use of only few images in time. Moreover, vegetation greenness is also delicately related to major changes in precipitation characteristics, a relationship that is complex and varying with site-specific factors (Malo & Nicholson 1990; Davenport & Nicholson 1993; Farrar et al. 1994; Mishra & Mainali 2017). Forests and other natural vegetation are at risk of being lost to agriculture, and efforts should be made to make agriculture more sustainable – so

that food production can be increased while fostering sustainability of Earth's environmental systems (Atzberger 2013).

The representation of vulnerability as a single index is beneficial as it helps to identify areas of highest relative vulnerability – from an integration of multiple variables. Such information is important for better environmental conservation and livelihood improvement. PCA can be useful in such environmental vulnerability assessments: it evaluates how multiple variables interact, aggregate and affect a given location (Defne et al. 2020). This is important, as human-environment systems are known to have complex interactions and therefore intricate interrelationships among biophysical and socio-political factors. By aggregating these variables into a single vulnerability index, therefore, locations experiencing highest cumulative vulnerability can be delineated. In addition to an aggregate index, vulnerability assessments should explore spatio-temporal trends in variables used in the index. This can give a clearer picture of how the vulnerability of an ecosystem has evolved over time and variables associated with this evolution.

APPENDICES

Appendix A: Field Study Questionnaire

Introduction

The questions below will enable me to collect data about farmers' interactions with each other, external stakeholders, and their environment in order to understand the various factors that influence natural-vegetation-to-cropland conversion and the impacts of such a change on crop yields. Here I will collect farmers and other stakeholders' knowledge, perceptions, actions, and attitudes in their use of the natural environment to meet their livelihood needs under the changing weather and climate. Additionally, family demographics will be collected to understand the various factors that may necessitate the conversion of the natural vegetation into cropland and settlement. Please circle, fill the blanks or tables as applicable.

Background prompts

Qa. How long have you lived on your current farm?

	0-5 years	6-10 years	11-20 years	21-30 years	30+ years
Please choose one.	○	○	○	○	○

Qb. What's your nationality?

- ○ Kenyan
- ○ Ugandan
- ○ Other

Qc. If Other, please list your nationality below.

_____
_____
_____
_____

1. Family Demographics

a. Name Code

_____
_____
_____
_____

b. Year of birth

_____
_____
_____
_____

c. Gender

- ○ Male
- ○ Female
- ○ Cannot answer

d. Are you the household head?

- ○ Yes
- ○ No

What is your marital status?

- ○ Married
- ○ Divorced
- ○ Widowed
- ○ Separated
- ○ Never married

f. What is your education level?

- ○ Less than high school
- ○ High school graduate
- ○ Some college
- ○ 2-year degree
- ○ 4-year degree
- ○ Professional degree
- ○ Doctorate

g. What is your primary occupation?

_____
_____
_____
_____

h. Are you salaried?

- ○ Yes
- ○ No

i. If yes, what is your net salary in local currency?

_____
_____
_____
_____

j. Are any of your children attending school?

- ○ Yes
- ○ No
- ○ NA

k. If yes, how much are you paying for school tuition and fees per year?

_____
_____
_____
_____

l. Do you hold any leadership positions in the community?

- ○ Yes
- ○ No

m. If yes, list the position in the community below

n. Using the scale below, indicate how much you are involved with your neighbors?

	Far below average	Moderately below average	Slightly below average	Average	Slightly above average	Moderately above average	Far above average
Click to write Statement 1							

o. Who is the major decision-maker in the household? Options include father, mother, children, any combination of these or other.

2. Please provide information about your family resources

Q2.1 Does your family own a phone(s)?

- ○ Yes
- ○ No

Q2.1.1 If Yes, state how many phones you own.

	1	2	3	4	5	6+
○ Please choose one.	○	○	○	○	○	○

Q2.2 Does your family own a radio and/or television?

- ○ Yes
- ○ No

Q2.2.1 If Yes, please state how many radio and/or television sets you have.

Q2.3 Do you own any agricultural machinery?

- ○ Yes
- ○ No

Q2.3.1 If Yes, please list the agricultural machinery you own.

Q2.4 Do you own any oxen?

- ○ Yes
- ○ No

Q2.4.1 If Yes, how many?

	1-2	3-5	6-10	10+
Please pick one.	○	○	○	○

3. Land use and ownership

Q3.1 What type of land tenure is practiced here?

- ○ Customary
- ○ Public
- ○ Private
- ○ Other

Q3.1.1 If Other, please specify

_____
_____
_____
_____

Q3.2 How many acres of land do you own?

_____
_____
_____
_____

Q3.3 Did you lease out any land in the last growing season?

- ○ Yes
- ○ No

Q3.3.1 If Yes, specify how many acres.

_____
_____
_____
_____

Q3.4 Did you rent-in any land in the last growing season?

- ○ Yes
- ○ No

Q3.4.1 If Yes, specify how many acres.

_____
_____
_____

Q3.5 Did you grow any crop(s) during the previous long growing season?

- ○ Yes
- ○ No

Q3.5.1 If you answered Yes, please specify the main crop?

_____
_____
_____
_____

Q3.6 Did you grow any crop(s) during the previous short growing season?

- ○ Yes
- ○ No

Q3.6.1 If you answered Yes, please specify the main crop.

_____
_____
_____
_____

Q3.7 Did you leave any land fallow?

- ○ Yes
- ○ No

Q3.7.1 If you answered Yes, please state how many acres.

_____
_____
_____
_____

Q3.8 Looking back at least 10 years, have you increased or reduced land under agriculture?

- ○ Increased
- ○ Reduced

Q3.9 If reduced, what did you convert the land to and why?

_____
_____
_____
_____

Q3.10 If increased, which land uses were converted?

- ○ Forest
- ○ Shrub
- ○ Grassland
- ○ Bare land
- ○ Other

Q3.10.1 If Other, please specify.

Q3.11 Please explain reasons that necessitated expansion of land under agriculture.

4. Farm labor and sources

Q4.1 What is the major source of your farm labor?

- ○ Family
- ○ Hired casual laborers
- ○ Family relatives
- ○ 2&3
- ○ Other

Q4.1.1 If Other, please specify

5. Farm credit and subsidy access

Q5.1 Have you received any fertilizer subsidies in the past 3 years?

- ○ Yes
- ○ No

Q5.1.1 If Yes, please list the year, amount (in Kg) and source.

Q5.2 Have you received any other agricultural subsidies in the past 3 years?

- ○ Yes
- ○ No

Q5.2.1 If Yes, please list the year, amount and source.

Q5.3 Have you received any agricultural credit in the past 3 years?

- ○ Yes
- ○ No

Q5.3.1 If Yes, please list the year, amount and source.

_____
_____
_____
_____

Q5.4 Compared to the past 5-10 years, how easy or difficult is it to access these resources?

	Extremely easy	Moderately easy	Slightly easy	Neither easy nor difficult	Slightly difficult	Moderately difficult	Extremely difficult
Click to write Statement 1	○	○	○	○	○	○	○

6. Income

Q6.1 Do you consider your previous season's yields to be below average, average or above average?

- ○ Below average
- ○ Average
- ○ Above average

Q6.2 How much did you earn from agriculture (in local currency)?

_____
_____
_____
_____

Q6.3 Do you have any other income-generating activity, apart from agriculture?

- ○ Yes
- ○ No

Q6.3.1 If Yes, please list them alongside the monthly wage.

	Job type	Monthly wage (in local currency)	Is it a constant amount every month?	How long have you been working (in years)?
Click to write Statement 1				
Click to write Statement 2				

7. Involvement in civil society organizations and other non-governmental groups

Q7.1 Are you a member of any civil society organization (CSO) or any other groups?

- ○ Yes
- ○ No

Q7.1.1 If yes, please list the services you receive from the organization.

_____
_____
_____
_____

Q7.2 Have you received any sort of training or sensitization about environmental conservation?

- ○ Yes
- ○ No

Q7.2.1 If Yes, how has this influenced your agricultural practices?

_____
_____
_____
_____

Q7.3 Are you aware of any government legislation about local land use and access?

- ○ Yes
- ○ No

Q7.3.1 If Yes, how have these influenced your agricultural practices?

_____
_____
_____
_____

Q7.4 Are there any agricultural extension officers who visit and advise you about agriculture and climate issues?

- ○ Yes
- ○ No

Q7.4 Are there any agricultural extension officers who visit and advise you about agriculture and climate issues?

- ○ Yes
- ○ No

Q7.4 Are there any agricultural extension officers who visit and advise you about agriculture and climate issues?

- ○ Yes
- ○ No

Q7.4.1 If Yes, how many of such visits did you receive in the past growing season?

- ○ 1-2

- ○ 3-5
- ○ 5+

8. Changes in the weather and climate

Q8.1 Looking back 10 years, have you noticed any changes in rainfall patterns?

- ○ Yes
- ○ No

Q8.1.1 If Yes, what changes have you observed?

Q8.2 How has the change in Q8.1.1 impacted your crop yields and agricultural practices?

Q8.3 How have you adapted to or mitigated the impacts of the change in Q8.1.1?

Q8.4 Looking back 10 years, have you noticed any changes in temperature?

- ○ Yes
- ○ No

Q8.5.1 If Yes, what changes have you observed?

Q8.6 How has the change in Q8.5.1 impacted your crop yields and agricultural practices?

Q8.7 How have you adapted to or mitigated the impacts of the change in Q8.5.1?

Q8.8 General comment about location's LULC/interviewee.

Appendix B: Sensitivity of Model to Forcing Independent Variables to be Constant

Results from sensitivity analysis of explanatory variables used in the M0109 model are shown in Tables A2-A4. Table A1 represents the explanatory variables.

Table A.1. *Explanatory variables used in the M0109 model.*

Var. 1	Distance from 2001-2009 cropland areas
Var. 2	AMJ_LTSD (mm)
Var 3.	Annual LTSD (mm)
Var. 4	Distance from rivers (m)
Var. 5	Elevation (m)
Var. 6	Slope (%)
Var. 7	Distance from 2001 urban areas (m)

Table A.2. *Forcing a single independent variable to be constant*

Model	Accuracy (%)	Skill measure	Influence order
With all variables	92.80	0.9041	N/A
Var. 1 constant	64.43	0.5257	2
Var. 2 constant	92.80	0.9041	6
Var. 3 constant	92.80	0.9041	7 (least influential)
Var. 4 constant	92.63	0.9018	5
Var. 5 constant	59.00	0.4533	1 (most influential)
Var. 6 constant	91.89	0.8918	3
Var. 7 constant	92.50	0.9000	4

Table A.3. *Forcing all independent variables except one to be constant.*

Model	Accuracy (%)	Skill measure
With all variables	92.80	0.9041
All constant but Var. 1	48.07	0.3075
All constant but Var. 2	15.92	-0.1211
All constant but Var. 3	15.92	-0.1211
All constant but Var. 4	38.76	0.1835
All constant but Var. 5	63.24	0.5098
All constant but Var. 6	57.03	0.4270
All constant but Var. 7	43.72	0.2496

Table A. 4. *Backwards stepwise constant forcing.*

Model	Variables included	Accuracy (%)	Skill measure
With all variables	All variables	92.80	0.9041
Step 1: Var. [2] constant	[1,3,4,5,6,7]	92.80	0.9041
Step 2: var. [2,4] constant	[1,3,5,6,7]	92.63	0.9018
Step 3: Var. [2,4,7] constant	[1,3,5,6]	92.06	0.8941
Step 4: Var. [2,4,7,3] constant	[1,5,6]	90.33	0.8710
Step 5: Var. [2,4,7,3,6] constant	[1,5]	87.41	0.8321
Step 6: Var. [2,4,7,3,6,1] constant	[5]	63.24	0.5098

REFERENCES

REFERENCES

Abson DJ, Dougill AJ, Stringer LC. 2012. Using Principal Component Analysis for information-rich socio-ecological vulnerability mapping in Southern Africa. Appl Geogr [Internet]. 35:515–524. http://dx.doi.org/10.1016/j.apgeog.2012.08.004

Aburas MM, Ho YM, Pradhan B, Salleh AH, Alazaiza MYD. 2021. Spatio-temporal simulation of future urban growth trends using an integrated CA-Markov model. Arab J Geosci. 14(2).

Alavipanah S, Wegmann M, Qureshi S, Weng Q, Koellner T. 2015. The role of vegetation in mitigating urban land surface temperatures: A case study of Munich, Germany during the warm season. Sustain. 7(4):4689–4706.

Alcaraz-Segura D, Chuvieco E, Epstein HE, Kasischke ES, Trishchenko A. 2010. Debating the greening vs. browning of the North American boreal forest: Differences between satellite datasets. Glob Chang Biol. 16(2):760–770.

Aleksandrova M, Gain AK, Giupponi C. 2016. Assessing agricultural systems vulnerability to climate change to inform adaptation planning: an application in Khorezm, Uzbekistan. Mitig Adapt Strateg Glob Chang [Internet]. 21(8):1263–1287. http://dx.doi.org/10.1007/s11027-015-9655-y

Ansari A, Golabi MH. 2019. Prediction of spatial land use changes based on LCM in a GIS environment for Desert Wetlands – A case study: Meighan Wetland, Iran. Int Soil Water Conserv Res [Internet]. 7(1):64–70. http://dx.doi.org/10.1016/j.iswcr.2018.10.001

Anseeuw W, Alden C, editors. 2010. The struggle over land in Africa: Conflicts, politics and change. Cape Town, South Africa: HSRC Press.

Anyamba A, Eastman JR. 1996. Interannual variability of ndvi over africa and its relation to el niño/southern oscillation. Int J Remote Sens. 17(13):2533–2548.

AppEEARS Team. 2019. Application for Extracting and Exploring Analysis Ready Samples (AppEEARS). Sioux Falls, SD, USA: LP DAAC.

Appelhans AT, Detsch F, Nauss T, Appelhans MT. 2016. Package ‘ remote .’

Aretano R, Semeraro T, Petrosillo I, De Marco A, Pasimeni MR, Zurlini G. 2015. Mapping ecological vulnerability to fire for effective conservation management of natural protected areas. Ecol Modell [Internet]. 295:163–175. http://dx.doi.org/10.1016/j.ecolmodel.2014.09.017

Arowolo AO, Deng X. 2018. Land use/land cover change and statistical modelling of cultivated land change drivers in Nigeria. Reg Environ Chang. 18(1):247–259.

Atzberger C. 2013. Advances in remote sensing of agriculture: Context description, existing operational monitoring systems and major information needs. Remote Sens. 5(2):949–981.

Aydi A. 2018. Evaluation of groundwater vulnerability to pollution using a GIS-based multi-criteria decision analysis. Groundw Sustain Dev [Internet]. 7:204–211. https://doi.org/10.1016/j.gsd.2018.06.003

Ayugi B, Tan G, Rouyun N, Zeyao D, Ojara M, Mumo L, Babaousmail H, Ongoma V. 2020. Evaluation of meteorological drought and flood scenarios over Kenya, East Africa. Atmosphere (Basel). 11(3).

Ayuyo IO, Sweta L. 2014. Land Cover and Land Use Mapping and Change Detection of Mau Complex in Kenya Using Geospatial Technology. Int J Sci Res. 3(3):767–778.

Baca M, Läderach P, Haggar J, Schroth G, Ovalle O. 2014. An integrated framework for assessing vulnerability to climate change and developing adaptation strategies for coffee growing families in mesoamerica. PLoS One. 9(2).

Badjana HM, Helmschrot J, Selsam P, Wala K, Flugel W-A, Afouda A, Akpagana K. 2015. Land Cover Changes assessment using object-based image analysis in the Binah River watereshed (Togo and Benin). Earth Sp Sci. 2:403–416.

Ballantyne A, Smith W, Anderegg W, Kauppi P, Sarmiento J, Tans P, Shevliakova E, Pan Y, Poulter B, Anav A, et al. 2017. Accelerating net terrestrial carbon uptake during the warming hiatus due to reduced respiration. Nat Clim Chang. 7(2):148–152.

Bamutaze Y, Tenywa MM, Majaliwa M, Vanacker V, Bagoora F, Magunda M, Obando J, Wasige JE. 2010. Infiltration characteristics of volcanic sloping soils on Mount Elgon, Eastern Uganda. Catena. 80.

Barasa B, Kakembo V. 2013. The impact of land use/cover change on soil organic carbon and its implication on food security and climate change vulnerability on the slopes of Mt. Elgon, Eastern Uganda. Port Elizabeth, South Africa: Nelson Mandela Metropolitan University.

De Beurs KM, Henebry GM. 2010. A land surface phenology assessment of the northern polar regions using MODIS reflectance time series. Can J Remote Sens. 36:S87–S110.

BirdLife International. Important Bird and Biodiversity Areas (IBAs) [Internet]. [accessed 2020 May 1]. https://www.birdlife.org/worldwide/programme-additional-info/important-bird-and-biodiversity-areas-ibas

Boori MS, Choudhary K, Paringer R, Kupriyanov A. 2021. Eco-environmental quality assessment based on pressure-state-response framework by remote sensing and GIS. Remote Sens Appl Soc Environ [Internet]. 23. https://doi.org/10.1016/j.rsase.2021.100530

Bradley BA, Jacob RW, Hermance JF, Mustard JF. 2007. A curve fitting procedure to derive inter-annual phenologies from time series of noisy satellite NDVI data. Remote Sens Environ. 106(2):137–145.

Brink AB, Bodart C, Brodsky L, Defourney P, Ernst C, Donney F, Lupi A, Tuckova K. 2014. Anthropogenic pressure in East Africa - Monitoring 20 years of land cover changes by means of medium resolution satellite data. Int J Appl Earth Obs Geoinf [Internet]. 28(1):60–69. http://dx.doi.org/10.1016/j.jag.2013.11.006

Broeckx J, Maertens M, Isabirye M, Vanmaercke M, Namazzi B, Deckers J, Tamale J, Jacobs L, Thiery W, Kervyn M, et al. 2019. Landslide susceptibility and mobilization rates in the Mount Elgon region, Uganda. Landslides. 16(3):571–584.

Bryan E, Ringler C, Okoba B, Roncoli C, Silvestri S, Herrero M. 2013. Adapting agriculture to climate change in Kenya: Household strategies and determinants. J Environ Manage. 114:26–35.

Camacho Olmedo MT, Pontius RG, Paegelow M, Mas JF. 2015. Comparison of simulation models in terms of quantity and allocation of land change. Environ Model Softw [Internet]. 69:214–221. http://dx.doi.org/10.1016/j.envsoft.2015.03.003

Campbell DJ, Olson JM. 1991. Framework for Environment and Development : The Kite. East Lansing.

Chamaille-Jammes S, Fritz H, Murindagomo F. 2006. Spatial patterns of the NDVI-rainfall relationship at the seasonal and interannual time scales in an African savanna. Int J Remote Sens. 27(23):5185–5200.

Chen C, Li T, Li J, Fu W, Wang G. 2018. Vegetation Change Analyses Considering Climate Variables and Anthropogenic Variables in the Three-River Headwaters Region. 3:419–409.

Chinese Ministry of Natural Resources. 2019. GlobeLand30: Global Geo-information Public Product [Internet]. [accessed 2021 Jun 1]. http://www.globeland30.org/home_en.html?type=data

Climate Hazards Center. 2018. CHIRTSmonthly [Internet]. [accessed 2020 Jul 3]. https://www.chc.ucsb.edu/data/chirtsmonthly

Crist E.P., Cicone R.C. 1984. A Physically-Based Transformation of Thematic Mapper Data-The TM Tasseled Cap. IEEE Trans Geosci Remote Sens. 22(3):256–263.

Daron JD. 2014. Regional Climate Messages for East Africa. Ottawa, ON: CARIAA.

Das P, Behera MD, Pal S, Chowdary VM, Behera PR, Singh TP. 2019. Studying land use dynamics using decadal satellite images and Dyna-CLUE model in the Mahanadi River basin, India. Environ Monit Assess. 191.

Davenport ML, Nicholson SE. 1993. On the relation between rainfall and the Normalized Difference Vegetation Index for diverse vegetation types in East Africa. Int J Remote Sens. 14(12):2369–2389.

Defne Z, Aretxabaleta AL, Ganju NK, Kalra TS, Jones DK, Smith KEL. 2020. A geospatially resolved wetland vulnerability index: Synthesis of physical drivers. PLoS One [Internet]. 15(1):1–27. http://dx.doi.org/10.1371/journal.pone.0228504

DeVries B, Verbesselt J, Kooistra L, Herold M. 2015. Robust monitoring of small-scale forest disturbances in a tropical montane forest using Landsat time series. Remote Sens Environ [Internet]. 161:107–121. http://dx.doi.org/10.1016/j.rse.2015.02.012

Didan K. 2015. MOD13Q1 MODIS/Terra Vegetation Indices 16-Day L3 Global 250m SIN Grid V006. Sioux Falls, SD, USA: NASA EOSDIS Land Processes DAAC.

DIVA-GIS. Download Data by Country [Internet]. [accessed 2021 Jun 2]. https://www.diva-gis.org/gdata

Doumenge C, Gilmour D, Pérez MR, Blockhus J. 1995. Tropical montane cloud forests: Conservation status and management issues. In: Hamilton LS, Juvik JO, Scatena FN, editors. Trop Mont cloud For. New York, NY: Springer; p. 24–37.

Duarte L, Teodoro AC, Gonçalves JA, Guerner Dias AJ, Espinha Marques J. 2015. A dynamic map application for the assessment of groundwater vulnerability to pollution. Environ Earth Sci. 74(3):2315–2327.

EAC, UNEP, GRID-Arendal. 2016. Sustainable mountain development in East Africa in a changing climate. Arusha, Tanzania: EAC.

Eastman JR. 2016a. TerrSet Geospatial Monitoring and Modeling System Manual. [place unknown].

Eastman JR. 2016b. TerrSet Geospatial Monitoring and Modeling System Tutorial. :283.

Eastman JR, He J. 2020. A regression-based procedure for markov transition probability estimation in land change modeling. Land. 9(11):1–12.

Eliasson Å, Jones RJA, Nachtergaele F, Rossiter DG, Terres JM, Van Orshoven J, van Velthuizen H, Böttcher K, Haastrup P, Le Bas C. 2010. Common criteria for the redefinition of Intermediate Less Favoured Areas in the European Union. Environ Sci Policy. 13(8):766–777.

Ellis E. 2007. Land-use and land-cover change and Climate change. Encycl Earth.:4.

Ellis EC, Ramankutty N. 2008. Putting people in the map: Anthropogenic biomes of the world. Front Ecol Environ. 6(8):439–447.

Emmett KD, Renwick KM, Poulter B. 2019. Disentangling Climate and Disturbance Effects on Regional Vegetation Greening Trends. Ecosystems [Internet]. 22(4):873–891. https://doi.org/10.1007/s10021-018-0309-2

Enea M, Salemi G. 2001. Fuzzy approach to the environmental impact evaluation. Ecol Modell. 136(2–3):131–147.

Fabricante I, Oesterheld M, Paruelo JM. 2009. Annual and seasonal variation of NDVI explained by current and previous precipitation across Northern Patagonia. J Arid Environ [Internet]. 73(8):745–753. http://dx.doi.org/10.1016/j.jaridenv.2009.02.006

Fan Z, Liu M, Shen W, Lin L. 2009. GIS-based assessment on eco-vulnerability of Jiangxi Province. Proc - 2009 Int Conf Environ Sci Inf Appl Technol ESIAT 2009. 3:426–431.

FAO. 2016. The state of food and agriculture: climate change, agriculture and food security. Rome.

FAO, UNEP. 2020. The State of the World's Forests 2020: Forests, biodiversity and people. Rome. https://doi.org/10.4060/ca8642en

Farrar TJ, Nicholson SE, Lare AR. 1994. The influence of soil type on the relationships between NDVI, rainfall, and soil moisture in semiarid Botswana. I. NDVI response to rainfall. Remote Sens Environ. 50(2):107–120.

Feddema JJ, Oleson KW, Bonan GB, Mearns LO, Buja LE, Meehl GA. 2005. The Importance of Land-Cover Change in Simulating Future Climates. Science (80-). 310:1674–1678.

Fensholt R, Langanke T, Rasmussen K, Reenberg A, Prince SD, Tucker C, Scholes RJ, Le QB, Bondeau A, Eastman R, et al. 2012. Greenness in semi-arid areas across the globe 1981-2007 - an Earth Observing Satellite based analysis of trends and drivers. Remote Sens Environ [Internet]. 121:144–158. http://dx.doi.org/10.1016/j.rse.2012.01.017

Fetene A, Hilker T, Yeshitela K, Prasse R, Cohen W, Yang Z. 2016. Detecting Trends in Landuse and Landcover Change of Nech Sar National Park, Ethiopia. Environ Manage. 57(1):137–147.

FEWS Net. 2013. Kenya Food Security Brief. Washington, DC, USA: USAID.

Foley JA, Barford C, Coe MT, Gibbs HK, Helkowski JH, Holloway T, Howard EA, Kucharik CJ, Monfreda C, Patz JA, et al. 2005. Global consequences of land use. Science (80-). 309(5734):570–574.

Foody GM. 2002. Status of land cover classification accuracy assessment. Remote Sens Environ. 80(1):185–201.

Forzieri G, Alkama R, Miralles DG, Cescatti A. 2018. Response to Comment on “Satellites reveal contrasting responses of regional climate to the widespread greening of Earth.” Science. 360(6394):1180–1184.

Funk C, Peterson P, Landsfeld M, Pedreros D, Verdin J, Shukla S, Husak G, Rowland J, Harrison L, Hoell A, Michaelsen J. 2015. The climate hazards infrared precipitation with stations - A new environmental record for monitoring extremes. Sci Data. 2:1–21.

Funk C, Peterson P, Peterson S, Shukla S, Davenport F, Michaelsen J, Knapp KR, Landsfeld M, Husak G, Harrison L, et al. 2019. A high-resolution 1983–2016 TMAX climate data record based on infrared temperatures and stations by the climate hazard center. J Clim. 32(17):5639–5658.

Gashu K, Aminu O. 2019. Participatory forest management and smallholder farmers’ livelihoods improvement nexus in Northwest Ethiopia. J Sustain For [Internet]. 38(5):413–426. https://doi.org/10.1080/10549811.2019.1569535

Gemitzi A, Banti M, Lakshmi V. 2019. Vegetation greening trends in different land use types: natural variability versus human-induced impacts in Greece. Environ Earth Sci [Internet]. 78(5):1–10. http://dx.doi.org/10.1007/s12665-019-8180-9

Georganos S, Abdi AM, Tenenbaum DE, Kalogirou S. 2017. Examining the NDVI-rainfall relationship in the semi-arid Sahel using geographically weighted regression. J Arid Environ [Internet]. 146:64–74. http://dx.doi.org/10.1016/j.jaridenv.2017.06.004

Getachew Tesfaye Ayehu SA. 2015. Land Suitability Analysis for Rice Production: A GIS Based Multi-Criteria Decision Approach. Am J Geogr Inf Syst . 4(3):95–104.

Gharaibeh A, Shaamala A, Obeidat R, Al-Kofahi S. 2020. Improving land-use change modeling by integrating ANN with Cellular Automata-Markov Chain model. Heliyon [Internet]. 6(9):e05092. https://doi.org/10.1016/j.heliyon.2020.e05092

Gibson L, Münch Z, Palmer A, Mantel S. 2018. Future land cover change scenarios in South African grasslands – implications of altered biophysical drivers on land management. Heliyon. 4(7).

Githui FW. 2008. Assessing the Impacts of Environmental Change on the Hydrology of the Nzoia Catchment, in the Lake Victoria Basin. [place unknown]: Vrije Universiteit Brussel. http://twws6.vub.ac.be/hydr/wbauwens/PhD-Thesis/Thesis/PhD_Githui.pdf

Global Historical Climatology Network - Daily (GHCN-Daily). 2012. Asheville, NC: National Centers for Environmental Information.

Gómez C, White JC, Wulder MA. 2016. Optical remotely sensed time series data for land cover classification: A review. ISPRS J Photogramm Remote Sens. 116:55–72.

Google Earth Pro. 2020. Menlo Park, CA, USA: Google LLC.

Gorelick N, Hancher M, Dixon M, Ilyushchenko S, Thau D, Moore R. 2017. Google Earth Engine: Planetary-scale geospatial analysis for everyone. Remote Sens Environ.

Government of Kenya. 2009. AGRICULTURAL SECTOR DEVELOPMENT strategy (ASDS) 2009 - 2020. [place unknown].

Guan DJ, Li HF, Inohae T, Su W, Nagaie T, Hokao K. 2011. Modeling urban land use change by the integration of cellular automaton and Markov model. Ecol Modell [Internet]. 222(20–22):3761–3772. http://dx.doi.org/10.1016/j.ecolmodel.2011.09.009

Guan Q, Yang L, Pan N, Lin J, Xu C, Wang F, Liu Z. 2018. Greening and browning of the Hexi Corridor in northwest China: Spatial patterns and responses to climatic variability and anthropogenic drivers. Remote Sens. 10(8).

Gunton RM, Firbank LG, Inman A, Winter DM. 2016. How scalable is sustainable intensification? Nat Plants [Internet]. 2(5):1–4. http://dx.doi.org/10.1038/nplants.2016.65

Guo B, Fan Y, Yang F, Jiang L, Yang W, Chen S, Gong R, Liang T. 2019. Quantitative assessment model of ecological vulnerability of the Silk Road Economic Belt, China, utilizing remote sensing based on the partition–integration concept. Geomatics, Nat Hazards Risk [Internet]. 10(1):1346–1366. https://doi.org/10.1080/19475705.2019.1568313

Guzha AC, Rufino MC, Okoth S, Jacobs S, Nóbrega RLB. 2018. Impacts of land use and land cover change on surface runoff, discharge and low flows: Evidence from East Africa. J Hydrol Reg Stud. 15(May 2017):49–67.

Haghtalab N, Moore N, Heerspink BP, Hyndman DW. 2020. Evaluating spatial patterns in precipitation trends across the Amazon basin driven by land cover and global scale forcings. Theor Appl Climatol. 140(1–2):411–427.

Haghtalab N, Moore N, Ngongondo C. 2019. Spatio-temporal analysis of rainfall variability and seasonality in Malawi. Reg Environ Chang. 19(7):2041–2054.

Hailemariam SN, Soromessa T, Teketay D. 2016. Land use and land cover change in the Bale Mountain eco-region of Ethiopia during 1985 to 2015. Land. 5(4).

Halmy MWA, Gessler PE, Hicke JA, Salem BB. 2015. Land use/land cover change detection and prediction in the north-western coastal desert of Egypt using Markov-CA. Appl Geogr [Internet]. 63:101–112. http://dx.doi.org/10.1016/j.apgeog.2015.06.015

Hamilton AC, Perrott RA. 1981. A study of altitudinal zonation in the montane forest belt of Mt. Elgon, Kenya/Uganda. Vegetatio. 45:107–125.

Han J, Park S, Kim S, Son S, Lee S, Kim J. 2019. Performance of logistic regression and support vector machines for seismic vulnerability assessment and mapping: A case study of the 12 September 2016 ML5.8 Gyeongju earthquake, South Korea. Sustain. 11(24):1–19.

Hasan S, Shi W, Zhu X, Abbas S, Khan HUA. 2020. Future simulation of land use changes in rapidly urbanizing South China based on land change modeler and remote sensing data. Sustain. 12(11):4–6.

Hatfield JL, Prueger JH. 2015. Temperature extremes: Effect on plant growth and development. Weather Clim Extrem. 10:4–10.

Hawinkel P, Thiery W, Lhermitte S, Swinnen E, Verbist B, Van Orshoven J, Muys B. 2016. Vegetation response to precipitation variability in East Africa controlled by biogeographical factors. J Geophys Res Biogeosciences. 121(9):2422–2444.

He L, Shen J, Zhang Y. 2018. Ecological vulnerability assessment for ecological conservation and environmental management. J Environ Manage. 206:1115–1125.

Helman D, Zaitchik BF. 2020. Temperature anomalies affect violent conflicts in African and Middle Eastern warm regions. Glob Environ Chang. 63.

Van den Hende C, Van Schaeybroeck B, Nyssen J, Van Vooren S, Van Ginderachter M, Termonia P. 2021. Analysis of rain-shadows in the Ethiopian Mountains using climatological model data. Clim Dyn [Internet]. 56(5–6):1663–1679. https://doi.org/10.1007/s00382-020-05554-2

Hermance JF, Jacob RW, Bradley BA, Mustard JF. 2007. Extracting phenological signals from multiyear AVHRR NDVI time series: Framework for applying high-order annual splines with roughness damping. IEEE Trans Geosci Remote Sens. 45(10):3264–3276.

Hou K, Li X, Zhang J. 2015. GIS analysis of changes in ecological vulnerability using a SPCA model in the Loess Plateau of Northern Shaanxi, China. Int J Environ Res Public Health.:4292–4305.

Huang J, Wu Y, Gao T, Zhan Y, Cui W. 2015. An integrated approach based on Markov chain and cellular automata to simulation of urban land use changes. Appl Math Inf Sci. 9(2):769–775.

Huong NTL, Yao S, Fahad S. 2019. Assessing household livelihood vulnerability to climate change: The case of Northwest Vietnam. Hum Ecol Risk Assess [Internet]. 25(5):1157–1175. https://doi.org/10.1080/10807039.2018.1460801

IPCC. 2001. Climate change 2001: impacts, adaptation, and vulnerability. Cambridge, United Kingdom.

Iversen P, Lee D, Rocha M. 2014. Understanding land use in the UNF-CCC. [place unknown].

Ji W, Cui J. 2021. Application of land ecological environment risk assessment based on SAR image. Arab J Geosci. 14(1713):1–13.

Jiang L, Huang X, Wang F, Liu Y, An P. 2018. Method for evaluating ecological vulnerability under climate change based on remote sensing: A case study. Ecol Indic [Internet]. 85(2):479–486. https://doi.org/10.1016/j.ecolind.2017.10.044

Jolliffe IT. 1990. Principal component analysis: A beginner's guide - I. Introduction and application. Weather. 45(10):375–382.

Jun C, Ban Y, Li S. 2014. Open access to Earth land-cover map. Nature. 514(7253):434.

Kabubo-Mariara J, Kabara M. 2015. Climate Change and Food Security in Kenya. Environ Dev.

Kelly PM, Adger WN. 2000. Theory and practice in assessing vulnerability to climate change and facilitating adaptation. Clim Change. 47(4):325–352.

Kennedy RE, Yang Z, Cohen WB. 2010. Detecting trends in forest disturbance and recovery using yearly Landsat time series: 1. LandTrendr - Temporal segmentation algorithms. Remote Sens Environ [Internet]. 114(12):2897–2910. http://dx.doi.org/10.1016/j.rse.2010.07.008

Khambhammettu P. 2005. Annual Groundwater Monitoring Report, Appendix D - Mann-Kendall Analysis for the Fort Ord Site. Monterey County, CA, USA: HydroGeoLogic, Inc.

Kibret S, Lautze J, McCartney M, Nhamo L, Yan G. 2019. Malaria around large dams in Africa: Effect of environmental and transmission endemicity factors. Malar J [Internet]. 18(1):1–12. https://doi.org/10.1186/s12936-019-2933-5

Kogo BK, Kumar L, Koech R, Kariyawasam CS. 2019. Modelling climate suitability for rainfed maize cultivation in Kenya using a maximum entropy (MAXENT) approach. Agronomy. 9(11).

Kolb M, Mas JF, Galicia L. 2013. Evaluating drivers of land-use change and transition potential models in a complex landscape in Southern Mexico. Int J Geogr Inf Sci [Internet]. 27(9):1804–1827. http://dx.doi.org/10.1080/13658816.2013.770517

Kotikot SM, Flores A, Griffin RE, Sedah A, Nyaga J, Mugo R, Limaye A, Irwin DE. 2018. Mapping threats to agriculture in East Africa: Performance of MODIS derived LST for frost identification in Kenya's tea plantations. Int J Appl Earth Obs Geoinf. 72:131–139.

Lambin EF, Meyfroidt P. 2011. Global land use change, economic globalization, and the looming land scarcity. Proc Natl Acad Sci. 108(9):3465–3472.

Lamchin M, Lee WK, Jeon SW, Wang SW, Lim CH, Song C, Sung M. 2018. Long-term trend of and correlation between vegetation greenness and climate variables in Asia based on satellite data. MethodsX [Internet]. 5:803–807. https://doi.org/10.1016/j.mex.2018.07.006

Landmann T, Dubovyk O. 2014. Spatial analysis of human-induced vegetation productivity decline over eastern Africa using a decade (2001-2011) of medium resolution MODIS time-series data. Int J Appl Earth Obs Geoinf [Internet]. 33(1):76–82. http://dx.doi.org/10.1016/j.jag.2014.04.020

Leutner B, Horning N, Schwalb-Willmann J, Hijmans RJ, Leutner MB. 2019. Package ‘ RStoolbox .’

Li A, Wang A, Liang S, Zhou W. 2006. Eco-environmental vulnerability evaluation in mountainous region using remote sensing and GIS - A case study in the upper reaches of Minjiang River, China. Ecol Modell. 192(1–2):175–187.

Li C, Chai Y, Yang L, Li H. 2016. Spatio-temporal distribution of flood disasters and analysis of influencing factors in Africa. Nat Hazards. 82(1):721–731.

Li J, Oyana TJ, Mukwaya PI. 2016. An examination of historical and future land use changes in Uganda using change detection methods and agent-based modelling. African Geogr Rev [Internet]. 6812:1–25. http://dx.doi.org/10.1080/19376812.2016.1189836

Li Q, Shi X, Wu Q. 2021. Effects of protection and restoration on reducing ecological vulnerability. Sci Total Environ. 761.

Liao A, Chen L, Chen Jun, He C, Cao X, Chen Jin, Peng S, Sun F, Gong P. 2014. High-resolution remote sensing mapping of global land water. Sci China Earth Sci. 57(10):2305–2316.

Liou YA, Nguyen AK, Li MH. 2017. Assessing spatiotemporal eco-environmental vulnerability by Landsat data. Ecol Indic [Internet]. 80:52–65. http://dx.doi.org/10.1016/j.ecolind.2017.04.055

Lu Y, Wu P, Ma X, Li X. 2019. Detection and prediction of land use/land cover change using spatiotemporal data fusion and the Cellular Automata–Markov model. Environ Monit Assess. 191(2).

De Luis M, González-Hidalgo JC, Brunetti M, Longares LA. 2011. Precipitation concentration changes in Spain 1946-2005. Nat Hazards Earth Syst Sci. 11(5):1259–1265.

Maitima JM, Mugatha SM, Reid RS, Gachimbi LN, Majule A, Lyaruu H, Pomery D, Mathai S, Mugisha S. 2009. The linkages between land use change, land degradation and biodiversity across East Africa. African J Agric Res. 3(10):310–325.

Malo AR, Nicholson SE. 1990. A study of rainfall and vegetation dynamics in the African Sahel using normalized difference vegetation index. J Arid Environ [Internet]. 19(1):1–24. http://dx.doi.org/10.1016/S0140-1963(18)30825-5

Mann HB. 1945. Nonparametric Tests Against Trend. Econometrica. 13(3):245–259.

Mawa C, Babweteera F, Tumusiime DM. 2020. Conservation Outcomes of Collaborative Forest Management in a Medium Altitude Semideciduous Forest in Mid-western Uganda. J Sustain For [Internet].:1–20. https://doi.org/10.1080/10549811.2020.1841006

McKinney L, Wright DC. 2021. Climate Change and Water Dynamics in Rural Uganda. Sustainability. 13(15):8322.

McNally A, Verdin K, Harrison L, Getirana A, Jacob J, Shukla S, Arsenault K, Peters-Lidard C, Verdin JP. 2019. Acute water-scarcity monitoring for Africa. Water (Switzerland). 11(10).

Metzger MJ, Rounsevell MDA, Acosta-Michlik L, Leemans R, Schröter D. 2006. The vulnerability

of ecosystem services to land use change. Agric Ecosyst Environ. 114(1):69–85.

Ministry of Water and Environment Uganda. 2016. Uganda Wetlands Atlas. Kampala, Uganda: Ministry of Water and Environment Uganda.

Mishra NB, Mainali KP. 2017. Greening and browning of the Himalaya: Spatial patterns and the role of climatic change and human drivers. Sci Total Environ [Internet]. 587–588(March):326–339. http://dx.doi.org/10.1016/j.scitotenv.2017.02.156

Mishra VN, Rai PK. 2016. A remote sensing aided multi-layer perceptron-Markov chain analysis for land use and land cover change prediction in Patna district (Bihar), India. Arab J Geosci [Internet]. 9(4). http://dx.doi.org/10.1007/s12517-015-2138-3

Morrison J, Higginbottom TP, Symeonakis E, Jones MJ, Omengo F, Walker SL, Cain B. 2018. Detecting vegetation change in response to confining elephants in forests using MODIS time-series and BFAST. Remote Sens. 10(7).

Mugagga F, Kakembo V, Buyinza M. 2012. Land use changes on the slopes of Mount Elgon and the implications for the occurrence of landslides. Catena [Internet]. 90:39–46. http://dx.doi.org/10.1016/j.catena.2011.11.004

Mugagga F, Nagasha B, Barasa B, Buyinza M. 2015. The Effect of Land Use on Carbon Stocks and Implications for Climate Variability on the Slopes of Mount Elgon, Eastern Uganda. Int J Reg Dev. 2(1):58.

Muhweezi AB, Sikoyo GM, Chemonges M. 2007. Introducing a Transboundary Ecosystem Management Approach in the Mount Elgon Region. Mt Res Dev. 27(3):215–219.

Mumba M, Kutegeka S, Nakangu B, Munang R, Sebukeera C. 2016. Ecosystem-based Adaptation (EbA) of African Mountain Ecosystems: Experiences from Mount Elgon, Uganda. In: Salzmann N, Huggel C, Nussbaumer SU, Ziervogel G, editors. Clim Chang Adapt Strateg – An Upstream-downstream Perspect. [place unknown]: Springer International Publishing Switzerland; p. 121–140.

Mungai LM, Messina JP, Snapp S. 2020. Spatial pattern of agricultural productivity trends in Malawi. Sustain. 12(4):1–22.

Murthy K, Bagchi S. 2018. Spatial patterns of long-term vegetation greening and browning are consistent across multiple scales: Implications for monitoring land degradation. L Degrad Dev. 29(8):2485–2495.

Musau J, Patil S, Sheffield J, Marshall M. 2018. Vegetation dynamics and responses to climate anomalies in East Africa. Earth Syst Dyn Discuss.:1–27.

Musau J, Sang J, Gathenya J, Luedeling E. 2015. Hydrological responses to climate change in Mt. Elgon watersheds. J Hydrol Reg Stud [Internet]. 3:233–246. http://dx.doi.org/10.1016/j.ejrh.2014.12.001

Muthoni FK, Odongo VO, Ochieng J, Mugalavai EM, Mourice SK, Hoesche-Zeledon I, Mwila M, Bekunda M. 2019. Long-term spatial-temporal trends and variability of rainfall over Eastern and Southern Africa. Theor Appl Climatol. 137(3–4):1869–1882.

Mwangi HM, Lariu P, Julich S, Patil SD, McDonald MA, Feger KH. 2017. Characterizing the intensity and dynamics of land-use change in the Mara River Basin, East Africa. Forests. 9(1):1–17.

Mwangi KK, Mutua F. 2015. Modeling Kenya's vulnerability to climate change - A multifactor approach. Int J Sci Res [Internet]. 4(6):12–19. https://www.researchgate.net/publication/279885203_Modeling_Kenya's_Vulnerability_to_Climate_Change_-_A_Multifactor_Approach

Mwanjalolo MGJ, Bernard B, Paul MI, Joshua W, Sophie K, Cotilda N, Bob N, John D, Edward S, Barbara N. 2018. Assessing the extent of historical, current, and future land use systems in Uganda. Land. 7(4):1–17.

Mwendwa P, Giliba RA. 2012. Climate Change Impacts and Adaptation Strategies in Kenya. Chinese J Popul Resour Environ. 10(4):22–29.

Myhren SM. 2007. Rural Livelihood and Forest Management in Mount Elgon , Kenya. [place unknown]: Norwegian University of Life Sciences, Ås, Norway.

NAAIAP, KARI. 2014. Soil Suitability Evaluation for Maize Production in Kenya. Nairobi, Kenya: Ministry of Agriculture Kenya.

Nakakaawa C, Moll R, Vedeld P, Sjaastad E, Cavanagh J. 2015. Collaborative resource management and rural livelihoods around protected areas: A case study of Mount Elgon National Park, Uganda. For Policy Econ. 57:1–11.

Nakileza BR, Nedala S. 2020. Topographic influence on landslides characteristics and implication for risk management in upper Manafwa catchment, Mt Elgon Uganda. Geoenvironmental Disasters. 7(27):1–13.

Nandy S, Singh C, Das KK, Kingma NC, Kushwaha SPS. 2015. Environmental vulnerability assessment of eco-development zone of Great Himalayan National Park, Himachal Pradesh, India. Ecol Indic [Internet]. 57:182–195. http://dx.doi.org/10.1016/j.ecolind.2015.04.024

Nelson GC, Rosegrant MW, Koo J, Robertson R, Sulser T, Zhu T, Ringler C, Msangi S, Palazzo A, Batka M, et al. 2009. Climate Change and Agriculture Impacts and costs of adaptation. [place unknown].

Newbold T, Hudson LN, Hill SLL, Contu S, Lysenko I, Senior RA, Börger L, Bennett DJ, Choimes A, Collen B, et al. 2015. Global effects of land use on local terrestrial biodiversity. Nature. 520(7545):45–50.

Nguvava M, Abiodun BJ, Otieno F. 2019. Projecting drought characteristics over East African basins at specific global warming levels. Atmos Res. 228(May):41–54.

Nguyen K-A, Liou Y-A. 2019. Mapping global eco-environment vulnerability due to human and nature disturbances. MethodsX [Internet]. 6:862–875. https://doi.org/10.1016/j.mex.2019.03.023

Nguyen K-A, Liou Y-A, Li M-H, Tran TA. 2016. Zoning eco-environmental vulnerability for environmental management and protection. Ecol Indic [Internet]. 69:100–117. http://dx.doi.org/10.1016/j.ecolind.2016.03.026

Nguyen P, Thorstensen A, Sorooshian S, Hsu K, AghaKouchak A, Ashouri H, Tran H, Braithwaite D. 2018. Global precipitation trends across spatial scales using satellite observations. Bull Am Meteorol Soc. 99(4):689–697.

Norrington-Davies G, Thornton N. 2011. Climate Change Financing and Aid Effectiveness Kenya Case Study. (March).

O'Brien K, Leichenko R, Kelkar U, Venema H, Aandahl G, Tompkins H, Javed A, Bhadwal S, Barg S, Nygaard L, West J. 2004. Mapping vulnerability to multiple stressors: Climate change and globalization in India. Glob Environ Chang. 14(4):303–313.

Okello SV, Nyunja RO, Netondo GW, Onyango JC. 2010. Ethnobotanical study of medicinal plants used by the Sabaots of Mt. Elgon, Kenya. African J Tradit Contemp Altern Med. 7(1):1–10.

Oliver JE. 1980. Monthly precipitation distribution: A comparative index. Prof Geogr. 32(3):300–309.

Olsson L, Eklundh L, Ardö J. 2005. A recent greening of the Sahel - Trends, patterns and potential causes. J Arid Environ. 63(3):556–566.

Omwenga JM, Daudi F, Jebet C. 2019. Understanding ecosystem-based adaptation to climate in Kenya' s Mt Elgon Forest Ecosystem: Definitions, opportunities and constraints. Environ Sustain Clim Chang. 1(1):1–8.

One Acre Fund. One Acre Fund: Our Model [Internet]. https://oneacrefund.org/what-we-do/our-model/

Ongoma V, Chen H. 2017. Temporal and spatial variability of temperature and precipitation over East Africa from 1951 to 2010. Meteorol Atmos Phys. 129(2):131–144.

Ongugo P, Owuor B, Osano P. 2017. Detecting Forest degradation in Kenya: An analysis of hot spots and rehabilitation techniques in Mt. Elgon and Cherangani Hills ecosystems [Internet]. Nairobi, Kenya: KEFRI. https://kefri.org/WaterTowers/PDF/AFROMONT_Paul Paper-22nd Feb 2017_Paul edits.pdf

Ordway EM, Asner GP, Lambin EF. 2017. Deforestation risk due to commodity crop expansion in sub-Saharan Africa. Environ Res Lett. 12(4).

Overmars KP, de Groot WT, Huigen MGA. 2007. Comparing inductive and deductive modeling of land use decisions: Principles, a model and an illustration from the Philippines. Hum Ecol. 35(4):439–452.

Overmars KP, De Koning GHJ, Veldkamp A. 2003. Spatial autocorrelation in multi-scale land use models. Ecol Modell. 164(2–3):257–270.

Paegelow M, Teresa M, Olmedo C, Mas J, Houet T, Gilmore R, Jr P. 2013. Land change modelling : moving beyond projections. 8816.

Pan N, Feng X, Fu B, Wang S, Ji F, Pan S. 2018. Increasing global vegetation browning hidden in overall vegetation greening: Insights from time-varying trends. Remote Sens Environ [Internet]. 214(May):59–72. https://doi.org/10.1016/j.rse.2018.05.018

Parker L, Bourgoin C, Martinez-Valle A, Läderach P. 2019. Vulnerability of the agricultural sector to climate change: The development of a pan-tropical Climate Risk Vulnerability Assessment to inform sub-national decision making. PLoS One. 14(3):1–25.

Pearson K. 1901. LIII. On lines and planes of closest fit to systems of points in space . London, Edinburgh, Dublin Philos Mag J Sci. 2(11):559–572.

Pellikka PKE, Clark BJF, Gosa AG, Himberg N, Hurskainen P, Maeda E, Mwang'ombe J, Omoro LMA, Siljander M. 2013. Kenya: A Natural Outlook: Geo-Environmental Resources and Hazards - Agricultural expansion and its consequences in the Taita Hills, Kenya. In: Paron P, Olago DO, Omuto CT, editors. Dev Earth Surf Process. Vol. 16. Oxford; p. 165–179.

Petersen B, Snapp S. 2015. What is sustainable intensification? Views from experts. Land use policy [Internet]. 46:1–10. http://dx.doi.org/10.1016/j.landusepol.2015.02.002

Petursson JG, Vedeld P. 2017. Rhetoric and reality in protected area governance: Institutional change under different conservation discourses in Mount Elgon National Park, Uganda. Ecol Econ [Internet]. 131:166–177. http://dx.doi.org/10.1016/j.ecolecon.2016.08.028

Petursson JG, Vedeld P, Sassen M. 2013. An institutional analysis of deforestation processes in protected areas: The case of the transboundary Mt. Elgon, Uganda and Kenya. For Policy Econ. 26:22–33.

Pijanowski BC, Brown DG, Shellito BA, Manik GA. 2002. Using neural networks and GIS to forecast land use changes: a Land Transformation Model Bryan. Comput Environemnt Urban Syst. 26:553–575.

Pretty JN. 1997. The sustainable intensification of agriculture. Nat Resour Forum. 21(4):247–256.

Qualtrics. 2019. Provo, UT, USA: Qualtrics.

Le Quéré C, Raupach MR, Canadell JG, Marland G, Bopp L, Ciais P, Conway TJ, Doney SC, Feely RA, Foster P, et al. 2009. Trends in the sources and sinks of carbon dioxide. Nat Geosci. 2(12):831–836.

R Core Team. 2016. Package ' grDevices .'

R Core Team. 2018. R: A Language and Environment for Statistical Computing. Vienna, Austria: R Core Team.

Rama Rao CA, Raju BMK, Subba Rao AVM, Rao K V., Rao VUM, Ramachandran K, Venkateswarlu B, Sikka AK, Srinivasa Rao M, Maheswari M, Rao CS. 2016. A district level assessment of vulnerability of Indian agriculture to climate change. Curr Sci. 110(10):1939–1946.

Ratemo S, Bamutaze Y. 2017. Spatial analysis of elements at risk and household vulnerability to landslide hazards on Mt. Elgon, Uganda. African J Environ Sci Technol. 11(8):438–447.

RCMRD. 2020. Eastern and Southern Africa Land Cover Viewer [Internet]. [accessed 2021 Jun 2].
https://rcmrd.maps.arcgis.com/apps/webappviewer/index.html?id=c954194840d74c48a760485fe00ffb1e

Rindfuss RR, Walsh SJ, Ii BLT, Fox J, Mishra V. 2004. Developing a science of land change: Challenges and methodological issues. 101(39).

Rukundo E, Liu S, Dong Y, Rutebuka E, Asamoah EF, Xu J, Wu X. 2018. Spatio-temporal dynamics of critical ecosystem services in response to agricultural expansion in Rwanda, East Africa. Ecol Indic [Internet]. 89(February):696–705. https://doi.org/10.1016/j.ecolind.2018.02.032

Sahoo S, Dhar A, Kar A. 2016. Environmental vulnerability assessment using Grey Analytic Hierarchy Process based model. Environ Impact Assess Rev [Internet]. 56:145–154. http://dx.doi.org/10.1016/j.eiar.2015.10.002

Salami AO, Kamara AB, Brixiova Z. 2010. Smallholder Agriculture in East Africa: Trends, Constraints and Opportunities. In: Work Pap Ser. Abidjan, Côte d'Ivoire: African Development Bank Group.

Salazar A, Baldi G, Hirota M, Syktus J, McAlpine C. 2015. Land use and land cover change impacts on the regional climate of non-Amazonian South America: A review. Glob Planet Change. 128:103–119.

Schmidt H, Gitelson A. 2000. Temporal and spatial vegetation cover changes in Israeli transition zone: AVHRR-based assessment of rainfall impact. Int J Remote Sens. 21(5):997–1010.

Sen PK. 1968. Estimates of the Regression Coefficient Based on Kendall's Tau. J Am Stat Assoc. 63(324):1379–1389.

Seneviratne SI, Nicholls N, Easterling D, Goodess CM, Kanae S, Kossin J, Luo Y, Marengo J, McInnes K, Rahimi M, et al. 2012. Changes in climate extremes and their impacts on the naturalphysical environment. In: Manag Risks Extrem Events Disasters to Adv Clim Chang Adapt. Cambridge, United Kingdom: Cambridge University Press; p. 109–230.

Shafizadeh-Moghadam H, Tayyebi A, Helbich M. 2017. Transition index maps for urban growth simulation : application of artificial neural networks , weight of evidence and fuzzy multi-criteria evaluation.

Shafizadeh Moghadam H, Helbich M. 2013. Spatiotemporal urbanization processes in the megacity of Mumbai, India: A Markov chains-cellular automata urban growth model. Appl Geogr. 40:140–149.

Simane B, Zaitchik BF, Foltz JD. 2016. Agroecosystem specific climate vulnerability analysis: application of the livelihood vulnerability index to a tropical highland region. Mitig Adapt Strateg Glob Chang. 21(1):39–65.

Smith V, Portillo-Quintero C, Sanchez-Azofeifa A, Hernandez-Stefanoni JL. 2019. Assessing the accuracy of detected breaks in Landsat time series as predictors of small scale deforestation in tropical dry forests of Mexico and Costa Rica. Remote Sens Environ [Internet]. 221(December 2018):707–721. https://doi.org/10.1016/j.rse.2018.12.020

Struik PC, Kuyper TW. 2017. Sustainable intensification in agriculture : the richer shade of green . A review. Agron Sustain Dev.

Sulla-Menashe D, Friedl MA. 2018. User Guide to Collection 6 MODIS Land Cover (MCD12Q1

and MCD12C1) Product [Internet]. Reston, VA, USA: USGS. https://doi.org/10.5067/MODIS/MCD12Q1.006

Tadesse S, Woldetsadik M, Senbeta F. 2017. Forest users' level of participation in a participatory forest management program in southwestern Ethiopia. Forest Sci Technol [Internet]. 13(4):164–173. https://doi.org/10.1080/21580103.2017.1387613

Teodoro A, Santos P, Marques JE, Ribeiro J, Mansilha C, Melo A, Duarte L, de Almeida CR, Flores D. 2021. An integrated multi-approach to environmental monitoring of a self-burning coal waste pile: The são pedro da cova mine (porto, portugal) study case. Environ - MDPI. 8(6).

Torresan S, Critto A, Rizzi J, Marcomini A. 2012. Assessment of coastal vulnerability to climate change hazards at the regional scale: The case study of the North Adriatic Sea. Nat Hazards Earth Syst Sci. 12(7):2347–2368.

Tucker CJ. 1979. Red and photographic infrared linear combinations for monitoring vegetation. Remote Sens Environ. 8(2):127–150.

Turner II BL, Lambin EF, Reenberg A. 2007. The emergence of land change science for global environmental change and sustainability. PNAS. 104(12):5252.

Uddin K, Chaudhary S, Chettri N, Kotru R, Murthy M, Chaudhary RP, Ning W, Shrestha SM, Gautam SK. 2015. The changing land cover and fragmenting forest on the Roof of the World: A case study in Nepal's Kailash Sacred Landscape. Landsc Urban Plan [Internet]. 141:1–10. http://dx.doi.org/10.1016/j.landurbplan.2015.04.003

UNEP. 2015. Green Economy Sector Study on Agriculture in Kenya. Nairobi, Kenya: UNEP.

United States Geological Service. 2000. USGS EROS Archive - Digital Elevation - Shuttle Radar Topography Mission (SRTM) 1 Arc-Second Global [Internet]. https://www.usgs.gov/centers/eros/science/usgs-eros-archive-digital-elevation-shuttle-radar-topography-mission-srtm-1-arc?qt-science_center_objects=0#qt-science_center_objects

USGS. Landsat Satellite Missions. Landsat Mission [Internet]. [accessed 2020 May 12]. https://www.usgs.gov/land-resources/nli/landsat/landsat-satellite-missions?qt-science_support_page_related_con=2#qt-science_support_page_related_con

Vaz de NE, Nijkamp P, Painho M, Caetano M, Cover CL. 2012. Landscape and Urban Planning A multi-scenario forecast of urban change : A study on urban growth in the Algarve. Landsc Urban Plan [Internet]. 104(2):201–211. http://dx.doi.org/10.1016/j.landurbplan.2011.10.007

Vedeld P, Cavanagh C, Petursson J, Nakakaawa C, Moll R, Sjaastad E. 2016. The political economy of conservation at mount elgon, Uganda: Between local deprivation, regional sustainability, and global public goods. Conserv Soc. 14(3):183.

Venkatesh R, Abdul Rahaman S, Jegankumar R, Masilamani P. 2020. Eco-environemntal vulnerability zonation in essense of environmental monitoring and management. Int Arch Photogramm Remote Sens Spat Inf Sci - ISPRS Arch. 43(B5):149–155.

Verbesselt J, Herold M, Hyndman R, Zeileis A, Culvenor D. A robust approach for phenological change detection within satellite image time series. In: 2011 6th Int Work Anal Multi-Temporal

Remote Sens Images, Multi-Temp 2011 - Proceedings, Trento, Italy, 12–14 July 2011. [place unknown]; p. 41–44.

Verbesselt J, Hyndman R, Newnham G, Culvenor D. 2010. Detecting trend and seasonal changes in satellite image time series. Remote Sens Environ [Internet]. 114(1):106–115. http://dx.doi.org/10.1016/j.rse.2009.08.014

Verbesselt J, Hyndman R, Zeileis A, Culvenor D. 2010. Phenological change detection while accounting for abrupt and gradual trends in satellite image time series. Remote Sens Environ [Internet]. 114(12):2970–2980. http://dx.doi.org/10.1016/j.rse.2010.08.003

Verbesselt J, Zeileis A, Herold M. 2012. Near real-time disturbance detection using satellite image time series. Remote Sens Environ [Internet]. 123:98–108. http://dx.doi.org/10.1016/j.rse.2012.02.022

Vermeulen SJ, Aggarwal PK, Ainslie A, Angelone C, Campbell BM, Challinor AJ, Hansen JW, Ingram JSI, Jarvis A, Kristjanson P, et al. 2012. Options for support to agriculture and food security under climate change. Environ Sci Policy. 15(1):136–144.

Vlaeminck P, Maertens M, Isabirye M, Vanderhoydonks F, Poesen J, Deckers S, Vranken L. 2016. Coping with landslide risk through preventive resettlement. Designing optimal strategies through choice experiments for the Mount Elgon region, Uganda. Land use policy. 51:301–311.

Vrieling A, de Beurs KM, Brown ME. 2011. Variability of African farming systems from phenological analysis of NDVI time series. Clim Change. 109(3–4):455–477.

Vrieling A, De Leeuw J, Said MY. 2013. Length of growing period over africa: Variability and trends from 30 years of NDVI time series. Remote Sens. 5(2):982–1000.

Waiyasusri K, Wetchayont P. 2020. Assessing long-term deforestation in nam san watershed, loei province, thailand using a dyna-clue model. Geogr Environ Sustain. 13(4):81–97.

Wang W. 2015. Evaluating land suitability to increase food production in Kenya [Internet]. [place unknown]: Massahusetts Institute of Technology. http://hdl.handle.net/1721.1/99627

Wang XD, Zhong XH, Liu SZ, Liu JG, Wang ZY, Li MH. 2008. Regional assessment of environmental vulnerability in the Tibetan Plateau: Development and application of a new method. J Arid Environ. 72(10):1929–1939.

Wanyama D. 2017. A Spatial Analysis of Climate Change Effects on Maize Productivity in Kenya [Internet]. Florence, AL, USA: University of North Alabama. https://ir.una.edu/gmt/1

Wanyama D, Kar B, Moore NJ. 2021. Quantitative multi-factor characterization of eco-environmental vulnerability in the Mount Elgon ecosystem. GIScience Remote Sens [Internet].:1–22. https://doi.org/10.1080/15481603.2021.2000351

Wanyama D, Mighty M, Sim S, Koti F. 2019. A spatial assessment of land suitability for maize farming in Kenya. Geocarto Int. 36(12):1378–1395.

Wanyama D, Moore NJ, Dahlin KM. 2020. Persistent vegetation greening and browning trends related to natural and human activities in the Mount Elgon Ecosystem. Remote Sens. 12(13).

Wasonga D V., Opiyo J. 2018. Biodiversity status of Mount Elgon Forest ecosystem. Nairobi, Kenya: Kenya Forestry Research Institute (KEFRI). http://kefriwatertowers.org/PDF/Biodiversity status report _ Mt Elgon FF.pdf

Wei W, Shi S, Zhang X, Zhou L, Xie B, Zhou J, Li C. 2020. Regional-scale assessment of environmental vulnerability in an arid inland basin. Ecol Indic [Internet]. 109. https://doi.org/10.1016/j.ecolind.2019.105792

Winkler JA, Soldo L, Tang Y, Forbush T, Douches DS, Long CM, Leisner CP, Buell CR. 2018. Potential impacts of climate change on storage conditions for commercial agriculture: an example for potato production in Michigan. Clim Change. 151(2):275–287.

Woodcock CE, Allen R, Anderson M, Belward A, Bindschadler R, Cohen W, Gao F, Goward SN, Helder D, Helmer E, et al. 2008. Free Access to Landsat Imagery. Science (80-). 320(May):1011–1012.

World Bank. Indicators [Internet]. [accessed 2019 Apr 17]. https://data.worldbank.org/indicator/

World Resources Institute. Kenya GIS Data [Internet]. [accessed 2021 Jun 2]. https://www.wri.org/data/kenya-gis-data

WorldPop Project. 2020. World population data [Internet]. [accessed 2020 Jul 2]. http://www.worldpop.org

Wu KY, Zhang H. 2012. Land use dynamics, built-up land expansion patterns, and driving forces analysis of the fast-growing Hangzhou metropolitan area, eastern China (1978-2008). Appl Geogr [Internet]. 34:137–145. http://dx.doi.org/10.1016/j.apgeog.2011.11.006

Xiong J, Li J, Cheng W, Wang N, Guo L. 2019. A GIS-based support vector machine model for flash flood vulnerability assessment and mapping in China. ISPRS Int J Geo-Information. 8(7).

Zhang X, Chen M, Guo K, Liu Yang, Liu Yi, Cai W, Wu H, Chen Z, Chen Y, Zhang J. 2021. Regional land eco-security evaluation for the mining city of Daye in China using the GIS-based grey topsis method. Land. 10(2):1–18.

Zhao J, Ji G, Tian Y, Chen Y, Wang Z. 2018. Environmental vulnerability assessment for mainland China based on entropy method. Ecol Indic [Internet]. 91:410–422. https://doi.org/10.1016/j.ecolind.2018.04.016

Zhong-Wu L, Guang-Ming Z, Hua Z, Bin Y, Sheng J. 2006. The integrated eco-environment assessment of the red soil hilly region based on GIS-A case study in Changsha City, China. Ecol Modell. 202(3–4):540–546.

Zhu Z, Piao S, Myneni RB, Huang M, Zeng Z, Canadell JG, Ciais P, Sitch S, Friedlingstein P, Arneth A, et al. 2016. Greening of the Earth and its drivers. Nat Clim Chang. 6(8):791–795.

Zou T, Yoshino K. 2017. Environmental vulnerability evaluation using a spatial principal components approach in the Daxing'anling region, China. Ecol Indic [Internet]. 78:405–415. http://dx.doi.org/10.1016/j.ecolind.2017.03.039

Žurovec O, Čadro S, Sitaula BK. 2017. Quantitative assessment of vulnerability to climate change

in rural municipalities of Bosnia and Herzegovina. Sustain. 9(7):1–18.